Synthesis and kinetic characterisation of water-soluble fluorogenic acyl donors for transglutaminase 2

Wodtke, R.; Schramm, G.; Pietzsch, J.; Pietsch, M.; Löser, R.;

Originally published:

May 2016

ChemBioChem 17(2016), 1263-1281

DOI: https://doi.org/10.1002/cbic.201600048

Perma-Link to Publication Repository of HZDR:

https://www.hzdr.de/publications/Publ-23553

Synthesis and kinetic characterisation of water-soluble fluorogenic acyl donors for transglutaminase 2

Robert Wodtke,[a,c] Georg Schramm,[a,d] Jens Pietzsch,[a,c] Markus Pietsch,[b]* and Reik Löser[a,c]*

Abstract: Small glutamate-containing peptides that bear coumarin derivatives as fluorescent leaving groups attached to the γ-carboxylic group of the Glu residue were synthesised and investigated towards their potential to act as substrates for transglutaminase 2 (TGase 2). Their synthesis was accomplished by an efficient solid-phase approach. The excellent water solubility of the compounds enabled their extensive kinetic characterisation regarding TGase 2-catalysed hydrolysis and aminolysis. The influence of the substitution pattern at the coumarin skeleton on the kinetic properties was studied. Derivatives containing 7-hydroxy-4-methylcoumarin (HMC) revealed superior properties over their 7-hydroxycoumarin counterparts; analogous amides are not accepted as substrates. Z-Glu(HMC)-Gly-OH, which exhibited the most optimal substrate properties among the investigated derivatives, was selected for the exemplary kinetic characterisation of acyl acceptor substrates and irreversible inhibitors.

Introduction

The quantitative determination of enzyme activities is of outstanding importance in biochemical research. Enzymatic assays provide the basis for the functional characterisation of enzymes with regards to kinetic parameters and are crucial for studying these biocatalysts in their biological contexts. In the field of drug discovery, the availability of methods that allow for assaying enzymes is a prerequisite for the identification and characterisation of inhibitors. In addition, the development of substrate-based probes that can efficiently monitor enzymes for diagnostic or imaging purposes requires their evaluation based on kinetic properties. To facilitate a sensitive and facile quantification, enzyme substrates should contain moieties that are released upon conversion and can be reliably detected by spectroscopic methods/analytical instruments. Enzymes that catalyse the transfer of acyl moieties to water or alternative nucleophiles, such as hydrolases and acyl transferases, respectively, often accept chromophores or fluorophores as leaving groups within the acyl donor substrate. When these chromophores or fluorophores contain electron-donating groups, such as OH or NH_2, attachment of acyl residues to these groups usually results in attenuation of the absorption and emission intensities, respectively. Upon enzyme-catalysed cleavage, the spectroscopic properties are restored, which couples enzymatic activity to signal increase.[1]

Acyl transferases of particular importance are transglutaminases, among which transglutaminase 2 (TGase 2, tissue transglutaminase) seems to be most obviously involved in human disease progression. TGase 2 is an ubiquitously occurring enzyme in mammals that exhibits several important biological functions.[2] The eponymous and best characterised role is its function as Ca^{2+}-dependent catalyst of the acyl transfer reaction between protein-bound glutamine residues and primary amines, particularly protein-bound lysine-residues and low-molecular weight polyamines.[3] In addition to catalysing such transamidation reactions, TGase 2 is able to hydrolyse the γ-carboxamide group of glutamine residues, thus, generating glutamate residues.[4]

The acyl transferase activity of TGase 2 is considered to be latent under physiological conditions but rapid activation occurs in stress situations, such as apoptosis, where cross-linking of proteins will stabilise dying cells.[5] In the course of TGase 2 research, further diverse enzymatic and non-enzymatic functions were ascribed to this enzyme, which might be more relevant under physiological conditions for maintaining the integrity of the cell.[6]

TGase 2, particularly its acyl transferase activity, contributes to different pathophysiological conditions, such as celiac disease,[7] diseases related to fibrotic processes,[8] neurodegenerative disorders,[9] and cancer.[10] Therefore, this enzyme appears to be an attractive target for pharmacological inhibition to potentially treat these diseases. In addition, the development of imaging agents targeted against TGase 2 will provide further insight into its pathological functions and will support clinical translation of inhibitors. One of the prerequisites for the development of TGase 2 inhibitors is the availability of reliable assay methods for precise measurement of the enzymatic activity, which will enable the evaluation of the compounds' inhibitory potency. Various continuous and discontinuous assay methods for TGase 2 have been described so far, which were recently discussed in detail.[11] Among these assay methods, the continuous fluorimetric activity assay described by Gillet *et al.*[12] seems to be well-suitable for inhibitor characterisation as it allows for the

[a] *Robert Wodtke, Dr. Georg Schramm, Prof. Dr. Jens Pietzsch, Dr. Reik Löser*
Helmholtz-Zentrum Dresden-Rossendorf
Institut für Radiopharmazeutische Krebsforschung
Bautzner Landstraße 400, D-01328 Dresden (Germany)
E-mail: r.loeser@hzdr.de
[b] *Dr. Markus Pietsch*
Zentrum für Pharmakologie, Medizinische Fakultät
Universität zu Köln
Gleueler Straße 24, D-50931 Köln (Germany)
E-mail: markus.pietsch@uk-koeln.de
[c] *Robert Wodtke, Prof. Dr. Jens Pietzsch, Dr. Reik Löser*
Fachrichtung Chemie und Lebensmittelchemie
Technische Universität Dresden
Mommsenstraße 4, D-01062 Dresden (Germany)
[d] *Dr. Georg Schramm*
present address: KU Leuven, Department of Imaging and Pathology
3000 Leuven, Belgium

Supporting information for this article is given via a link at the end of the document.

sensitive detection of the TGase 2 activity through the measurement of an increase in fluorescence (**Scheme 1**).

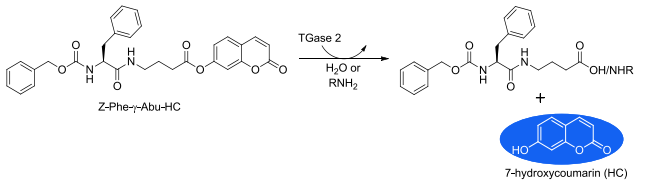

Scheme 1. Principle of the fluorimetric TGase 2 activity assay according to Gillet *et al.*[12] Release of 7-hydroxycoumarin (HC) by TGase 2-catalysed hydrolysis or aminolysis of Z-Phe-γ-Abu-HC results in a measureable increase in fluorescence.

The synthetic access to the required fluorogenic acyl donors consisting of a Z-protected amino acid (Z: benzyloxycarbonyl, also referred to as carbobenzoxy (Cbz) group) connected to umbelliferon (7-hydroxycoumarine, HC) via a γ-aminobutyric linker acting as mimetic of the glutamine side chain is rather facile. In addition, the assay allows for the kinetic characterisation of both inhibitors and acyl acceptor substrates. Therefore, we aimed to establish this fluorimetric assay in our laboratories by using the fluorogenic acyl donor Z-Phe-γ-Abu-HC. However, as outlined later in this article, both Z-Phe-γ-Abu-HC and its 7-hydroxy-4-methylcoumarin (HMC)-based derivative revealed the disadvantage of low solubility in aqueous media. Depending on the experimental setup, this may limit the applicability of these compounds for detailed kinetic studies as such investigations require activity measurements over a broad range of substrate concentration. In particular, simultaneous measurements of various substrate concentrations in a microplate format may be more affected by solubility limits than single measurements in a cuvette[12] due to the different time delay caused by preparation. Therefore, we intended to develop analogues with improved solubility. A general approach to render molecules more soluble in water is the attachment of ionisable functionalities such as carboxylic groups.[13] Applied to the above-mentioned TGase 2 substrates such derivatisation seems to be most facile to realise by replacing the γ-aminobutyric moiety with glutamate.

Herein, we describe the synthesis and kinetic characterisation of six novel glutamate-derived fluorogenic acyl donors. A solid phase synthesis strategy was developed for this purpose and the compounds were evaluated with regards to their enzymatic hydrolysis and aminolysis by both standard regression analysis and numerical integration. Beside the investigations on different peptidic scaffolds for recognition by TGase 2, the influence of substitutions on the fluorophore was explored. Since all compounds exhibit distinct rates of spontaneous reactions, this feature was used in turn to assess their solubility. In addition to the coumarinyl esters, two coumarinyl amides were synthesised to determine their potential to act as fluorogenic acyl donors. Furthermore, the applicability of the novel acyl donors for kinetic characterisation of amine-based acyl acceptor substrates, *i.e.* aminoacetonitrile and *N*-(biotinyl)cadaverine, and irreversible inhibitors, *i.e.* iodoacetamide and the recently described N^{α}-phenylacetyl-N^{ε}-acryloyl-lysine-4-(6-methylpyridine-2-yl)piperazide,[14] was verified.

Results and Discussion

Synthesis and kinetic evaluation of the γ-Abu-derived acyl donors

Initially, it was envisaged to establish the fluorimetric activity assay for TGase 2 using the acyl donors described by Gillet *et al.*[12] Since the reported kinetic data were more favourable for Z-Phe-γ-Abu-HC (**2a**) compared to those of its glycine derivative Z-Gly-γ-Abu-HC, we focused on the former compound. Moreover, other coumarin derivatives, *i.e.* HMC and 7-amino-4-methylcoumarin (AMC), were employed as fluorogenic leaving groups. The syntheses of these three compounds were accomplished in two steps according to the published procedure with some modifications starting from commercially available Z-Phe-OH (see **Scheme 2** and Discussion S1 in Supporting Information for the detailed experimental procedures).[12] After purification by column chromatography and recrystallisation, the fluorogenic acyl donors **2a**-**2c** were obtained in sufficient yields (55-68%) and high purities.

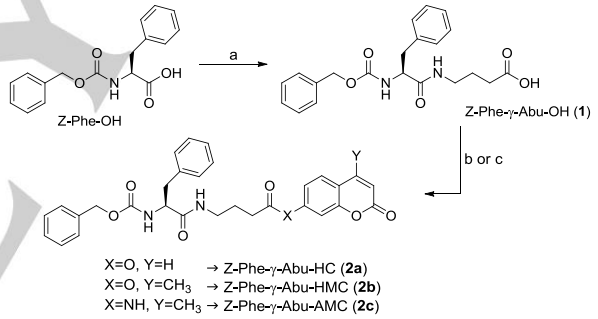

Scheme 2. Synthesis of the γ-aminobutyric acid-derived fluorogenic acyl donors **2a**-**2c**. Reagents and conditions: **a**) NMM, IBCF, γ-Abu-OH, aqueous NaOH, THF, -30 → 10 °C, 2.5 h; **b**) HC/HMC, DCC, DMAP, CH_2Cl_2/THF (4:1), 25 h; **c**) AMC, NMM, IBCF, THF/DMF (12:1), -25 °C → 10 °C, 5 h.

Initial investigations were focussed on the enzymatic aminolysis of the acyl donors **2a** and **2b** at pH=8.0 using aminoacetonitrile as acyl acceptor in the presence of (±)-*threo*-dithiothreitol (DTT) as antioxidant. According to the reported assay procedure, a final concentration of 5% DMF or DMSO was used to achieve sufficient solubility of the acyl donors in aqueous media.[12] The increase in fluorescence was monitored in 96-well microplates at different concentrations of **2a** (5-40 µM) and **2b** (1-20 µM) and initial rates (v_{0total}) were calculated as outlined in the Experimental section. Unexpectedly, plots of v_{0total} *versus* the acyl donor concentration for both compounds exhibited a maximum at ~5 µM, after which the rates suddenly dropped and further increased with rising substrate concentrations (see Figure S1 in Supporting Information). Concomitantly, visual inspection of plate wells revealed the formation of precipitates

even at acyl donor concentrations below 20 µM independently of the used organic co-solvent. This observation suggested that the anomalous Michaelis-Menten plots are caused by the limited solubility of **2a** and **2b**. Generally, poorly soluble substrates will follow the Michaelis-Menten hyperbola only up to the solubility limit without reaching V_{max}, "since the concentration of substrate which saturates an aqueous solution is insufficient to saturate the enzyme".[15] To investigate the solubility behaviour of the acyl donors more in detail, we decided to take advantage of their spontaneous decay, which takes place in the absence of TGase 2 and aminoacetonitrile. As this reaction follows a pseudo-first-order kinetics, plots of initial rates ($v_{0control}$) *versus* concentration should display a linear dependence in the case of complete solubility.[16] The results of this investigation confirmed the initial observations on the low solubility of the γ-Abu-derived acyl donors as the curves deviate from linearity even at low concentrations (<15 µM, see Figure S2 in Supporting Information) before precipitation can be visually noticed, which indicates aggregation prior to precipitate formation. Moreover, as shown in Figure S2, the solubility of the two γ-Abu derivates is highly time-dependent and strongly influenced by the organic co-solvent as well as the present antioxidant. However, to demonstrate their potential as substrates, compounds **2a** and **2b** were evaluated towards gpTGase 2-catalysed hydrolysis within their solubility limits (see Figure S3 in Supporting Information). Nonlinear regression according to the Michaelis-Menten equation (equation III) revealed K_m and k_{cat} values of 1.47 µM and 0.30 s^{-1} for acyl donor **2a** and 1.14 µM and 0.52 s^{-1} for acyl donor **2b** resulting in performance constants of 204,000 $M^{-1}s^{-1}$ and 456,000 $M^{-1}s^{-1}$, respectively **(Table 2)**. These results clearly confirm the favourable substrate properties of the γ-Abu derivatives.[12] Interestingly, despite similar K_m values, substitution of HC by HMC resulted in an almost two times higher k_{cat} value for acyl donor **2b** compared to **2a**. Due to their low K_m values, both coumarinyl esters can be applied for investigations on the hydrolytic activity of TGase 2 up to concentrations of 3-6×K_m depending on the used buffer conditions.

In contrast to the coumarinyl esters **2a** and **2b**, neither spontaneous nor enzymatic release of AMC was observed for coumarinyl amide **2c** (data not shown), which will be discussed later in this article.

Synthesis and spontaneous reactivity of the glutamate-derived acyl donors

To overcome the low solubility, derivatisation of fluorogenic acyl donors with a carboxylic group as solubilising moiety was envisaged.[13] From a synthetic point of view, the most straightforward way to realise this attempt seemed to be the replacement of the γ-aminobutyric acid linker that connects Z-Phe and the fluorophore by a glutamic moiety resulting in Z-Phe-Glu(fluorophore)-OH as basic dipeptidic structure. Moreover, this scaffold allows for the C-terminal extension of the scaffold structure by an additional amino acid such as glycine, which would place the solubility-mediating carboxylic group further away from the reaction centre. In order to define the minimal structural motif for efficient TGase 2-catalysed conversion, the effect of deleting the N-terminal Phe moiety had to be studied. Therefore, Z-Glu(fluorophore)-OH, Z-Glu(fluorophore)-Gly-OH and Z-Phe-Glu(fluorophore)-Gly-OH were taken into account as amino acid-based and peptidic scaffolds for substrate synthesis in addition to Z-Phe-Glu(fluorophore)-OH. As γ-Abu derivative **2b** exhibits more favourable substrate properties than **2a**, HMC was selected as fluorophore for all peptidic scaffolds. However, to investigate the influence of methyl substitution at the coumarin fluorophore on the substrate properties towards TGase 2, HC derivatives of the most favourable peptidic structures Z-Glu-Gly-OH and Z-Phe-Glu-Gly-OH (see Kinetics section) were also synthesised. Finally, Z-Glu(AMC)-Gly-OH (**5c**) was prepared to ascertain whether or not coumarinyl amides can be used as fluorogenic acyl donors for TGase 2.

A major challenge for the synthesis of the glutamate-derived acyl donors is faced with the regioselective installation of the fluorogenic leaving group into the side chain of the glutamate residue. Therefore, a strategy based on solid phase synthesis using orthogonal protecting groups was developed to provide the different glutamate-derived acyl donors (**Scheme 3**). In addition, this modular approach should account for an efficient access to a broad spectrum of potential acyl donors. For this purpose, the 2-chlorotrityl chloride (2-ClTrtCl) resin was considered as optimal polymeric support as the anchoring moiety readily reacts with carboxylic groups and the corresponding highly acid-labile 2-chlorotrityl esters can be easily cleaved under mildly acidic conditions (see below).[17] Final esterification at the glutamate side chain required careful optimisation with regards to the selection of the coupling reagents (see Discussion S2 in Supporting Information). In result, the use of the uronium-based coupling agent HATU and DIPEA as base accounted for a complete conversion of the carboxylic acids to the respective coumarinyl esters (see Discussion S3 in Supporting Information).[18] Subsequent release of the acyl donors from the resin was achieved under mild conditions by treatment with a 1:4 mixture of hexafluoroisopropanol (HFIP) and dichloromethane.[19] In this context, the use of HFIP instead of TFA ensures the integrity of the coumarinyl esters as they are potentially susceptible to acid-mediated hydrolysis. All compounds were obtained in sufficient yields (26-36%) and high purities after purification by preparative RP-HPLC (see Discussion S4 in Supporting Information for details on the experimental procedures).

The established modular solid-phase synthesis approach allows for the facile access to a variety of peptidic coumarinyl esters in small amounts. Alternatively, Chung *et al.* prepared the analogous chromogenic acyl donor Z-Glu(O*p*Np)-Gly-OH in solution starting from Z-protected glutamic anhydride, which offers the advantage to obtain the final product in larger scale.[20] The transfer of the conditions for on-resin esterification to the coupling of AMC to the glutamate side chain carboxylic group of resin-linked Z-Glu-Gly-OH yielded only minor amounts of the desired coumarinyl amide **5c** (yield 3%, see Discussion S5 in Supporting Information) along with different side products. This may originate from the less nucleophilic character of the

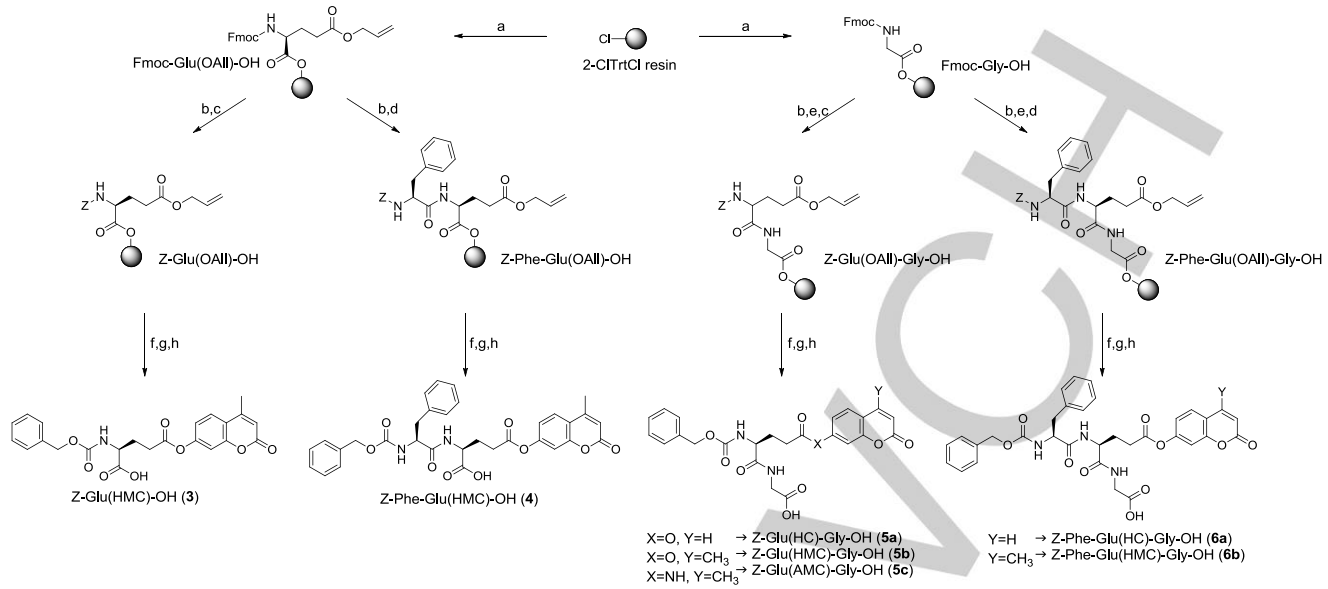

Scheme 3. Solid phase synthesis of the glutamate-derived fluorogenic acyl donors **3**-**6**. Reagents and conditions: **a**) 1. Fmoc-AA, DIPEA, CH_2Cl_2, 4 h, 2. CH_2Cl_2/CH_3OH/DIPEA (17:1:2); **b**) 20% piperidine/DMF; **c**) Z-OSu, DIPEA, CH_2Cl_2, 17 h; **d**) Z-Phe-OH, HBTU, DIPEA, DMF; **e**) 1. Fmoc-Glu(OAll)-OH, HBTU, DIPEA, DMF, 2. 20% piperidine/DMF; **f**) $Pd(PPh_3)_4$, CH_2Cl_2/NMM/HOAc (8:2:1), 4 h, Ar; **g**) HATU, DIPEA, HMC or HC or AMC, DMF, 5 h; **h**) HFIP/CH_2Cl_2 (1:4), 3x10 min.

aromatic amine AMC under these conditions compared to the aromatic alcohols HMC and HC. To increase the yield for this amidation, different coupling procedures were tested with limited success (for details and further information see Discussion S5 in Supporting Information). However, the amounts of **5c** obtained by the various synthetic methods were sufficient for initial investigations concerning its behaviour towards TGase 2.

To determine the solubility of the novel glutamate-derived fluorogenic acyl donors **3**-**6**, the compounds were investigated concerning the rates of their spontaneous reactions at pH=8.0 in the presence of 5% DMSO as done for **2a** and **2b**. The resulting plots showed linearity up to concentrations of 250 µM (see **Figure 1** for the acyl donor **5b** and Figure S4 in Supporting Information), which highlights that the presence of the carboxylic group significantly increases the solubility compared to the γ-Abu derivatives. While linearity predominates over the entire concentration range for compound **4**, a slight bend between 100 and 200 µM is visible for compound **5b**, which indicates a diminished solubility at 200 and 250 µM. This behaviour can be also observed for the other glutamate-derived acyl donors **3**, **5a**, **6a** and **6b** (see Figure S4 in Supporting Information). Nevertheless, enzyme-kinetic investigations up to substrate concentrations of 200-250 µM should be also possible for these acyl donors as they still exhibit a sufficient solubility in this concentration range. Noteworthy, all glutamate-derived acyl donors do not form visible precipitates up to concentrations as high as 500 µM. Furthermore, as indicated by Figure S4, the extent of the spontaneous reaction varies within the different acyl donors. To quantify these characteristics, pseudo-first-order rate constants k_{obs} for the spontaneous reactions were determined for all ester-based acyl donors, which are summarised in **Table 1**.

Table 1. Pseudo-first-order rate constants k_{obs} for the spontaneous reactions of the different acyl donors

acyl donor	k_{obs} (×10^{-3} min^{-1})		k_{obs}(TCEP)/ k_{obs}(DTT)
	DTT	TCEP	
2a	15.8 (0.6)	2.11 (0.05)	0.13
2b	14.3 (0.5)	1.86 (0.08)	0.13
3	-	4.60 (0.36)	-
4	12.2 (0.2)	4.75 (0.13)	0.39
5a	25.1 (2.8)	16.9 (0.6)	0.67
5b	24.3 (1.1)	17.1 (0.3)	0.70
6a	29.2 (4.0)	18.1 (0.5)	0.62
6b	32.7 (1.1)	25.3 (0.4)	0.77

Data shown are mean values ±standard error of the mean (±SEM) of 2-3 separate experiments, each performed in duplicate. The corresponding plots of $v_{0control}$=f([acyl donor]) are enclosed in the Supporting Information (Figure S5).

Since the assay of TGase 2 requires the presence of an antioxidant to prevent oxidation of the active-site cysteine

residue, both DTT and tris(2-carboxyethyl)phosphine (TCEP) were employed for the investigations on the spontaneous reactivity of the compounds at a concentration of 500 µM. In the presence of TCEP, the obtained k_{obs} values reveal distinct spontaneous reactions for all compounds, which seem to depend on the kind of the peptidic scaffold and thus allow for a classification into three groups. The γ-aminobutyric acid derivatives **2a** and **2b** display the lowest k_{obs} values. Compounds **3** and **4**, which bear the free carboxylic groups directly at the glutamate residue, exhibited pseudo-first order rate constants that were approximately twice as high compared to their descarboxy analogues. Interestingly, C-terminal extension by glycine resulted in k_{obs} values that increased by the factor of approximately four, as observed for the acyl donors **5a**, **5b**, **6a** and **6b**. These results suggest that the carboxylate group might act as an intramolecular general base to facilitate the nucleophilic attack of water on the coumarinyl ester bond. General intramolecular base catalysis is obviously more effective for the glycine derivatives, since a spatial orientation of the glycine carboxylic group in proximity to the coumarinyl ester bond is probably sterically less strained compared to the glutamate carboxylic group (see Figure S5 in Supporting Information). Compared to TCEP, monitoring the spontaneous reactions in the presence of DTT resulted in k_{obs} values which are up to 1.6 times greater for the glutamate-derived acyl donors and up to 7.6 times greater for the γ-Abu derivatives **2a** and **2b** (**Figure 1** and **Table 1**). Due to the nucleophilic character of its two thiol groups, DTT may contribute to the spontaneous reaction of the ester substrates. This pathway of spontaneous substrate disintegration is very likely to occur because the reaction of activated aryl esters with thiols to thioesters has previously been reported.[21] In general, thioesters are distinctly more stable towards hydrolysis than the corresponding *O*-esters[22] and, therefore, thiolysis of the coumarinyl ester-based substrates by DTT should be considered as independent pathway for spontaneous reaction. To prove this assumption and to identify the thiolysis products, compound **5b** was exposed to a 10-fold excess of DTT in acetonitrile as solvent in the presence of one equivalent triethylamine. After 5 h at room temperature, analysis of the reaction mixture by RP-HPLC indicated the formation of three major components in addition to remaining educt, the released 4-methylumbelliferon and the corresponding γ-carboxylic acid, which were identified as DTT-thioester, DTT-*O*-ester and glutarimide **5d** (**Scheme 4** and Figures S6 and S7 in Supporting Information). The **5b**-derived DTT-thioester and *O*-ester as well as the corresponding glutarimide **5d** were also detectable under assay conditions (pH=8.0, 500 µM DTT) in the absence of TGase 2 (see Figure S8 in Supporting Information). Notably, the rate of spontaneous reaction in the absence of DTT and TCEP is nearly identical to that observed in the presence of TCEP, which illustrates that the presence of TCEP does not contribute to the spontaneous disintegration of the acyl donors (**Figure 1**). Glutarimide formation from **5b** under assay conditions was unexpected, however, this cyclisation does not substantially contribute to the spontaneous disintegration of **5b** (Figure S8).

Another type of spontaneous reaction that can occur during investigations on TGase 2-catalysed aminolysis is spontaneous aminolysis. However, as exemplarily shown for compound **5b** in **Figure 1**, no increased rate constant for spontaneous disintegration was observed in the presence of aminoacetonitrile and concomitant absence of any reducing agent.

In conclusion, as all coumarinyl esters exhibit distinct rates of spontaneous reactions at pH=8.0, these nonenzymatic conversions must be considered for the analyses of the TGase 2-mediated hydrolyses and aminolyses to ensure correct data evaluation. For this purpose, control measurements in the absence of TGase 2 were carried out for the characterisation of all substrates to determine the proportion of the enzyme-catalysed reactions.

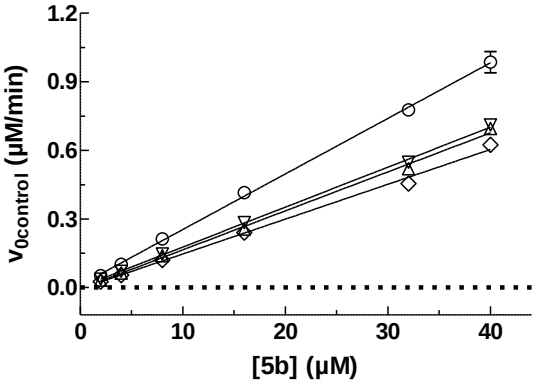

Figure 1. Spontaneous reactions of the fluorogenic acyl donor **5b**. Plots of $v_{0control}$=f([**5b**]) at pH=8.0 and 30 °C in the presence of 5% DMSO and 500 µM DTT (○), 500 µM TCEP (△), no additive (▽) and 400 µM aminoacetonitrile (◇). Analysis by linear regression (–) gave rate constants k_{obs} of 24.3 ± 1.1 ×10^{-3} min^{-1} (DTT), 17.1 ± 0.4 ×10^{-3} min^{-1} (TCEP), 17.5 ± 0.2 ×10^{-3} min^{-1} (no additive) and 15.3 ± 0.2 ×10^{-3} min^{-1} (aminoacetonitrile). Data shown are mean values ±SEM of 2 separate experiments, each performed in duplicate. When not apparent, error bars are smaller than the symbols.

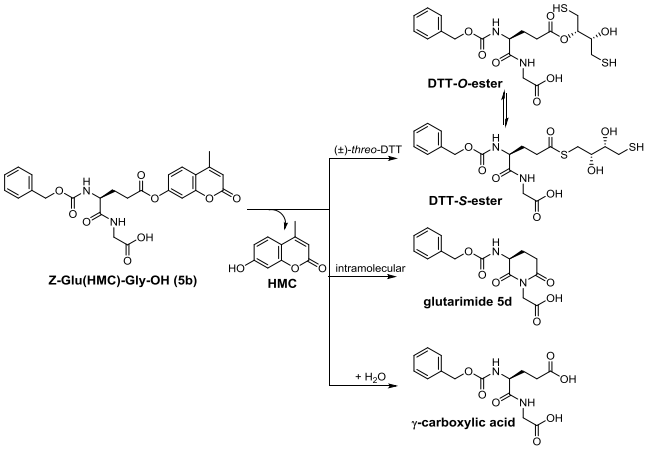

Scheme 4. Structures of identified products from spontaneous reactions of **5b**

Kinetic analysis of TGase 2-catalysed conversions of the glutamate-derived acyl donors

TGase 2-catalysed hydrolyses

Prior to the characterisation of the different acyl donors, fluorescence coefficients for the used fluorophores HC and HMC were determined. As seen in Figure S17 in the Supporting Information, sufficient linearity between the concentration of fluorophore and the respective fluorescence signal is predominant up to a concentration of 20 µM. Typical kinetic runs for the enzymatic hydrolysis and the spontaneous reaction at pH=8.0 are exemplarily depicted for compound **5b** in **Figure 2**. The enzymatic measurements for compound **5b** generated nonlinear progress curves over 900 s, which have also been observed for the other compounds including the γ-amino butyric acid derivatives **2a** and **2b**. To ensure that inactivation of TGase 2 does not occur due to protein instability under the experimental conditions (which could also account for nonlinear progress curves), the Selwyn test was performed with acyl donor **5b**.[23] The results clearly indicate the absence of enzyme inactivation over the entire measurement period of 900 s (plots of RFU=f([E]*t) are almost congruent for three different enzyme concentrations, see Figure S9 in Supporting Information). Therefore, nonlinear progress curves result from a rapid enzymatic conversion of the acyl donors, which gradually leads to substrate depletion for TGase 2. Typically, this effect can be simply reduced by using a lower enzyme concentration, as demonstrated by the Selwyn test, which was performed at 1, 2 and 3 µg/ml of TGase 2. However, with the reduced amount of enzyme the relative proportion of the spontaneous reaction increases (Figure S10 in Supporting Information). Despite the fact that the portion of the enzymatic rate is even at the lowest enzyme concentration greater than that of the spontaneous rate (over the applied range of substrate concentration), a TGase 2 concentration of 3 µg/ml provides the best compromise between signal/background ratio and speed of enzymatic reaction. If the concentration of the released fluorophore exceeds 20 µM during the enzymatic conversion of the acyl donor, fluorescence quenching might contribute to the bend of the curves. Hence, progress curves for the enzymatic hydrolyses were analysed over the first 300 s by nonlinear regression using equation I,[24] which maintained the limits for the fluorescence coefficient mentioned above.

Michaelis-Menten plots for the enzymatic hydrolysis of compound **5b** by gpTGase 2 and hTGase 2, respectively, at pH=8.0 are depicted in **Figure 3** (for the other compounds see Figures S11 and S12 in Supporting Information). The obtained kinetic parameters for all compounds are summarised in **Table 2**. The ratio k_{cat}/K_m, which we decided to denote as performance constant according to Koshland's suggestion, can be regarded as the most appropriate parameter to compare the synthesised fluorogenic acyl donors with regards to their TGase 2-catalysed conversion.[25] Compared to **2b**, changing γ-Abu to glutamate resulted in a significantly decreased k_{cat}/K_m value for compound **4** (456,000 $M^{-1}s^{-1}$ and 16,400 $M^{-1}s^{-1}$ for **2b** and **4**, respectively), which is mainly due to an increase in K_m. This result indicates a detrimental effect on the affinity towards gpTGase 2 when the carboxylic group is directly attached at the glutamate residue, which is in agreement to previous results observed with substrates that contain glutamine[26] or inhibitors based on reactive glutamine analogues.[27] Therefore, a shift of the carboxylic group further away from the reaction centre might be beneficial for the recognition by gpTGase 2.

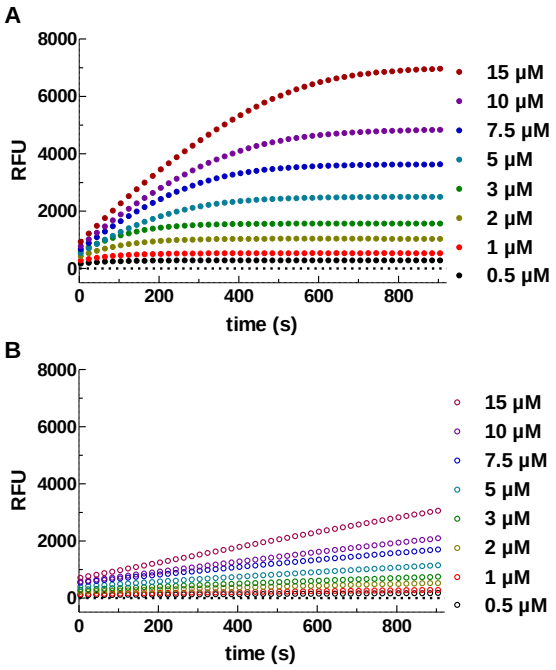

Figure 2. Progress curves for TGase 2-catalysed hydrolysis (**A**) and spontaneous reaction (**B**) of acyl donor **5b**. Conditions: pH=8.0, 30 °C, 5% DMSO, 500 µM DTT, 3 µg/mL gpTGase 2.

Indeed, compound **6b** with Z-Phe-Glu-Gly-OH as peptidic scaffold shows a performance constant that is more than one order of magnitude higher (k_{cat}/K_m=207,000 $M^{-1}s^{-1}$) compared to that of **4**. In order to define the minimal peptidic motif for efficient TGase 2-mediated conversion, N-terminal deletion of the Phe residue was envisaged. For this purpose, we synthesised compounds **3** and **5b** that are derived from Z-Glu-OH and Z-Glu-Gly-OH, respectively. Based on the kinetic data, it can be concluded that the presence of the N-terminal phenylalanine residue does not seem to be crucial for efficient conversion by gpTGase 2 as the performance constants even increase upon its deletion (compare **3** and **4** as well as **5b** and **6b**). Again, the presence of a C-terminal glycine residue positively influenced the recognition by gpTGase 2 (k_{cat}/K_m values of 41,300 $M^{-1}s^{-1}$ and 300,000 $M^{-1}s^{-1}$ for **3** and **5b**, respectively). In order to evaluate the influence of the fluorophore on the substrate properties, HC analogues of the best HMC bearing substrates **5b** and **6b** were synthesised. Surprisingly, while **5a** displays almost unaltered kinetic parameters, characterisation of tripeptide **6a** revealed a considerably lower performance

constant in comparison to its methyl-substituted counterpart **6b**. This result suggests that the methyl group in 4-position of the coumarin system might be beneficial but in detail its influence seems to depend on the peptidic scaffold. Finally, when comparing **5b** (k_{cat}/K_m=300,000 $M^{-1}s^{-1}$) with literature-reported acyl donors, the compound shows not only the most favourable substrate properties of all well-soluble fluorogenic substrates investigated in this study, but also belongs to the kinetically most favourable acyl donor substrates described so far for gpTGase 2.[11] However, it should be pointed out that among all investigated fluorogenic acyl donors, compound **2b** (k_{cat}/K_m=456,000 $M^{-1}s^{-1}$) clearly exhibits the best kinetic properties, even though it is the least soluble compound of the series.

In accordance with this result, the corresponding non-fluorescent substrate Z-Gln-Gly-OH exhibits favourable kinetic parameters towards gpTGase 2[26] and a microbial transglutaminase.[28] In addition to the evaluation of the acyl donors towards gpTGase 2, compounds **5a**, **5b** and **6b**, which display favourable substrate properties towards that enzyme, were also characterised with regards to their hydrolysis catalysed by human TGase 2. Both orthologues share 83% of sequence identity, which in turn renders TGase 2 from guinea pig liver a cost-efficient model for the human enzyme (see Figure S13 in Supporting Information).[29] Notably, all three compounds are also suitable substrates for hTGase 2,

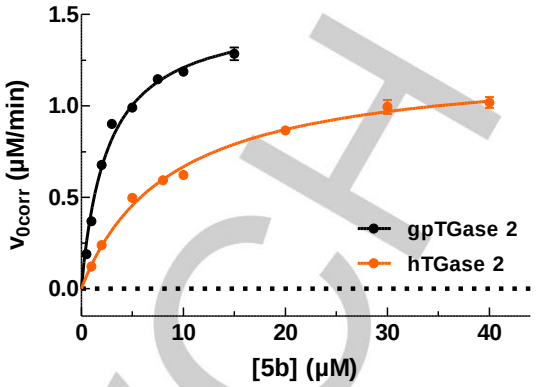

Figure 3. gpTGase 2- and hTGase 2-catalysed hydrolysis of the acyl donor **5b** at pH=8.0. Plots of v_{0corr}=f([acyl donor]) with the nonlinear regressions (—) using equation III (Michaelis-Menten equation). Data shown are mean values ±SEM of 3 separate experiments, each performed in duplicate. When not apparent, error bars are smaller than the symbols. Conditions: pH=8.0, 30 °C, 5% DMSO, 500 µM DTT (for gpTGase 2) or 500 µM TCEP (for hTGase 2), 3 µg/ml of either gpTGase 2 or hTGase 2.

even though performance constants are diminished compared to the guinea pig enzyme (**Table 2**).

Table 2. Kinetic parameters for the TGase 2-catalysed hydrolyses of the acyl donors **2**-**6** at pH=8.0

	Regression analysis			Numerical integration		
	K_m (µM)	k_{cat} (s^{-1})	k_{cat}/K_m ($M^{-1}*s^{-1}$)	K_m (µM)	k_{cat} (s^{-1})	k_{cat}/K_m ($M^{-1}*s^{-1}$)
cpd	**gpTGase 2**					
2a	1.47 (0.02)	0.30 (0.03)	204,000	1.24 (0.06)	0.25 (0.01)	202,000
2b	1.14 (0.16)	0.52 (0.03)	456,000	1.20 (0.27)	0.46 (0.04)	383,000
3	12.1 (0.5)	0.50 (0.01)	41,300	10.9 (0.9)	0.43 (0.01)	39,500
4	17.7 (0.5)	0.29 (0.03)	16,400	12.4 (0.6)	0.23 (0.02)	18,500
5a	2.83 (0.17)	0.71 (0.02)	251,000	2.57 (0.46)	0.62 (0.02)	241,000
5b	2.53 (0.14)	0.76 (0.02)	300,000	2.49 (0.23)	0.71 (0.02)	285,000
6a	11.0 (0.6)	0.64 (0.03)	58,200	8.87 (0.64)	0.55 (0.01)	62,000
6b	2.66 (0.11)	0.55 (0.02)	207,000	2.14 (0.13)	0.54 (0.02)	252,000
	hTGase 2					
5a	12.7 (0.9)	0.84 (0.05)	66,100	9.72 (0.62)	0.74 (0.04)	76,100
5b	8.62 (0.09)	0.68 (0.02)	78,900	6.06 (0.16)	0.64 (0.02)	106,000
6b	13.6 (1.3)	0.50 (0.03)	36,800	7.73 (0.54)	0.48 (0.03)	62,100

For details on calculation of the kinetic parameters see Experimental section. Data shown are mean values (±SEM) of 3 separate experiments, each performed in duplicate. Active concentrations of TGase 2 from guinea pig liver (E_T=31.6-35.3 nM, various lots) and human (E_T=30.8 nM) were calculated from activity data of Zedira® or determined by active site titration as recently described,[30] respectively.

Their K_m values are 4-5 times higher than for the gpTGase 2. Trends are similar as for gpTGase 2 and compound **5b** turned out to be the acyl donor with the most favourable substrate properties towards the human enzyme (k_{cat}/K_m=78,900 $M^{-1}s^{-1}$). A Michaelis constant similar to that of **5b** has been reported for the chromogenic analogue Z-Glu(O*p*Np)-Gly-OH towards hTGase 2, with a similar tendency being found when compared to the guinea pig enzyme.[31]

As an experimental setup with 96-well plates was used to simultaneously record spontaneous and enzymatic hydrolyses, there is a time delay between the start of the reaction and the data acquisition. In consequence, those substrate concentrations pipetted at earlier time points might be lower than intended at the start of the measurement. Although this problem was tried to be minimised by pipetting in the right order of substrate concentrations, *i.e.* from low to high, it cannot be completely avoided. The resulting variation of the substrate concentrations is not considered by the classical regression analysis but can be quantified by analysis with numerical integration. Furthermore, application of this method was envisaged to prove whether or not separate recording of spontaneous and enzymatic reactions is of sufficient accuracy to calculate the kinetic parameters for the enzyme-catalysed reactions. For this purpose, the differential equations for the time dependence of [E], [SL], [ESL] and [P] of the classical two-step Michaelis-Menten model extended by the pathway for spontaneous reaction of the acyl donor substrates were formulated (**Scheme 5**) and implemented in the freely available statistical software R (www.R-project.org) (see Experimental section for further details). The kinetic parameters K_m and k_{cat} obtained from nonlinear regressions were then used as initial values for numerical integration of the respective progress curves

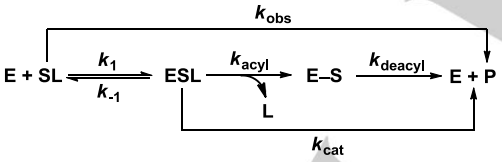

$$\frac{d[E]}{dt} = -k_1[E]\cdot[SL] + k_{-1}[ESL] + k_{cat}[ESL]$$

$$\frac{d[SL]}{dt} = -k_1[E]\cdot[SL] + k_{-1}[ESL] + k_{obs}[SL]$$

$$\frac{d[ESL]}{dt} = k_1[E]\cdot[SL] - k_{-1}[ESL] - k_{cat}[ESL]$$

$$\frac{d[P]}{dt} = k_{obs}[SL] + k_{cat}[ESL]$$

Scheme 5. Kinetic model for substrate hydrolysis by TGase 2 and the respective differential rate laws derived thereof. The kinetic model was prepared according to [32]. For all calculations, rate constants k_{acyl} and k_{deacyl} were combined to rate constant k_{cat} according to the equation: $k_{cat}=k_{acyl}*k_{deacyl}/(k_{acyl}+k_{deacyl})$. Abbreviations used in the Scheme: E: enzyme, SL: Substrate (fluorogenic acyl donor), ESL: initial enzyme-substrate complex, L: coumarin derivative, E-S: acyl enzyme intermediate, P: product.

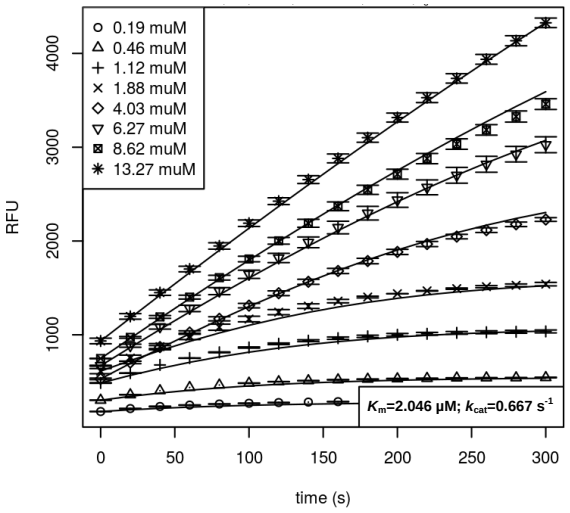

Figure 4. Global fit of progress curves for gpTGase 2-catalysed hydrolysis of acyl donor **5b** at pH=8.0. Concentrations of **5b** at the start of the reaction were 0.5 (○), 1 (△), 2 (+), 3 (×), 5 (◇), 7.5 (▽), 10 (⊠) and 15 µM (✳). Data shown {mean ±standard deviation (±SD)} are of one experiment which was performed in duplicate. The calculated concentrations at the time point of data acquisition are given in the box at the top, left corner. Fitted values for K_m and k_{cat} are given in the box at the bottom, right corner; values calculated from three independent experiments can be found in **Table 2**. Conditions: pH=8.0, 30 °C, 5% DMSO, 500 µM DTT, 3 µg/mL gpTGase 2.

(same data sets as for analysis by nonlinear regression) over the first 300 s. Global fits to the data of one experiment are exemplarily shown for compound **5b** in **Figure 4**. As obvious, a global fit to the experimental data provided the best fit-traces of sufficient quality for all concentrations. In this context, deviations of fit-traces from experimental data are a common problem of the analysis by global fitting as "it is not permissive to even small deviations from ideal progress curves, *i.e*. data should not contain errors and should perfectly adhere to the model".[33] Concerning the calculation of mean values and errors for K_m and k_{cat}, the experiments for each acyl donor were separately analysed by global fitting followed by statistical analysis of the obtained fitted parameters (**Table 2**). Noteworthy, both methods for data analysis gave reasonably comparable results for the values of K_m and k_{cat}. Thus, the approach to get the proportion of enzyme-catalysed reaction within the regression analysis by simple subtraction of the rates for spontaneous reaction from those of the overall reaction seems to be of sufficient accuracy. However, the systematic deviation to lower values for the parameters derived from numerical integration compared to those obtained by nonlinear regression might occur due to the corrected substrate concentrations, which highlights the advantage of the former method.

*Kinetic behaviour of coumarinyl amide **5c***

The distinct spontaneous reaction of the coumarinyl esters requires careful handling of these compounds and a more

complex data evaluation. Therefore, a substrate analogue with similar substrate properties as the coumarinyl esters that is devoid of spontaneous disintegration would be of advantage. A promising way to obtain such a substrate seems to be the exchange of the ester bond between the fluorophore and the peptidic scaffold for an amide bond. Resulting from the investigations done in this study with regards to the substrate properties of different peptidic scaffolds, the dipeptide Z-Glu-Gly-OH seems to be most suitable for performing such a substitution. Therefore, compound **5c** bearing AMC attached at the carboxyl group of the glutamate side chain was synthesised. Indeed, no spontaneous release of AMC was observed in the absence of TGase 2 (see Discussion S6 in Supporting Information). Surprisingly, initial investigations of **5c** towards its enzymatic hydrolysis and aminolysis also revealed no TGase 2-mediated release of AMC (see Discussion S6 in Supporting Information) which was also observed for the γ-Abu-derived coumarinyl amide **2c** as mentioned above. This was not expected for the coumarinyl amides, as TGase 2 is actually specialised in the interconversion of amide bonds. Moreover, compared to aliphatic amides, aryl amides should be easier to cleave from a merely electronic point of view due to the less pronounced double bond character of the amide bond adjacent to an aromatic ring system. This situation can also result in faster reactions catalysed by enzymes involving acyl enzyme intermediates such as the serine protease trypsin, for which nitroanilide substrates exhibited greater performance constants than the corresponding primary amides.[34] However, results comparable to those herein were obtained from studies on chromogenic and fluorogenic acyl donor substrates for factor XIIIa. Rapid cleavage of the aryl amide bond to release *p*-nitroaniline was observed by factor XIIIa whereas the conversion of corresponding AMC derivatives was considerably slower. In contrast, the conversion of both aryl amide-based substrates by TGase 2 was negligible.[35] To obtain further information on the kinetic behaviour of compound **5c**, the gpTGase 2-catalysed hydrolysis of coumarinyl ester **5b** in the presence of increasing concentrations of **5c** was studied (see Discussion S6 in Supporting Information). Judged from these results, **5c** has an inhibitory effect on the enzymatic hydrolysis of **5b**. A detailed kinetic analysis of the recorded data along with the respective discussion can be found in Discussion S6 in Supporting Information. In summary, the obtained results indicate that the coumarinyl amide seems most likely to act as a linear (β=0) mixed, predominantly specific (1<α<∞) inhibitor according to the systematic classification of enzyme-modifier interactions suggested by Baici[36] [1] Considering the high structural similarity between the coumarinyl ester **5b** and the coumarinyl amide **5c**, the observed pronounced competitive component for inhibition of gpTGase 2 by **5c** is comprehensible. On the other hand, binding of **5c** to sites distinct from the active site also appears to be reasonable if one considers the multidomain structure of the TGase 2 protein, which is known to harbour several binding sites for various ligands apart from the catalytic centre. As a representative example, Yi *et al.* recently reported on an acylideneoxindole derivative which also exhibits inhibitory potency of noncompetitive character on the transamidase activity.[37]

TGase 2-catalysed aminolyses

As transglutaminases are specialised in the catalysis of transamidation reactions to primary amine-derived acyl acceptors, the kinetics of TGase 2-catalysed aminolysis of the glutamate-derived acyl donors was investigated in addition to hydrolysis using aminoacetonitrile as amine substrate.

The corresponding kinetic data are shown in **Table 3**, with the parameters K_m and k_{cat} being of apparent character (see Discussion S7 in Supporting Information for detailed explanation). Nevertheless, K_m^{app} and k_{cat}^{app} can be used to evaluate the different substrates as they were determined under identical conditions at an aminoacetonitrile concentration of 400 µM, which warrants excess over the respective acyl donor. However, the calculated ratios of k_{cat}^{app} over K_m^{app} represent the true performance constants for aminolysis, as V_{max}/K_m is independent of the concentrations of either substrate, if the enzyme-catalysed reaction adheres to a ping-pong mechanism,[38] which is true for TGase 2.[39,32b] The dependence of the kinetic parameters K_m^{app} and k_{cat}^{app} on substrate structure followed the trends observed for hydrolysis; however, the values are considerably greater (**Table 3** and **Figure 5**). This result is reasonable as the deacylation step with aminoacetonitrile as acyl acceptor substrate proceeds considerably faster compared to water.[20b] As the Michaelis constant is the ratio of the sum of the rate constants that describe the steps of disintegration of the Michaelis complex ($k_{-1}+k_{cat}$) divided by the second-order rate constant for the association of free enzyme and substrate (k_1),

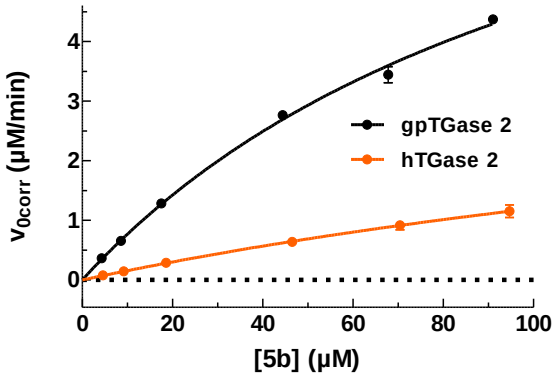

Figure 5. gpTGase 2- and hTGase 2-catalysed aminolysis of acyl donor **5b** at pH=8.0. Plots of v_{0corr}=f([**5b**]) with nonlinear regressions (–) using the Michaelis-Menten equation III. Data shown are mean values ±SEM of 3 separate experiments, each performed in duplicate. When not apparent, error bars are smaller than the symbols. Conditions: pH=8.0, 30 °C, 5% DMSO, 500 µM TCEP, 400 µM aminoacetonitrile, 0.3 µg/ml of either gpTGase 2 or hTGase 2

[1] According to that system for classification of enzyme-modifier interactions, competitive inhibition is referred to as specific inhibition whereas noncompetitive inhibition is referred to as catalytic inhibition.

Table 3. Kinetic parameters for the TGase 2-catalysed aminolyses of the acyl donors **3**-**6** at pH=8.0 using aminoacetonitrile (400 µM) as acyl acceptor.

	Regression analysis			Numerical integration		
	K_m^{app} (µM)	k_{cat}^{app} (s^{-1})	k_{cat}/K_m ($M^{-1}*s^{-1}$)	K_m^{app} (µM)	k_{cat}^{app} (s^{-1})	k_{cat}/K_m ($M^{-1}*s^{-1}$)
cpd	**gpTGase 2**					
3	148 (52)	6.26 (1.26)	42,300	99.5 (13.9)	4.28 (0.17)	43,000
4	140 (24)	3.05 (0.39)	21,800	135 (19)	2.66 (0.29)	19,600
5a	120 (12)	47.1 (3.6)	393,000	82.9 (7.6)	34.3 (1.1)	414,000
5b	121 (8)	52.7 (1.7)	436,000	82.1 (3.6)	35.7 (0.5)	435,000
6a*	236	29.7	126,000	249 (104)	29.8 (9.5)	120,000
6b*	238	70.4	296,000	150 (21)	45.6 (4.2)	304,000
hTGase 2						
5b*	252	22.7	90,100	171 (51)	16.7 (4.6)	97,800

For details on calculation of the kinetic parameters see Experimental section. Data shown are mean values (±SEM) of 3 separate experiments, each performed in duplicate. Active concentrations of TGase 2 from guinea pig liver (E_T=3.16 nM for **5**-**6** and 21.0 nM for **3** and **4**) and human TGase 2 (E_T=3.08 nM) were calculated from activity data of Zedira® or determined by active site titration as recently described,[30] respectively. *Data obtained by the method of Cornish-Bowden and Eisenthal.[40]

the values for K_m have to increase as deacylation becomes faster. This relationship results in apparent K_m values that are approximately up to 100-fold higher than the Michaelis constants for hydrolysis. Consequently, the increased single parameters K_m and k_{cat} compensate each other when the performance constants are calculated, with the latter ones being of similar value to those of the hydrolysis reaction. As in the case of hydrolysis, **5b** was revealed to be the most efficient substrate with a performance constant of 436,000 $M^{-1}s^{-1}$ towards TGase 2 from guinea pig, while its reaction with aminoacetonitrile catalysed by the human enzyme was much slower (k_{cat}/K_m=90,100 $M^{-1}s^{-1}$). Exemplarily for compound **5b**, additional investigations were performed that allowed for estimation of its true kinetic parameters k_{cat} and K_m (see Discussion S7 in Supporting Information). Due to the high values of K_m^{app}, measurements at higher acyl donor concentrations were necessary, which in turn resulted in higher rates of spontaneous reactions. For regression analysis, the initial substrate concentrations were therefore corrected according to the time delay between preparation of the reaction mixture and start of reaction by addition of the enzyme. Furthermore, fitting the Michaelis-Menten equation to the experimental data yielded unreliable results in the case of compounds **6a** and **6b** as well as for **5b** towards hTGase 2 due to the high K_m^{app} values and limitations in substrate concentration. For this reason, evaluation of these data sets was performed by the method of Cornish-Bowden and Eisenthal (see Figures S14 and S15 in Supporting Information).[41,40] Results of data analysis by numerical integration are in good agreement with those obtained by regression analysis (**Table 3**). Exceptions can be observed for the K_m^{app} values of **6b** towards gpTGase 2 and **5b** towards the human enzyme obtained from the different methods of data analysis. These discrepancies might result from the mentioned problem that in those cases substrate concentrations were restricted to values $<K_m^{app}$. In this context, it might seem that the improved solubility of the glutamate-derived acyl donors compared to the γ-Abu derivatives is of minor importance as substrate concentrations $<K_m^{app}$ could also be investigated for the latter compounds. However, the observed increase in K_m upon changing the acyl acceptor from water to aminoacetonitrile, which was also demonstrated for compound **2a** by Gillet *et al.*,[12] implicates that substrate concentrations for **2a** and **2b** would be restricted to even lower values in relation to K_m^{app}. Even though we refrained from attempts to characterise **2a** and **2b** with regards to their enzymatic aminolyses, it can be concluded that the increased solubility of the glutamate-derived acyl donors may indeed be beneficial, since a broader concentration range is available for these substrates.

To prove the occurrence of TGase 2-catalysed transamidation in the presence of competing spontaneous reaction pathways, the assay mixture containing **5b** and aminoacetonitrile was analysed by RP-HPLC and ESI-MS, which confirmed the formation of the expected corresponding cyanomethyl amide (see Figure S16 in Supporting Information).

Application of acyl donor 5b for the kinetic characterisation of amine substrates and inhibitors

Characterisation of amine substrates

One motivation behind this study was to establish an activity assay for TGase 2 that allows for the kinetic evaluation of both amine-based acyl acceptor substrates and irreversible inhibitors of this enzyme. After identifying fluorogenic acyl donor

substrates with suitable properties, we therefore aimed to prove their applicability for that purpose. As **5b** exhibited the most optimal substrate properties among the studied analogues, the following investigations were performed with this acyl donor substrate. Since *N*-(biotinyl)cadaverine is often applied as amine substrate to determine the activity of TGase 2,[42] this compound was selected in addition to aminoacetonitrile to verify the applicability of the novel fluorogenic acyl donors for the kinetic characterisation of primary amines as acyl acceptors (for synthesis see Discussion S8 in Supporting Information).

The two primary amines were evaluated regarding their kinetic parameters K_m and k_{cat}, which were determined at a constant concentration of **5b** (100 µM). As this concentration of the acyl donor substrate is not sufficient to fulfil the condition K_m(**5b**)<<[**5b**], neither for the guinea pig nor for the human TGase 2, the parameters K_m and k_{cat} are of apparent character and therefore denoted as K_m^{app} and k_{cat}^{app}. The Michaelis-Menten plots are shown in **Figure 6** and the calculated parameters are summarised in **Table 4**.

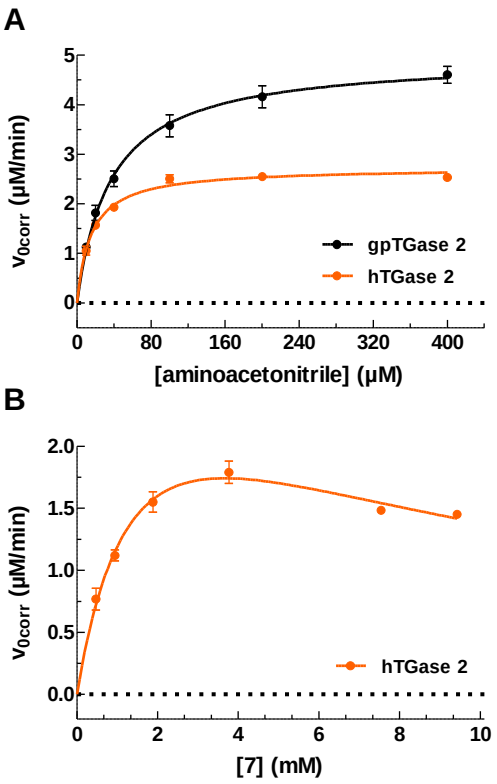

Figure 6. gpTGase 2- and hTGase 2-catalysed incorporation of different amines into compound **5b**. Plots of v_{0corr}=f([amine]) with nonlinear regressions (–) using equation III (Michaelis-Menten equation) for aminoacetonitrile (**A**) and equation IV (substrate inhibition) for *N*-(biotinyl)cadaverine (**7**) (**B**). Data shown for aminoacetonitrile are mean values ±SEM of 3 separate experiments, each performed in duplicate. Data shown for *N*-(biotinyl)cadaverine (**7**) are mean values ±SD of 1 experiment, which was performed in duplicate. When not apparent, error bars are smaller than the symbols. Conditions: pH=8.0, 30 °C, 5% DMSO, 100 µM acyl donor **5b**, 500 µM TCEP, 0.3 µg/mL gpTGase 2 or 0.6 µg/mL hTGase 2.

For aminoacetonitrile, values for K_m^{app} and k_{cat}^{app} of 37 µM and 27 s^{-1}, respectively, were determined on the guinea pig enzyme. On human TGase 2, the K_m^{app} of aminoacetonitrile was slightly lower, whereas its k_{cat}^{app} value decreased to a larger extent, which resulted in a somewhat reduced performance constant. To gain insights into the true Michaelis constant of aminoacetonitrile, K_m^{app} values were determined at four different concentrations of the fluorogenic acyl donor **5b**, which concomitantly provided insight into the true K_m value of **5b**. The detailed analysis of these kinetic data along with the respective discussion is given in Discussion S7 in Supporting Information.

Since *N*-(biotinyl)cadaverine (**7**) has been frequently used as molecular tool to study TGase 2 at the cellular level, the utility of **5b** to evaluate amine-based acceptor substrates was demonstrated for this compound on human TGase 2. In contrast to aminoacetonitrile, compound **7** displayed a K_m^{app} value in the millimolar range. This dramatical difference in the K_m^{app} values reflects the differing basicities of aminoacetonitrile and **7**. While the amino group of aminoacetonitrile exhibits a pK_a value of 5.6 for the conjugate ammonium ion, the corresponding value of **7** is in the range of 10-11.[20b] As the deacylation of acyl donor-derived TGase 2 thiolester intermediates can only be effected by unprotonated amines,[43] the free substrate concentration of **7** is much lower than that of aminoacetonitrile. Furthermore, Brønsted plots for a series of primary amines as acyl acceptor substrates of varying basicity indicated a correlation between the performance constants of TGase 2-catalysed transamidation and their pK_a values.[20b] It should be noted that the k_{cat}^{app} value of **7** on human TGase 2 is in the same range as that of aminoacetonitrile and its rate *versus* concentration plot indicates substrate inhibition (**Figure 6B**). The latter finding is in accordance with the behaviour of the analogous fluorescent acyl acceptor *N*-(dansyl)cadaverine, which displayed substrate

Table 4. Kinetic parameters of different amines as acyl acceptors on gpTGase 2 at pH=8.0

amine	K_m^{app} (mM)	k_{cat}^{app} (s^{-1})	k_{cat}/K_m ($M^{-1}*s^{-1}$)
	gpTGase 2		
aminoacetonitrile	0.037 (0.002)	27.0 (1.8)	736,000
	hTGase 2		
aminoacetonitrile	0.015 (0.001)	7.39 (0.15)	489,000
N*-(biotinyl)cadaverine (7)	1.67	9.02	5,410

For details on calculation of the kinetic parameters see Experimental section. Data shown are mean values (±SEM) of 1 (**7**) or 3 (aminoacetonitrile) separate experiments, each performed in duplicate. Active concentrations of TGase 2 from guinea pig liver (E_T=3.16 nM) and human TGase 2 (E_T=6.16 nM) were calculated from activity data of Zedira® or determined by active site titration as recently described,[30] respectively. * K_I=8.04 mM

inhibition for TGase 2-catalyzed transamidation in case of both the guinea pig and the human enzyme. This phenomenon has been attributed to the formation of an unproductive complex of the acyl acceptor substrate and free TGase 2.[32a] Moreover, substrate inhibition in enzyme-catalysed group-transferring reactions by the substrate that is devoid of the transferred group is very common due to its premature binding to the free enzyme.[44]

Characterisation of irreversible inhibitors

The evaluation of enzyme inhibitors for the purposes of drug discovery projects is often based on kinetic assays. This is particularly valid for inhibitors that interact with enzymes in an irreversible manner. Therefore, we aimed to validate the usefulness of the developed fluorogenic TGase 2 substrates for the characterisation of inhibitors exemplarily for substrate **5b** with the established irreversible TGase 2 inhibitors iodoacetamide and the recently reported selective N^{ε}-acryloyllysine derivative **8** (**Scheme 6**).[14]

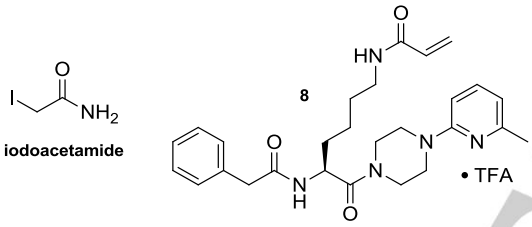

Scheme 6. Structures of iodoacetamide and acrylamide **8**

Inhibition studies with iodoacetamide for the TGase 2-catalysed hydrolysis of **5b** at pH=8.0 were problematic as the product-release progress plots were curved even in the absence of inhibitor due to substrate depletion (data not shown). To obtain steady-state conditions over a broad time window, both reducing the amount of enzyme and increasing the substrate concentration was impossible due to the susceptibility of **5b** to spontaneous hydrolysis. Therefore, the conversion of **5b** was decelerated by reducing the pH from 8.0 to 6.5, which slowed down the rate of the spontaneous reaction to less than 5%, whereas the enzymatic hydrolysis was reduced to a much less extent. These modified conditions resulted in linear progress curves for concentrations of **5b** greater than 20 µM for both gpTGase 2 and hTGase 2 over a time window of 900 s. This linearity ensures the absence of substrate depletion, which is of crucial importance for the correct kinetic evaluation of time-dependent enzyme inhibition.[45] The fluorescence coefficients of 4-methylumbelliferon and the Michaelis-Menten parameters were determined for pH=6.5 (**Figure 7**, **Table 5** and Figure S17 in Supporting Information).

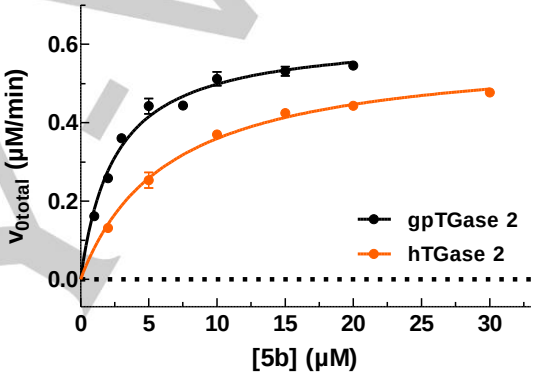

Figure 7. gpTGase 2- and hTGase 2-catalysed hydrolysis of acyl donor **5b** at pH=6.5. Plots of v_{0total}=f([**5b**]) with the nonlinear regressions (–) using equation III (Michaelis-Menten equation). Data shown are mean values ±SEM of 3 separate experiments, each performed in duplicate. When not apparent, error bars are smaller than the symbols. Conditions: pH=6.5, 30 °C, 5% DMSO, 500 µM TCEP, 3 µg/ml of either gpTGase 2 or hTGase 2.

Table 5. Kinetic parameters for the TGase 2-catalysed hydrolyses of the acyl donor **5b** at pH=6.5 and 30 °C

	Regression analysis			Numerical integration		
	K_m (µM)	k_{cat} (s^{-1})	k_{cat}/K_m ($M^{-1}*s^{-1}$)	K_m (µM)	k_{cat} (s^{-1})	k_{cat}/K_m ($M^{-1}*s^{-1}$)
cpd	**gpTGase 2**					
5b	2.53 (0.18)	0.33 (0.01)	132,000	2.67 (0.20)	0.34 (0.01)	129,000
hTGase 2						
5b	6.60 (1.06)	0.32 (0.02)	50,300	5.78 (1.03)	0.32 (0.02)	57,600

For details on calculation of the kinetic parameters see Experimental section. Data shown are mean values (±SEM) of 3 separate experiments, each performed in duplicate. Active concentrations of TGase 2 from guinea pig liver (E_T=31.6 nM) and human (E_T=30.8 nM) were calculated from activity data of Zedira® or determined by active site titration as recently described,[30] respectively. k_{obs} value for the spontaneous reaction of **5b** at pH=6.5 and 30 °C in the presence of TCEP was determined to be 0.70 ± 0.03×10^{-3} min^{-1}.

On gpTGase 2, the performance constants were reduced to 132,000 $M^{-1}s^{-1}$, *i.e.* to less than half of the value determined at pH=8.0 (**Table 2**), which is caused by a reduction in k_{cat}, while K_m was unaffected by the change of pH. A similar trend was observed for the human enzyme. Data analysis by numerical integration confirmed these results for the two TGase orthologues.

The reduction of pH in the assay medium enabled the analysis of inhibition by iodoacetamide under the formalism of slow-binding inhibition (equation V).[46] Iodoacetamide has been shown to inactivate TGase 2 irreversibly by alkylation of the active-site thiol Cys 277.[47] Irreversible enzyme inactivation usually results in steady-state rates that are equal to zero independent of inhibitor concentration. However, as substrate **5b** continues to react in the presence of completely inactivated enzyme, we use v_s as open parameter in equation V to take into account the remaining spontaneous reaction after completed enzyme inhibition. Replotting the obtained pseudo-first order rate constants k_{obs} against the inhibitor concentration and linear regression of the resulting line provided the ratio k_{obs}/[I] as slope. Correction of that value by the factor 1+[S]/K_m gave a value of 55,600 $M^{-1}s^{-1}$ for the second-order inactivation constant k_{inact}/K_I towards the guinea pig enzyme, with a similar value being obtained towards hTGase 2 (**Table 6**).[46,48] In contrast to the k_{obs} values, which linearly increased with rising inhibitor concentration, the initial velocities did not systematically vary when the iodoacetamide concentration was increased (see Figure S18 in Supporting Information). This finding indicates a one-step mechanism for inactivation of both guinea pig and human TGase 2 by iodoacetamide and suggests that no stable non-covalent enzyme-inhibitor complex is formed prior to the inactivating alkylation step. This result is in agreement with observations for the inactivation of factor XIIIa by iodoacetate[35a] and can be rationalised considering that this small inhibitor molecule does not provide many contact points for non-covalent interactions.

To characterise a pharmaceutically more relevant inhibitor with the established assay, compound **8** was investigated with regards to its interaction with guinea pig and human TGase 2. The N^6-acryloyllysine derivative **8** was prepared according to the published procedure with slight modifications;[14] details on its synthesis will be reported in the context of a follow-up study. The results of the kinetic characterisation of **8** are included in **Table 6**. Towards the guinea pig enzyme, compound **8** exhibited a second-order inactivation constant of 1,230 $M^{-1}s^{-1}$. No systematic variation of the initial velocities with increasing inhibitor concentration was discernible, which led to the conclusion that inactivation of gpTGase 2 by **8** follows a one-step mechanism. Notably, the situation is obviously different for the human enzyme (**Figure 8**). Here, the value for k_{inact}/K_I was approximately five-fold higher than that for the guinea pig orthologue and the initial velocities, v_i, hyperbolically decreased with increasing inhibitor concentration. This observation indicates the formation of a rapid-equilibrium non-covalent complex between acrylamide **8** and hTGase 2 prior to the inactivation step, for which a dissociation constant K_i of 5.73 µM was calculated from the plot of v_i *versus* [I] (see Figure S19 in Supporting Information). On the basis of the double reciprocal plot of 1/k_{obs} *versus* 1/[I] (**Figure 8B**) it was possible to obtain the isolated value for the first-order inactivation constant k_{inact} (21 min^{-1}) describing the transition of the initial non-covalent enzyme-inhibitor complex to the final covalent complex. Based on this value, K_I was calculated to be 68.7 µM. The meaning of this value is distinctly different from K_i as it represents a merely kinetic parameter that signifies the inhibitor concentration at which the inactivation proceeds with half the maximal rate in the absence of substrate.[46]

Usually, irreversible enzyme inhibition results in steady state rates equal to zero, whereas in the present case these rates are different to zero as substrate conversion continues after completed enzyme inactivation due to spontaneous hydrolysis. To take this fact into account for the kinetic analysis of TGase 2 inhibition, the kinetic parameters were independently determined by numerical integration.[33,23b] For this purpose, differential equations were formulated on the basis of **Scheme 7** and implemented into the statistical software R. The series of progress curves in the absence and presence of different inhibitor concentrations were globally fitted, which provided values for k_{inact}/K_I that are essentially similar to those obtained by conventional regression analysis (**Table 6**).

$$E + I \underset{k_{-2}}{\overset{k_2}{\rightleftharpoons}} EI \xrightarrow{k_{inact}} E\text{-}I$$

$$\frac{d[I]}{dt} = -k_2[E]\cdot[I] + k_{-2}[EI]$$

$$\frac{d[EI]}{dt} = -k_{-2}[EI] + k_2[E]\cdot[I] - k_{inact}[E\text{-}I]$$

$$\frac{d[E\text{-}I]}{dt} = k_{inact}[EI]$$

Scheme 7. Kinetic model for the two-step irreversible inhibition of TGase 2 and the respective differential rate laws derived thereof. For the case that the ratio $k_{-2}/k_2=K_i$ is high, the concentration of the initial non-covalent enzyme-inhibitor complex becomes negligible and, in consequence, the two-step mechanism for irreversible inhibition simplifies to a one-step mechanism. Abbreviations used in the Scheme: E: enzyme, I: inhibitor, EI: initial enzyme-inhibitor complex, E-I: covalent enzyme inhibitor complex.

Thus, it can be concluded that the common analysis using integrated rate equations and subsequent evaluation of the obtained data yields reliable parameters to describe the inhibitory potency. Taken together, the obtained results demonstrate the suitability of the established assay for the kinetic characterisation of TGase 2 inhibitors.

Conclusions

The recently described acyl donor substrate **2a** and compounds derived thereof which release fluorescent coumarins upon enzymatic conversion appear to be attractive substrates for the fluorimetric assay of TGase 2. However, both **2a** and its methyl-substituted analogue **2b** proved to be prone to aggregation in aqueous media, which can hamper detailed kinetic investigations depending on the particular conditions and intended application purposes. Therefore, analogues based on small glutamate-containing peptides were synthesised using a solid-phase approach and demonstrated to be soluble in assay medium up to concentrations of 250 µM. This remarkably

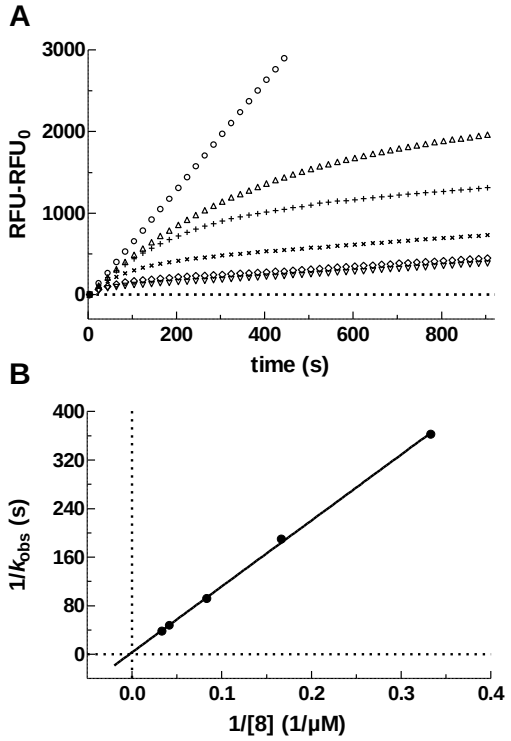

Figure 8. Kinetic characterisation of acrylamide **8** towards hTGase 2 using acyl donor **5b**. **A**) Typical time courses of the hTGase 2-catalysed hydrolysis of **5b** in the presence of different concentrations of acrylamide **8** (0 µM (○), 3 µM (△), 6 µM (+), 12 µM (×), 24 µM (◇) and 30 µM (▽)) in the presence of 30 µM (~4.5×K_m) of acyl donor **5b**; **B**) Double reciprocal plot ($1/k_{obs}$=f(1/[**8**])) with linear regression to the data for determination of k_{inact} and K_I; Conditions: pH=6.5, 30 °C, 5% DMSO, 500 µM TCEP, 3 µg/mL of hTGase 2.

Table 6. Kinetic parameters for the irreversible TGase 2 inhibitors iodoacetamide and acrylamide **8** at pH=6.5 and 30 °C

	Regression analysis	Numerical integration
	k_{inact}/K_I ($M^{-1}s^{-1}$)	k_{inact}/K_I ($M^{-1}s^{-1}$)
inhibitor	**gpTGase 2**	
iodoacetamide	55,600 (8,890)	38,400 (566)
acrylamide 8	1,230 (139)	789 (9)
	hTGase 2	
iodoacetamide	64,000 (4,040)	43,500 (2,770)
acrylamide 8*	5,110 (68)	5,100 (155)

* K_I=5.73 µM (0.77), K_I=68.7 µM (24.2), k_{inact}=21.0 s^{-1} (7.1)

For details on the calculation of the kinetic parameters see Experimental section. Inhibition experiments on gpTGase 2 and hTGase 2 were performed in the presence of 25 µM (~10×K_m) and 30 µM (~4.5×K_m) of acyl donor **5b**, respectively. Data shown are mean values (±SEM) of 2 separate experiments, each performed in duplicate.)

improved water solubility allowed for the extensive kinetic characterisation of the newly designed substrates regarding their TGase 2-catalysed hydrolysis and aminolysis by both conventional regression analysis as well as numerical integration. In addition, their spontaneous reactivity under assay conditions was studied in detail, which has revealed a significant contribution of spontaneous thiolysis in the presence of DTT to the overall rate of spontaneous disintegration, amongst other findings. This result suggests that TCEP should be used as antioxidant instead of DTT.

The influence of the fluorogenic leaving group on the kinetic properties was investigated. Substrates **5b** and **6b** containing 7-hydroxy-4-methylcoumarin attached to the γ-carboxylic group of the Glu residue showed superior kinetic properties over their unsubstituted counterparts **5a** and **6a**; analogous amides (**2c**, **5c**) containing 7-amino-4-methylcoumarin are not accepted as substrates. Z-Glu(HMC)-Gly-OH (**5b**) exhibited the most optimal substrate properties among the synthesised compounds, with performance constants of 300,000 and 436,000 $M^{-1}s^{-1}$ determined for the gpTGase 2-catalysed hydrolysis and aminolysis at pH=8.0, respectively. Therefore, **5b** was selected for the exemplary kinetic characterisation of amine-based acyl-acceptor substrates and irreversible inhibitors. The determination of performance constants at pH=8.0 was demonstrated for aminoacetonitrile and *N*-(biotinyl)cadaverine as representative primary amine substrates on both guinea pig and human TGase 2. Inhibitor characterisation was based on monitoring and analysing the TGase 2-catalysed hydrolysis of **5b** at pH=6.5, which resulted in reliable second-order inactivation constants for iodoacetamide and compound **8** towards both the guinea pig and human enzyme.

Furthermore, this study confirmed compounds **2a** and **2b** as potentially suitable substrates for fluorimetric activity determination of TGase 2. Considering their reduced susceptibility against spontaneous reaction in comparison to that of the glutamate-derived analogues introduced herein, **2a** and **2b** might be more advantageous for assaying cellular TGase 2 activities.[12]

Taken together, the results of this study prove compound **5b** to be a powerful fluorogenic substrate of guinea pig and human TGase 2. Therefore, this compound allows for robust assay methods to identify and characterise molecules capable of targeting TGase 2 for therapeutic inhibition and molecular imaging, even though its susceptibility to spontaneous decay may stimulate further developments towards fluorogenic substrates for this important enzyme.

Experimental Section

General

All commercial reagents and solvents were used without further purification unless otherwise specified. Melting points were determined on a Galen III Boetius apparatus from Cambridge Instruments. Nuclear magnetic resonance spectra were recorded on a Varian Unity 400 MHz or an Agilent Technologies 400 MR spectrometer. Spectra were processed by using the programme MestreNova (version 6.1.1-6384).[49] NMR chemical shifts were referenced to the residual solvent resonances relative to tetramethylsilane (TMS). Mass spectra (ESI) were obtained on a Micromass Quattro LC or a Waters Xevo TQ-S mass spectrometer each driven by the Mass Lynx software. Elemental analysis was

performed on a LECO CHNS-932 apparatus. Determination of the resin loading was performed on a Thermo Scientific Helios á UV/Vis spectrophotometer.

Chromatography

Thin-layer chromatography (TLC) was performed on Merck silica gel F-254 aluminium plates with visualisation under UV (254 nm) and/or staining with a 0.1% (m/V) ninhydrin solution in ethanol. Preparative column chromatography was carried out on Merck silica gel (mesh size 230–400 ASTM) with solvent mixtures as specified for the particular compounds. Analytical and Preparative HPLC of compounds **2**-**7** were performed on a Varian Prepstar system equipped with UV detector (Prostar, Varian) and automatic fraction collector Foxy 200. Two Microsorb C18 60-8 columns (Varian Dynamax 250 × 4.6 mm and 250 × 21.4 mm) were used as the stationary phases for analytical and preparative HPLC, respectively. A binary gradient system of 0.1% CF_3COOH/water (solvent A) and 0.1% CF_3COOH/CH_3CN (solvent B) at a flow rate of 1 mL/min or 10 mL/min served as the eluent. With regards to analytical HPLC, the programme for elution of compounds **2**-**6** was as follows: 0-3 min 90% A, 3-25 min gradient to 90% B, 25-35 min 90% B, 35-36 min gradient back to 90% A, 36-40 min 90% A; whereas for compound **7** the following elution regime was used: 0-5 min 95% A, 5-25 min gradient to 95% B, 25-30 min 95% B, 30-31 min gradient back to 95 % A, 31-35 min 95% A. With regards to preparative HPLC, the conditions for the gradient elution of compounds **2**-**6** are as follows: 0-3 min 90% A, 3-25 min gradient to 90% B, 25-30 min 90% B, 30-31 min gradient back to 90% A, 31-35 min 90% A; whereas for compound **7**: 0-7 min 90% A, 7-22 min gradient to 80% B, 22-30 min 80% B, 30-31 min gradient back to 90% A, 31-35 min 90% A. HPLC for investigating the spontaneous reactivity of compound **5b** was carried out on a device consisting of a Merck Hitachi L7100 gradient pump combined with a Jasco DG2080 4-line degasser with UV detection by a Merck Hitachi L7450 diode array detector. The system was operated by the D-700 HSM software using a Merck Hitachi D7000 interface. A Luna C18 5 µm column (Phenomenex, 250 × 4.6 mm) served as stationary phase. The following elution programme (binary gradient system as detailed above, flow rate 1 mL/min) was run to separate the components: 0-3 min 80% A, 3-25 min gradient to 70% B, 25-26 min gradient to 95% B, 26-30 min 95% B, 30-35 min gradient back to 80% A, 35-40 min 80% A.

Analytical data for the glutamate-derived fluorogenic acyl donors

Z-L-Glu(HMC)-OH (3)

The synthesis using HMC yielded 67 mg (30%) of **3** as a yellow oil. As **3** tends to decomposition in the isolated state, this compound should be stored below 0 °C. **^{1}H-NMR (DMSO-d_6):** δ=7.81 (d, $^3J_{H,H}$=8.7 Hz, 1H, H–5 of coumarin), 7.70 (d, $^3J_{H,H}$=8.3 Hz, 1H, NH), 7.39–7.27 (m, 5H, H_{Phenyl}), 7.25 (d, $^4J_{H,H}$=2.1 Hz, 1H, H–8 of coumarin), 7.17 (dd, $^3J_{H,H}$=8.6 Hz, $^4J_{H,H}$=2.2 Hz, 1H, H–6 of coumarin), 6.39 (d, $^4J_{H,H}$=1.1 Hz, 1H, H–3 of coumarin), 5.10–5.01 (m, 2H, CH_2O of Z), 4.15–4.07 (m, 1H, $C_\alpha H$ of Glu), 2.78–2.65 (m, 2H, $C_\gamma H_2$ of Glu), 2.44 (d, $^4J_{H,H}$=1.0 Hz, 3H, CH_3), 2.20–2.09 (m, 1H, $C_\beta H$*H* of Glu), 2.01–1.89 (m, 1H, C_β*H*H of Glu); **^{13}C-NMR (DMSO-d_6):** δ=173.26, 170.75, 159.60, 156.19, 153.49, 152.95, 152.80, 136.92, 128.32, 127.81, 127.72, 126.40, 118.38, 117.53, 113.73, 110.07, 65.51 (CH_2O of Z), 52.84 (C_α of Glu), 30.24, 25.91, 18.17 (CH_3); ESI-MS (ESI+) *m/z*: calc. for $C_{23}H_{22}NNaO_8$ $[M+Na]^+$, 462.12, found 462.1; Elemental analysis: calc. for $C_{23}H_{21}NO_8$, C, 62.87; H, 4.82; N, 3.19; found C, 60.45; H, 5.14; N, 3.14.

Z-L-Phe-L-Glu(HMC)-OH (4)

The synthesis using HMC yielded 99 mg (36%) of **4** as a white solid. As **4** tends to decomposition in the isolated state, this compound should be stored below 0 °C. **^{1}H-NMR (DMSO-d_6):** δ=8.41 (d, ^3J=8.0 Hz, 1H, NH of Glu), 7.81 (d, ^3J=8.6 Hz, 1H, H–5 of coumarin), 7.53 (d, ^3J=8.6 Hz, 1H, NH of Phe), 7.36–7.15 (m, 12H, H_{Phenyl} and H–6,8 of coumarin), 6.39 (s, 1H, H–3 of coumarin), 4.95–4.87 (m, 2H, CH_2O of Z), 4.45–4.36 (m, 1H, $C_\alpha H$), 4.36–4.28 (m, 1H, C_α), 3.02 (dd, ^2J=13.8 Hz, ^3J=3.8 Hz, 1H, $C_\beta H$*H* of Phe), 2.81–2.69 (m, 3H, C_β*H*H of Phe and $C_\gamma H_2$ of Glu), 2.44 (s, 3H, CH_3), 2.26–2.14 (m, 1H, $C_\beta H$*H* of Glu), 2.00–1.88 (m, 1H, C_β*H*H of Glu); **^{13}C-NMR (DMSO-d_6):** δ=172.94, 171.91, 170.78, 159.60, 155.90, 153.50, 152.95, 152.87, 138.08, 136.89, 129.20, 128.21, 128.04, 127.63, 127.42, 126.38, 126.25, 118.41, 117.52, 113.72, 110.11, 65.21 (CH_2O of Z), 56.10, 50.69, 37.26, 29.86, 26.10, 18.17 (CH_3); ESI-MS (ESI+) *m/z*: calc. for $C_{32}H_{31}N_2O_9$ $[M+H]^+$, 587.20, found 587.3; Elemental analysis: calc. for $C_{32}H_{30}N_2O_9$, C, 65.52; H, 5.15; N, 4.78; found C, 63.94; H, 5.23; N, 4.81.

Z-L-Glu(HC)-Gly-OH (5a)

The synthesis using HC yielded 34 mg (35%) of **5a** as a white solid. **^{1}H-NMR (DMSO-d_6):** δ=8.32 (t, ^3J=5.9 Hz, 1H, NH of Gly), 8.07 (d, ^3J=9.3 Hz, 1H, H–4 of coumarin), 7.76 (d, ^3J=8.5 Hz, 1H, H–5 of coumarin), 7.57 (d, ^3J=8.3 Hz, 1H, NH of Glu), 7.39–7.25 (m, 6H, H_{Phenyl} and H–8 of coumarin), 7.15 (dd, ^3J=8.4 Hz, ^4J=2.2 Hz, 1H, H–6 of coumarin), 6.48 (d, ^3J=9.6 Hz, 1H, H–3 of coumarin), 5.10–4.98 (m, 2H, CH_2O of Z), 4.22–4.13 (m, 1H, C_α of Glu), 3.83 (dd, ^2J=17.5 Hz, ^3J=5.9 Hz, 1H, $C_\alpha H$*H* of Gly), 3.73 (dd, ^2J=17.5 Hz, ^3J=5.6 Hz, 1H, C_α*H*H of Gly), 2.78–2.64 (m, 2H, $C_\gamma H_2$ of Glu), 2.12–2.01 (m, 1H, $C_\beta H$*H* of Glu), 1.99–1.86 (m, 1H, C_β*H*H of Glu); **^{13}C-NMR (DMSO-d_6):** δ=171.54, 171.07, 170.85, 159.68, 155.94, 154.05, 152.82, 143.81, 136.89, 129.28, 128.30, 127.77, 127.69, 118.61, 116.64, 115.52, 110.08, 65.53 (CH_2O of Z) 53.49, 40.67, 30.01, 27.00; ESI-MS (ESI+) *m/z*: calc. for $C_{24}H_{23}N_2O_9$ $[M+H]^+$, 483.14, found 483.1; Elemental analysis: calc. for $C_{24}H_{22}N_2O_9$, C, 59.75; H, 4.60; N, 5.81; found C, 58.28; H, 4.58; N, 5.75.

Z-L-Glu(HMC)-Gly-OH (5b)

The synthesis using HMC yielded 63 mg (26%) of **5b** as a white solid. **^{1}H-NMR (DMSO-d_6):** δ=12.58 (s, 1H, COOH), 8.32 (t, ^3J=5.8 Hz, 1H, NH of Gly), 7.81 (d, ^3J=8.7 Hz, 1H, H–5 of coumarin), 7.57 (d, ^3J=8.3 Hz, 1H, NH of Glu), 7.39–7.25 (m, 6H, H_{Phenyl} and H–8 of coumarin), 7.18 (dd, ^3J=8.6 Hz, ^4J=2.2 Hz, 1H, H–6 of coumarin), 6.39 (d, ^4J=1.2 Hz, 1H, H–3 of coumarin), 5.10–4.99 (m, 2H, CH_2O of Z), 4.22–4.14 (m, 1H, $C_\alpha H$ of Glu), 3.83 (dd, ^2J=17.5 Hz, ^3J=5.9 Hz, 1H, $C_\alpha H$*H* of Gly), 3.73 (dd, ^2J=17.5 Hz, ^3J=5.7 Hz, 1H, C_α*H*H of Gly), 2.77–2.65 (m, 2H, $C_\gamma H_2$ of Glu), 2.44 (d, ^4J=1.1 Hz, 3H, CH_3), 2.13–2.01 (m, 1H, $C_\beta H$*H* of Glu), 1.98–1.86 (m, 1H, C_β*H*H of Glu); **^{13}C-NMR (DMSO-d_6):** δ=171.56, 171.09, 170.86, 159.60, 155.95, 153.49, 152.95, 152.83, 136.90, 128.31, 127.78, 127.71, 126.37, 118.39, 117.50, 113.72, 110.09, 65.54 (CH_2O of Z), 53.50, 40.68, 30.02, 27.00, 18.17 (CH_3); ESI-MS (ESI+) *m/z*: calc. for $C_{25}H_{25}N_2O_9$ $[M+H]^+$, 497.16, found 497.1; Elemental analysis: calc. for $C_{25}H_{24}N_2O_9$, C, 60.48; H, 4.87; N, 5.64; found C, 59.86; H, 4.84; N, 5.65.

Z-L-Glu(AMC)-Gly-OH (5c)

The synthesis using AMC yielded 7.3 mg (3%) of **5c** as a white solid. **^{1}H-NMR (DMSO-d_6):** δ=10.34 (s, 1H, NH of coumarin), 8.22 (t, ^3J=5.6 Hz, 1H, NH of Gly), 7.75 (d, ^4J=1.9 Hz, 1H, H–8 of coumarin), 7.70 (d, ^3J=8.7 Hz, 1H, H–5 of coumarin), 7.49–7.44 (m, 2H, H–6 of coumarin and NH of Glu), 7.40–7.25 (m, 5H, H_{Phenyl}), 6.25 (d, ^4J=1.0 Hz, 1H, H–3 of coumarin), 5.08–4.95 (m, 2H, CH_2O of Z), 4.14–3.99 (m, 1H, $C_\alpha H$ of Glu), 3.82 (dd, ^2J=17.4 Hz, ^3J=6.1 Hz, 1H, $C_\alpha H$*H* of Gly), 3.73 (dd, ^2J=17.8 Hz, ^3J=5.5 Hz, 1H, C_α*H*H of Gly), 2.54-2.43 (m, 2H, $C_\gamma H_2$ of Glu), 2.39 (d, ^4J=0.7 Hz, 3H, CH_3), 2.11–1.95 (m, 1H, $C_\beta H$*H* of Glu), 1.92–1.75 (m, 1H, C_β*H*H of Glu); **^{13}C-NMR (DMSO-d_6):** δ=171.84, 171.31, 171.08, 160.01, 159.74, 153.65, 153.09, 142.53, 128.30, 127.76, 127.69, 125.85, 115.04, 114.78, 112.08, 105.42, 65.49 (CH_2O of Z), 27.36, 17.95 (CH_3), 2xCα and Cγ not visible; ESI-MS (ESI+) *m/z*: calc. for $C_{25}H_{26}N_3O_8$ $[M+H]^+$, 496.17, found 496.2.

Z-L-Phe-L-Glu(HC)-Gly-OH (6a)

The synthesis using HC yielded 44 mg (35%) of **6a** as a white solid. **^{1}H-NMR (DMSO-d_6):** δ=12.59 (s, 1H, COOH), 8.29–8.22 (m, 2H, NH of Glu and Gly), 8.07 (d, ^3J=9.5 Hz, 1H, H–4 of coumarin), 7.77 (d, ^3J=8.5 Hz, 1H, H–5 of coumarin), 7.55 (d, ^3J=8.5 Hz, 1H, NH of Phe), 7.35–7.10 (m, 12H, H_{Phenyl} and H–6,8 of coumarin), 6.48 (d, ^3J=9.6 Hz, 1H, H–3 of coumarin), 4.96–4.87 (m, 2H, CH_2O of Z), 4.52–4.43 (m, 1H, $C_\alpha H$), 4.38–4.27 (m, 1H, $C_\alpha H$), 3.84 (dd, ^2J=17.5 Hz, ^3J=6.0 Hz, 1H, $C_\alpha H$*H* of Gly), 3.74 (dd, ^2J=17.5 Hz, ^3J=5.8 Hz, 1H, C_α*H*H of Gly), 3.04 (dd, ^2J=13.7 Hz, ^3J=3.8 Hz, 1H, $C_\beta H$*H* of Phe), 2.81–2.68 (m, 3H, C_β*H*H of Phe and $C_\gamma H_2$ of Glu), 2.16–2.05 (m, 1H, $C_\beta H$*H* of Glu), 1.98–1.86 (m, 1H, C_β*H*H of Glu); **^{13}C-NMR (DMSO-d_6):** δ=171.67, 171.12, 171.01, 170.88, 159.68, 155.88, 154.05, 152.89, 143.82, 138.06, 136.88, 129.28, 129.19, 128.20, 128.01, 127.62, 127.42, 126.20, 118.64, 116.64, 115.50, 110.11, 65.23 (CH_2O of Z), 56.14, 51.22, 40.67, 37.25, 29.64, 27.16; ESI-MS (ESI+) *m/z*: calc. for $C_{33}H_{32}N_3O_{10}$ $[M+H]^+$, 630.21, found 630.1; Elemental analysis: calc. for $C_{33}H_{31}N_3O_{10}$, C, 62.95; H, 4.96; N, 6.67; found C, 61.75; H, 5.15; N, 7.22.

Z-L-Phe-L-Glu(HMC)-Gly-OH (6b)

The synthesis using HMC yielded 88 mg (27%) of **6b** as a white solid. **^{1}H-NMR (DMSO-d_6):** δ=8.29–8.24 (m, 2H, NH of Glu and Gly), 7.81 (d, ^3J=8.7 Hz, 1H, H–5 of coumarin), 7.55 (d, ^3J=8.4 Hz, 1H, NH of Phe), 7.34–7.16 (m, 12H, H_{Phenyl} and H–6,8 of coumarin), 6.39 (d, ^4J=1.2 Hz, 1H, H–3 of coumarin), 4.95–4.88 (s, 2H, CH_2O of Z), 4.52–4.44 (m, 1H, $C_\alpha H$), 4.37–4.29 (m, 1H, $C_\alpha H$), 3.84 (dd, ^2J=17.6 Hz, ^3J=5.9 Hz, 1H, $C_\alpha H$*H* of Gly), 3.74 (dd, ^2J=17.5 Hz, ^3J=5.7 Hz, 1H, C_α*H*H of Gly), 3.04 (dd, ^2J=13.8 Hz, ^3J=3.7 Hz, 1H, $C_\beta H$*H* of Phe), 2.80–2.68 (m, 3H, C_β*H*H of Phe and $C_\gamma H_2$ of Glu), 2.44 (d, ^4J=0.9 Hz, 3H, CH_3), 2.17–2.05 (m, 1H, $C_\beta H$*H* of Glu), 1.98–1.86 (m, 1H, C_β*H*H of Glu); **^{13}C-NMR (DMSO-d_6):** δ=171.70, 171.14, 171.04, 170.89, 159.61, 155.89, 153.50, 152.96, 152.90, 138.08, 136.89, 129.20, 128.21, 128.03, 127.63, 127.42, 126.37, 126.22, 118.41, 117.50, 113.71, 110.12, 65.23 (CH_2O of Z), 56.15, 51.23, 40.68, 37.25, 29.64, 27.17, 18.17 (CH_3); ESI-MS (ESI+) *m/z*: calc. for $C_{34}H_{34}N_3O_{10}$ $[M+H]^+$, 644.22, found 644.3; Elemental analysis: calc. for $C_{34}H_{33}N_3O_{10}$, C, 63.45; H, 5.17; N, 6.53; found C, 62.10; H, 5.17; N, 6.46.

Fluorimetric Assay

Buffer systems and TGase 2 stock solutions

For the measurements at pH=8.0 and pH=6.5, the following two assay buffers of the respective pH value were used.

buffer A: 100 mM MOPS (pH=8.0), 3 mM $CaCl_2$, 50 µM EDTA, adjusted to pH=8.0 with 1M NaOH

buffer B: 100 mM MES (pH=6.5), 3 mM $CaCl_2$, 50 µM EDTA, adjusted to pH=6.5 with 1M NaOH

Two different enzyme buffers were used for the preparation of the TGase 2 stock solutions:

buffer I: 100 mM MOPS (pH=8.0), 3 mM $CaCl_2$, 10 mM DTT, 20% v/v Glycerol

buffer II: 100 mM MOPS (pH=8.0), 3 mM $CaCl_2$, 10 mM TCEP, 20% v/v Glycerol

For kinetic measurements at pH=6.5, TGase 2 stock solutions in buffer **II** were used which were diluted with buffer **III**.

buffer III: 100 mM MES (pH=6.5), 3 mM $CaCl_2$, 10 mM TCEP, 20% v/v Glycerol

All buffers were stored at 0 °C for a period of two weeks and freshly prepared after that period. The concentrations of the enzyme stock solutions were 0.5 mg/mL and 1 mg/mL for gpTGase 2 and hTGase 2, respectively.

General assay procedure and analysis

All measurements were conducted at 30 °C over 900 s (interval of 20 s) using a Synergy™ 4 Multi-Mode Microplate Reader (BioTek Instruments) and black 96-well BRANDplates® with transparent bottom (BRAND). Fluorescence was detected in bottom read mode. To detect released HMC or HC, a combination of optical filters adjusted to 365/40 nm and 465/40 nm as ranges of wavelengths for excitation and emission were used, respectively. Measurements at pH=8.0 and pH=6.5 were conducted with a sensitivity of 35 and 45, respectively. The assay mixture (200 µL) contained 190 µL aqueous solution and 10 µL DMSO (5% v/v). All regression analyses were accomplished using GraphPad Prism (version 5.02, 17.12.2008). To provide values of mean and SEM, the respective regression analyses were separately accomplished for each experiment and the obtained fit values were collected and statistically analysed.

Assay procedure and kinetic analysis of the enzymatic hydrolyses

For investigations on enzyme-catalysed hydrolysis reactions, six or eight different concentrations of the acyl donors were used (three independent measurements for each concentration in duplicate). The respective stock solutions were prepared in DMSO. To 180 µL assay buffer were added 5 µL of DMSO and 5 µL of the acyl donor stock solution. The reactions were initiated upon addition of 10 µL (60 µg/mL) TGase 2. For the measurements of the spontaneous reactions, the TGase 2 solution was replaced by the respective enzyme buffer. The recorded time courses of type (RFU-RFU_0)=f(t) for the enzymatic conversions were analysed by nonlinear regression to the experimental data over the first 300 s using equation I (one-phase association). Subsequently, the first derivative of this function at t=0 (equation II) afforded the initial slopes, which are equal to the values of v_{0total} (units of RFU/s).

$$\mathrm{RFU} - \mathrm{RFU}_0 = \mathrm{Plateau} * (1 - \mathrm{e}^{-k*\mathrm{t}}) \qquad \text{(I)}$$

RFU_0: $RFU_{t=0}$ Plateau: $RFU_{t\to\infty}$ *k*: rate constant to reach the plateau

$$\mathrm{v}_{0\mathrm{total}} = k * \mathrm{Plateau} \qquad \text{(II)}$$

Regarding the measurements of compound **5b** at pH=6.5, time courses of type (RFU-RFU_0)=f(t) were either analysed by nonlinear (equation I) or linear regression over the first 300 s to the experimental data depending on the shape of the curve.

The rates for the spontaneous reactions ($v_{0control}$) in the absence of enzyme were determined as described below. All fluorescence rates (RFU/s) were converted into molar rates (µM/min) by dividing by the respective fluorescence coefficient. Subsequently, the two sets of initial rates (v_{0total}=f([acyl donor]) and $v_{0control}$=f([acyl donor])) were globally analysed using the model of total and nonspecific binding as implemented in GraphPad Prism to determine the kinetic parameters for the enzymatic conversion. Accordingly, the following rule was defined,

$$\mathrm{v}_{0\mathrm{total}} = \mathrm{v}_{0\mathrm{corr}} + \mathrm{v}_{0\mathrm{control}}$$

where v_{0corr} represents the rates for the enzymatic conversions. Within this model, the portion of v_{0corr}=f([acyl donor]) and $v_{0control}$=f([acyl donor]) were analysed by nonlinear regression using equation III (Michaelis-Menten equation) and linear regression ($v_{0control}=k_{obs}$*[acyl donor]) to the

data, respectively (see Figures S11 and S12 for global plots in Supporting Information).

$$v_{0corr} = \frac{V_{max}*[S]}{K_m+[S]} \qquad (III)$$

Due to the negligible spontaneous reaction of compound **5b** at pH=6.5, plots of v_{0total}=f([acyl donor]) were directly analysed by nonlinear regression to the data using equation III.

Analysis of the spontaneous reactions

The recorded time courses of type (RFU-RFU_0)=f(t) for the spontaneous reactions were analysed by linear regression to the experimental data over the first 120 s. The respective slopes are equal to the values of $v_{0control}$ (units of RFU/s).

To determine the pseudo-first-order rate constants (k_{obs}), plots of $v_{0control}$=f([acyl donor]) were analysed by linear regression to the data. The obtained slopes are identical to the k_{obs} values.

Assay procedure and kinetic analysis of the enzymatic aminolyses

For investigations on enzyme-catalysed aminolysis reactions, six different concentrations of the acyl donors were used (three independent measurements, each concentration in duplicate). The respective stock solutions were prepared in DMSO. Aminoacetonitrile was chosen as reference acyl acceptor. To 180 µL assay buffer were added 5 µL of 16 mM aminoacetonitrile in DMSO and 5 µL of the acyl donor stock solution. The reactions were initiated upon addition of 10 µL TGase 2 (6 µg/mL for **5a**, **5b**, **6a** and **6b** or 40 µg/mL for **3** and **4**). For the measurement of the spontaneous reactions, the TGase 2 solution was replaced by the respective enzyme buffer. The recorded time courses of type (RFU-RFU_0)=f(t) for the enzymatic conversions were analysed by nonlinear regression to the experimental data over 180 s using equation I (one-phase association). Values of v_{0total} and $v_{0control}$ were obtained as described for the enzymatic hydrolysis. Due to high rates of spontaneous and enzymatic reactions, the calculated substrate concentrations from the numerical integration were used. Finally, the two sets of initial rates (v_{0total} and $v_{0control}$) were globally analysed using a model of total and nonspecific binding as described for the enzymatic hydrolysis (see Figures S14 and S15 for global plots in Supporting Information). The evaluation of the data sets for compounds **6a** and **6b** (gpTGase 2) and compound **5b** (hTGase 2) were performed by the method of Cornish-Bowden und Eisenthal.[40]

Characterisation of acyl acceptors

To characterise the kinetic properties of the chosen acyl acceptor substrates (aminoacetonitrile and *N*-(biotinyl)cadaverine×TFA **(7))** six different concentrations of the acyl acceptors were used. The respective stock solutions were prepared in DMSO. Compound **5b** was chosen as acyl donor. To 180 µL assay buffer were added 5 µL of acyl acceptor stock solution and 5 µL of 4 mM **5b** in DMSO. The reactions were initiated upon addition of 10 µL (12 µg/mL) TGase 2. For the measurement of the spontaneous reactions, the TGase 2 solution was replaced by the respective enzyme buffer. The two sets of initial rates (v_{0total} and $v_{0control}$) were obtained as described for the enzymatic hydrolysis. Subsequently, the $v_{0control}$ values were subtracted from the respective v_{0total} values and the resulting plot of v_{0corr}=f([S]) was analysed either by equation III for aminoacetonitrile or equation IV for *N*-(biotinyl)cadaverine (**7**).

$$v_{0corr} = \frac{V_{max}*[S]}{K_m+[S]*(1+\frac{[S]}{K_i})} \qquad (IV)$$

Since the measurements with *N*-(biotinyl)cadaverine (**7**) required highly concentrated amine stock solutions (400 mM), the volumes of the stock solutions were significantly greater than that of the added DMSO for dissolving the compounds due to the large amount of amine, which finally resulted in lower concentrations than intended. Therefore, the applied concentrations had to be corrected. For this purpose, the density of the respective stock solution was determined by weighing a defined volume and the correct concentration was calculated using the obtained density and the overall weight of the solution (DMSO+amine). The ratio between the actual and the intended concentration of the stock solution provided a factor (0.94), which was then used to correct the concentrations of all other solutions made from the stock solution.

Inhibition experiments

For the characterisation of coumarinyl amide **5c** towards gpTGase 2 at pH=8.0, the enzymatic hydrolysis of **5b** in the presence of four concentrations of **5c** (0, 200, 300 and 500 µM) was recorded. The respective stock solutions of **5b** and **5c** were prepared in DMSO. To 180 µL assay buffer were added 5 µL of **5c** stock solution and 5 µL of **5b** stock solution. The reactions were initiated upon addition of 10 µL (60 µg/mL) gpTGase 2. For the measurement of the spontaneous reactions, the TGase 2 solution was replaced by the respective enzyme buffer. Data evaluation was done as described in the Supporting Information (Discussion S7).

For the characterisation of iodoacetamide and acrylamide **8** towards gpTGase 2 and hTGase 2 at pH=6.5, eight or six concentrations of the inhibitors were used. The respective stock solutions were prepared in DMSO. Compound **5b** was chosen as acyl donor. To 180 µL assay buffer were added 5 µL of iodoacetamide stock solution and 5 µL of 1 mM **5b** (for gpTGase 2) or 1.2 mM **5b** (for hTGase 2) in DMSO. The reactions were initiated upon addition of 10 µL (60 µg/mL) TGase 2. The recorded time courses of type (RFU-RFU_0)=f(t) were analysed by nonlinear regression to the experimental data over the entire measurement period (900 s) using equation (V).

$$RFU - RFU_0 = v_S * t + \frac{(V_i - V_S)*(1-e^{-k_{obs}*t})}{k_{obs}} \qquad (V)$$

v_s: steady state velocity v_i: initial velocity

For iodoacetamide (gpTGase 2 and hTGase 2) and acrylamide **8** (gpTGase 2) the plot of k_{obs}=f([I]) was analysed by linear regression to the data. The respective slope (k_{obs}/I) was converted into k_{inact}/K_I by multiplication with (1+[S]/K_m). For the inhibition of hTGase 2 by acrylamide **8**, the double reciprocal plot $1/k_{obs}$=f([1/[I]) (equation VII) was analysed by linear regression to the data to determine the values for k_{incat}, K_I and k_{inact}/K_I. The respective K_i value was determined by analysis of v_i=f([I]) using equation VIII and the equation K_i=K_i'/(1+[S]/K_m), with K_m=6.60 µM.

$$k_{obs} = \frac{k_{inact}*[I]}{K_I+[I]} \qquad (VI)$$

$$\frac{1}{k_{obs}} = \frac{K_I}{k_{inact}} * \frac{1}{[I]} + \frac{1}{k_{inact}} \qquad (VII)$$

$$v_i = \frac{V_0}{1+\frac{[I]}{K_i}} + v_{0control} \qquad (VIII)$$

Numerical integration

For analysis of progress curves (RFU=f(t)) by numerical integration the differential equations shown in **Scheme 5** and **Scheme 7** were implemented in the freely available software R (www.R-project.org). A series of parameters were also implemented: Fluorescent coefficients of

HMC or HC (coP), the acyl donors (coSL) and the background fluorescence (bg), active concentrations of TGase 2, the rate constants k_{obs} for spontaneous reactions of the acyl donors, time span between data points (20 s), the entire time period for analysis (same as for the analysis by nonlinear regression) and starting values for the concentrations of the acyl donors and inhibitors. These parameters had to be defined depending on the data set prior to performing numerical integration. Furthermore, following relations were also implemented:

Enzymatic hydrolysis and aminolysis

$$k_{-1} = k_1 * K_{\mathrm{m}} - k_{\mathrm{cat}}$$

where k_1 was kept constant at the assumed value of 1 $\mu M^{-1}s^{-1}$

$$\mathrm{RFU} = \mathrm{coP} * [\mathrm{P}] + \mathrm{coSL} * [\mathrm{SL}] + \mathrm{bg}$$

For fitting of the progress curves, the kinetic parameters (K_m and k_{cat}) obtained by nonlinear regression or by the method of Cornish-Bowden and Eisenthal were used as initial values.

Enzymatic hydrolysis in the presence of an irreversible inhibitor

$$k_1 = \frac{k_{-1} + k_{\mathrm{cat}}}{K_{\mathrm{m}}}$$

where k_{-1} was kept constant at the assumed value of 1 s^{-1}

$$k_2 = \frac{k_{-2} + k_{\mathrm{inact}}}{K_{\mathrm{I}}}$$

where k_{-2} was kept constant at the assumed value of 1 s^{-1}

$$k_{\mathrm{inact}} = \mathrm{r} * K_{\mathrm{I}}$$

with $r=k_{inact}/K_I$

$$\mathrm{RFU} = \mathrm{coP} * [\mathrm{P}] + \mathrm{coSL} * [\mathrm{SL}] + \mathrm{bg}$$

The value of k_{inact}/K_I obtained by regression analysis was used as initial value for r and an arbitrary value of K_I=15 µM was set. Therefore, this procedure only allowed for the reliable calculation of the second-order inactivation constant k_{inact}/K_I. Each experiment was fitted separately and final values of mean ± SEM shown in **Table 2** and **Table 3** were calculated by statistical analysis of all experiments.

Presetting of the parameters above to arbitrarily assumed values was necessary as the rate constants describing the reversible enzyme-substrate and enzyme-inhibitor complexes, respectively, cannot be calculated independently.[33]

Acknowledgements

The authors thank Martin Lohse (Helmholtz-Zentrum Dresden-Rossendorf, Institute of Radiopharmaceutical Cancer Research) for assisting in the synthesis of compound **5c** and are grateful to Gözde Sarican (Trakya University, Edirne, Turkey, financially supported by a scholarship within the Erasmus programme for residence at the University of Cologne) for initial investigations on compounds **2a**-**2c**. R. L. appreciates continuing support by Prof. Dr. Jörg Steinbach. Partial financial support by the Helmholtz Portfolio Topic "Technologie und Medizin – Multimodale Bildgebung zur Aufklärung des in vivo-Verhaltens von polymeren Biomaterialien" (R. W., J. P. and R. L.) and by the Fonds der Chemischen Industrie (R. L.) is gratefully acknowledged. Furthermore, we wish to thank Prof. Dr. Jörg van den Hoff for helpful discussions concerning numerical integration.

Keywords: enzyme assays, inhibitors, reactive peptides, solid-phase synthesis, transferases

[1] (a) G. W. Jameson, D. V. Roberts, R. W. Adams, W. S. A. Kyle, D. T. Elmore *Biochem. J.* **1973**, *131*, 107-117; (b) S. P. Leytus, L. L. Melhado, W. F. Mangel *Biochem. J.* **1983**, *209*, 299-307; (c) J. L. Reymond, V. S. Fluxa, N. Maillard *Chem. Commun.* **2009**, 34-46 *(Review)*; (d) S. S. van Berkel, B. van der Lee, F. L. van Delft, R. Wagenvoord, H. C. Hemker, F. P. Rutjes *ChemMedChem* **2012**, *7*, 606-617; (e) M. Sakabe, D. Asanuma, M. Kamiya, R. J. Iwatate, K. Hanaoka, T. Terai, T. Nagano, Y. Urano *J. Am. Chem. Soc.* **2013**, *135*, 409-414; (f) M. Prost, L. Canaple, J. Samarut, J. Hasserodt *ChemBioChem* **2014**, *15*, 1413-1417; (g) K. R. Tallman, K. E. Beatty *ChemBioChem* **2015**, *16*, 70-75; (h) A. Zadlo, D. Koszelewski, F. Borys, R. Ostaszewski *ChemBioChem* **2015**, *16*, 677-682.

[2] (a) D. Park, S. S. Choi, K. S. Ha *Amino Acids* **2010**, *39*, 619-631; (b) S. Gundemir, G. Colak, J. Tucholski, G. V. Johnson *Biochim. Biophys. Acta* **2012**, *1823*, 406-419; (c) R. L. Eckert, M. T. Kaartinen, M. Nurminskaya, A. M. Belkin, G. Colak, G. V. Johnson, K. Mehta *Physiol. Rev.* **2014**, *94*, 383-417.

[3] (a) N. K. Sarkar, D. D. Clarke, H. Waelsch *Biochim. Biophys. Acta* **1957**, *25*, 451-452; (b) M. J. Mycek, D. D. Clarke, A. Neidle, H. Waelsch *Arch. Biochem. Biophys.* **1959**, *84*, 528-540; (c) J. Schrode, J. E. Folk *J. Biol. Chem.* **1978**, *253*, 4837-4840.

[4] M. J. Mycek, H. Waelsch *J. Biol. Chem.* **1960**, *235*, 3513-3517.

[5] (a) P. A. Smethurst, M. Griffin *Biochem. J.* **1996**, *313*, 803-808; (b) N. S. Caron, L. N. Munsie, J. W. Keillor, R. Truant *PLoS One* **2012**, *7*, e44159; (c) M. S. Pavlyukov, N. V. Antipova, M. V. Balashova, M. I. Shakhparonov *Biochem. Biophys. Res. Commun.* **2012**, *421*, 773-779.

[6] (a) H. Nakaoka, D. Perez, K. Baek, T. Das, A. Husain, K. Misono, M. Im, R. Graham *Science* **1994**, *264*, 1593-1596; (b) S. S. Akimov, D. Krylov, L. F. Fleischman, A. M. Belkin *J. Cell Biol.* **2000**, *148*, 825-838; (c) A. M. Belkin *FEBS J.* **2011**, *278*, 4704-4716.

[7] (a) W. Dieterich, T. Ehnis, M. Bauer, P. Donner, U. Volta, E. O. Riecken, D. Schuppan *Nat. Med.* **1997**, *3*, 797-801; (b) A. Di Sabatino, A. Vanoli, P. Giuffrida, O. Luinetti, E. Solcia, G. R. Corazza *Autoimmun. Rev.* **2012**, *11*, 746-753; (c) C. Klöck, T. R. DiRaimondo, C. Khosla *Semin. Immunopathol.* **2012**, *34*, 513-522.

[8] (a) L. Elli, C. M. Bergamini, M. T. Bardella, D. Schuppan *Dig. Liver Dis.* **2009**, *41*, 541-550; (b) D. Caccamo, M. Curro, R. Ientile *Expert Opin. Ther. Targets* **2010**, *14*, 989-1003; (c) K. C. Olsen, R. E. Sapinoro, R. M. Kottmann, A. A. Kulkarni, S. E. Iismaa, G. V. Johnson, T. H. Thatcher, R. P. Phipps, P. J. Sime *Am. J. Respir. Crit. Care Med.* **2011**, *184*, 699-707.

[9] (a) H. Grosso, M. M. Mouradian *Pharmacol. Ther.* **2012**, *133*, 392-410; (b) A. C. Brett, T. R. Rosenstock, A. C. Rego *Curr. Drug Targets* **2014**, *15*, 313-334; (c) R. Ientile, M. Curro, D. Caccamo *Amino Acids* **2015**, *47*, 19-26.

[10] (a) P. Kotsakis, M. Griffin *Amino Acids* **2007**, *33*, 373-384; (b) K. Mehta, A. Kumar, H. I. Kim *Biochem. Pharmacol.* **2010**, *80*, 1921-1929; (c) S. Kumar, K. Mehta *Amino Acids* **2013**, *44*, 81-88.

[11] M. Pietsch, R. Wodtke, J. Pietzsch, R. Löser *Bioorg. Med. Chem. Lett.* **2013**, *23*, 6528-6543.

[12] S. M. Gillet, J. N. Pelletier, J. W. Keillor *Anal. Biochem.* **2005**, *347*, 221-226.

[13] M. Walker *Top. Med. Chem.* **2015**, *9*, 69-106.

[14] J. Wityak, M. E. Prime, F. A. Brookfield, S. M. Courtney, S. Erfan, S. Johnsen, P. D. Johnson, M. Li, R. W. Marston, L. Reed, D. Vaidya, S. Schaertl, A. Pedret-Dunn, M. Beconi, D. Macdonald, I. Muñoz-Sanjuan, C. Dominguez *ACS Med. Chem. Lett.* **2012**, *3*, 1024-1028.

[15] M. Dixon, E. C. Webb, C. J. R. Thorne, K. F. Tipton, *Enzymes*, Academic Press, New York, **1979**, pp. 78-79.

[16] J. Polster, *Reaktionskinetische Auswertung spektroskopischer Meßdaten*, Vieweg, Braunschweig/Wiesbaden, **1995**, pp. 80-115.

[17] F. García-Martín, N. Bayó-Puxan, L. J. Cruz, J. C. Bohling, F. Albericio *QSAR Comb. Sci.* **2007**, *26*, 1027-1035.

[18] J. D. K. Twibanire, T. B. Grindley *Org. Lett.* **2011**, *13*, 2988-2991.

[19] R. Bollhagen, M. Schmiedberger, K. Barlos, E. Grell *J. Chem. Soc., Chem. Comm.* **1994**, 2559-2560.

[20] (a) S. I. Chung, R. I. Shrager, J. E. Folk *J. Biol. Chem.* **1970**, *245*, 6424-6435; (b) A. Leblanc, C. Gravel, J. Labelle, J. W. Keillor *Biochemistry* **2001**, *40*, 8335-8342.

[21] (a) W. P. Jencks, J. Carriuolo *J. Am. Chem. Soc.* **1960**, *82*, 1778-1786; (b) O. S. Tee, O. J. Yazbeck *Can. J. Chem.* **2000**, *78*, 1100-1108; (c) C. Gravel, D. Lapierre, J. Labelle, J. W. Keillor *Can. J. Chem.* **2007**, *85*, 164-174.

[22] (a) P. J. Bracher, P. W. Snyder, B. R. Bohall, G. M. Whitesides *Orig. Life Evol. Biosph.* **2011**, *41*, 399-412; (b) Z. P. Gates, J. R. Stephan, D. J. Lee, S. B. H. Kent *Chem. Commun.* **2013**, *49*, 786-788.

[23] (a) M. J. Selwyn *Biochim. Biophys. Acta* **1965**, *105*, 193-195; (b) A. Baici, *Kinetics of enzyme-modifier interactions*, Springer, Wien, **2015**, pp. 1-64.

[24] R. A. Copeland, *Enzymes: a practical introduction to structure, mechanism, and data analysis*, Wiley-VCH, New York, **2000**, pp. 109-145.

[25] (a) D. E. Koshland *Bioorg. Chem.* **2002**, *30*, 211-213; (b) R. Eisenthal, M. J. Danson, D. W. Hough *Trends Biotechnol.* **2007**, *25*, 247-249.

[26] J. E. Folk, P. W. Cole *J. Biol. Chem.* **1965**, *240*, 2951-2960.

[27] M. Griffin, A. Mongeot, R. Collighan, R. E. Saint, R. A. Jones, I. G. Coutts, D. L. Rathbone *Bioorg. Med. Chem. Lett.* **2008**, *18*, 5559-5562.

[28] M. Malesevic, A. Migge, T. C. Hertel, M. Pietzsch *ChemBioChem* **2015**, *16*, 1169-1174.

[29] V. Gentile, M. Saydak, E. A. Chiocca, O. Akande, P. J. Birckbichler, K. N. Lee, J. P. Stein, P. J. A. Davies *J. Biol. Chem.* **1991**, *266*, 478-483.

[30] C. Hauser, R. Wodtke, R. Löser, M. Pietsch *Amino Acids* **2016**, DOI 10.1007/s00726-00016-02192-00725.

[31] I. Roy, O. Smith, C. M. Clouthier, J. W. Keillor *Protein Expr. Purif.* **2013**, *87*, 41-46.

[32] (a) A. Case, R. L. Stein *Biochemistry* **2003**, *42*, 9466-9481; (b) J. W. Keillor, C. M. Clouthier, K. Y. Apperley, A. Akbar, A. Mulani *Bioorg. Chem.* **2014**, *57*, 186-197.

[33] A. Baici In *Proteases: Structure and Function,* (Eds.: Brix, K.; Stöcker, W.), Springer, Wien, **2013**, pp. 37-84.

[34] H. Tsunematsu, H. Nishimura, K. Mizusaki, S. Makisumi *J. Biochem.* **1985**, *97*, 617-623.

[35] (a) K. Hardes, G. L. Becker, M. Z. Hammamy, T. Steinmetzer *Anal. Biochem.* **2012**, *428*, 73-80; (b) K. Hardes, M. Zouhir Hammamy, T. Steinmetzer *Anal. Biochem.* **2013**, *442*, 223-230.

[36] A. Baici, *Kinetics of enzyme-modifier interactions*, Springer, Wien, **2015**, pp. 127-169.

[37] M. C. Yi, B. A. Palanski, S. A. Quintero, N. M. Plugis, C. Khosla *Bioorg. Med. Chem. Lett.* **2015**, *25*, 4922-4926.

[38] R. L. Stein, *Kinetics of enzyme action - essential principles for drug hunters*, John Wiley & Sons, Hoboken, **2011**, pp. 141-168.

[39] J. E. Folk *J. Biol. Chem.* **1969**, *244*, 3707-3713.

[40] A. Cornish-Bowden, *Fundamentals of enzyme kinetics*, Wiley-Blackwell, Weinheim, **2012**, pp. 45-51.

[41] (a) R. Eisenthal, A. Cornish-Bowden *Biochem. J.* **1974**, *139*, 715-720; (b) R. Eisenthal, A. Cornish-Bowden *Biochem. J.* **1974**, *139*, 721-730; (c) A. Baici *Biochemist* **2006**, *28*, 36-39.

[42] (a) T. F. Slaughter, K. E. Achyuthan, T. S. Lai, C. S. Greenberg *Anal. Biochem.* **1992**, *205*, 166-171; (b) J.-H. Jeon, C.-W. Kim, D.-M. Shin, K.-i. Kim, S.-Y. Cho, J.-C. Kwon, K.-H. Choi, H.-S. Kang, I.-G. Kim *FEBS Lett.* **2003**, *534*, 180-184; (c) X. Jin, J. Stamnaes, C. Klöck, T. R. DiRaimondo, L. M. Sollid, C. Khosla *J. Biol. Chem.* **2011**, *286*, 37866-37873.

[43] M. T. Gundersen, J. W. Keillor, J. N. Pelletier *Appl. Microbiol. Biotechnol.* **2014**, *98*, 219-230.

[44] A. Cornish-Bowden, *Fundamentals of enzyme kinetics*, Wiley-Blackwell, Weinheim, **2012**, pp. 211-213.

[45] R. L. Stein, *Kinetics of enzyme action - essential principles for drug hunters*, John Wiley & Sons, Hoboken, **2011**, pp. 122-137.

[46] R. A. Copeland, *Evaluation of Enzyme Inhibitors in Drug Discovery.*, John Wiley & Sons, Hoboken, **2005**, pp. 214-248.

[47] J. E. Folk, P. W. Cole *J. Biol. Chem.* **1966**, *241*, 3238-3240.

[48] A. G. McDonald, K. F. Tipton In *eLS*, John Wiley & Sons, Chichester, **2012**, pp. 1-17

[49] C. Cobas, S. Dominguez, N. Larin, I. Iglesias, C. Geada, F. Seoane, M. Sordo, P. Monje, S. Fraga, R. Cobas, C. Peng, J. A. Garcia, M. Goebel, E. Vaz, *MestReNova 6.1.1-6384*, Mestrelab Research S.L., **2010**, pp.

Entry for the Table of Contents

FULL PAPER

A set of fluorogenic acyl donor substrates for transglutaminase 2 was synthesised via a modular solid phase strategy. Their good solubility in aqueous media allowed for their detailed kinetic characterisation towards transglutaminase 2-catalysed hydrolysis and aminolysis. Additionally, their applicability to characterise amine substrates and inhibitors of TGase 2 was demonstrated.

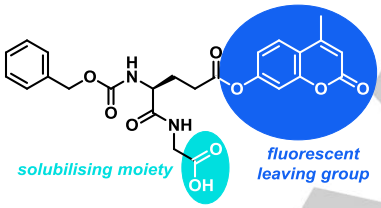

R. Wodtke, G. Schramm, J. Pietzsch, M. Pietsch, R. Löser**

Synthesis and kinetic characterisation of water-soluble fluorogenic acyl donors for transglutaminase 2

Supporting Information

Table of Contents

Discussion S1: Synthesis of the γ-Abu-derived acyl donors

General remarks

Preparation of Z-Phe-γ-Abu-OH (**1**) via mixed anhydride synthesis using isobutyl chloroformate (IBCF) and *N*-methylmorpholine was advantageous with regards to the reaction time over the published procedure, which employed *p*-nitrophenyl chloroformate as activating agent.[1] However, Z-Phe-γ-Abu-γ-Abu-OH (**1a**) was formed as side product in significant amounts (see below) in both procedures. This side product probably occurs as the carboxylic group in product **1** attacks either the initially formed mixed anhydride or the *p*-nitrophenyl ester of Z-Phe-OH. In both cases, the reaction results in a mixed anhydride of Z-Phe-OH and **1**, with the carbonyl C atom derived from the carboxylic group of **1** being more amenable to nucleophilic attack of γ-Abu-OH than that derived from Z-Phe-OH probably due to steric reasons. To avoid the formation of side product **1a**, attractive alternatives would be either the use of Z-Phe-OSu as acylating agent or the use of γ-Abu-O*t*Bu instead of free γ-Abu-OH. Furthermore, *N*,*O*-disilylation of γ-Abu-OH using trimethylchlorosilane *in situ* prior to the coupling of activated Z-Phe-OH should be a feasible way to obtain compound **1** without the undesired formation of **1a**.[2] Esterification of **1** with HC and HMC was accomplished by means of *N*,*N*'-dicyclohexylcarbodiimide (DCC) and Steglich's base (DMAP) following the procedure of Xu *et al.*[3] with slightly modified conditions. Coupling of AMC was achieved by the mixed anhydride approach analogously to the synthesis of **1**.

Synthesis of 4-(*N*-Benzyloxycarbonyl-L-phenylalanylamino)-butyric acid (Z-Phe-γ-Abu-OH; 1)

A solution of Z-L-Phe-OH (1.5 g, 5.01 mmol, 1 equiv.) in THF (15 mL) was cooled to -30 °C by a mixture of isopropanol and liquid nitrogen. Then, *N*-methylmorpholine (NMM; 551 µL, 5.01 mmol, 1 equiv.) and isobutylchloroformate (IBCF; 656 µL, 5.01 mmol, 1 equiv.) were sequentially added. After stirring for 1 min, a solution of γ-Abu-OH (0.78 g, 7.52 mmol, 1.5 equiv.) in a mixture of water (1 mL) and 4 M NaOH (1.88 mL, 7.52 mmol) was added. Cooling was stopped and the reaction mixture was stirred until the temperature reached 10 °C (approx. 2.5 h). Subsequently, the solvent was evaporated and the residuum dissolved in 1 M HCl to achieve pH<5 (approx. 12 mL). The aqueous phase was extracted with ethyl acetate (4×20 mL) and the combined organic fractions were washed with brine (50 mL). After that, the organic layer was dried over Na_2SO_4 and evaporated *in vacuo*. The crude product was purified by column chromatography (petrolether/ethyl acetate/acetic acid 1:1:0.01 for remaining Z-L-Phe-OH → 1:4:0.01 for product (**1**) → CH_3OH for side product (**1a**). To remove residual acetic acid, the products were washed several times with hexane and exposed to oil pump vacuum. Finally, 0.85 g (45%) of **1** were obtained as a white solid. R_f=0.15 (petrolether/ethyl acetate/acetic acid 1:1:0.01). **^{1}H-NMR (DMSO-d_6):** δ=12.04 (s, 1H, COOH), 8.00 (t, ^3J=5.5 Hz, 1H, NH of γ-Abu), 7.47 (d, ^3J=8.6 Hz, 1H, NH of Phe), 7.37–7.13 (m, 10H, H_{Phenyl}), 4.99–4.88 (m, 2H, CH_2O of Z), 4.22–4.13 (m, 1H, $C_\alpha H$ of Phe), 3.15–2.99

(m, 2H, $C_\gamma H_2$ of γ-Abu), 2.94 (dd, ^2J=13.6 Hz, ^3J=4.8 Hz, 1H, $C_\beta HH$ of Phe), 2.75 (dd, ^2J=13.6 Hz, ^3J=10.1 Hz, 1H, $C_\beta HH$ of Phe), 2.17 (t, ^3J=7.4 Hz, 2H, $C_\alpha H_2$ of γ-Abu), 1.64–1.53 (m, 2H, $C_\beta H_2$ of γ-Abu); **^{13}C-NMR (DMSO-d_6):** δ=174.20 (COOH), 171.25 (CO of Phe), 155.77 (CO of Z), 138.07, 137.03, 129.16, 128.26, 128.01, 127.65, 127.45, 126.22, 65.18 (CH_2O of Z), 56.27 (C_α of Phe), 37.92, 37.70, 30.93 (C_α of γ-Abu), 24.45 (C_β of γ-Abu); ESI-MS (ESI+) *m/z*: calc. for $C_{21}H_{25}N_2O_5$ $[M+H]^+$, 385.18, found 385.5; Elemental analysis: calc. for $C_{21}H_{24}N_2O_5$, C, 65.61; H, 6.29; N, 7.29; found C, 65.66; H, 6.30; N, 7.25. For characterisation of side product **1a** see below.

General procedure for esterification of 1 with coumarin derivatives

To a solution of **1** (0.4 g, 1.04 mmol, 1 equiv.) in CH_2Cl_2/THF (25 mL, 4:1) were successively added DCC (0.21 g, 1.04 mmol, 1 equiv.), the respective coumarin derivative (HC or HMC, 1.25 mmol, 1.2 equiv.), and DMAP (25 mg, 0.21 mmol, 0.2 equiv.). The reaction mixture was stirred for 25 h at room temperature in the dark and filtered through Celite. The filtrate was transferred to a separating funnel and successively washed with saturated $NaHCO_3$ (1×20 mL), 1 M HCl (2×20 mL) and brine (1×20 mL). After that, the organic layer was dried over Na_2SO_4 and evaporated *in vacuo*. The crude product was purified by column chromatography (petrolether/ethyl acetate 1:1 for HC → 1:4 for product) in the dark. The product was recrystallised in cyclohexane/ethyl acetate. To remove residual cyclohexane, the products were washed with hexane and exposed to oil pump vacuum.

4-(*N*-Benzyloxycarbonyl-L-phenylalanylamino)-butyric acid coumarin-7-yl-ester (Z-Phe-γ-Abu-HC; 2a)

The synthesis using umbelliferone (7-hydroxycoumarin, HC; 0.20 g) yielded 0.32 g (59%) of **2a** as a white solid. R_f=0.08 (petrolether/ethyl acetate 1:1); m.p. 166-169°C; **^{1}H-NMR (DMSO-d_6):** δ=8.08 (m, 2H, NH of γ-Abu and H–4 of coumarin), 7.77 (d, ^3J=8.5 Hz, 1H, H–5 of coumarin), 7.53 (d, ^3J=8.5 Hz, 1H, NH of Phe), 7.36–7.14 (m, 12H, H_{Phenyl} and H–6,8 of coumarin), 6.48 (d, ^3J=9.6 Hz, 1H, H–3 of coumarin), 5.01–4.90 (m, 2H, CH_2O of Z), 4.25–4.15 (m, 1H, $C_\alpha H$ of Phe), 3.22–3.12 (m, 2H, $C_\gamma H_2$ of γ-Abu), 2.97 (dd, ^2J=13.6 Hz, ^3J=5.0 Hz, 1H, $C_\beta HH$ of Phe), 2.78 (dd, ^2J=13.5 Hz, ^3J=10.1 Hz, 1H, $C_\beta HH$ of Phe), 2.57 (t, ^3J=7.1 Hz, 2H, $C_\alpha H_2$ of γ-Abu), 1.80–1.67 (m, 2H, $C_\beta H_2$ of γ-Abu); **^{13}C-NMR (DMSO-d_6):** δ=171.43 (CO), 171.13 (CO), 159.69 (C–2 of coumarin), 155.81 (CO of Z), 154.08, 152.91, 143.83, 138.04, 137.00, 129.32, 129.17, 128.24, 128.03, 127.64, 127.44, 126.23, 118.65, 116.63, 115.51, 110.09, 65.19 (CH_2O of Z), 56.34 (C_α of Phe), 37.64, 37.45, 30.63 (C_α of γ-Abu), 24.18 (C_β of γ-Abu); NMR data are in agreement to those reported by Gillet *et al*.[1b]; ESI-MS (ESI+) *m/z*: calc. for $C_{30}H_{29}N_2O_7$ $[M+H]^+$, 529.20, found 529.6; Elemental analysis: calc. for $C_{30}H_{28}N_2O_7$, C, 68.17; H, 5.34; N, 5.30; found C, 68.25; H, 5.35; N, 5.32.

4-(*N*-Benzyloxycarbonyl-L-phenylalanylamino)-butyric acid 4-methylcoumarin-7-yl-ester (Z-Phe-γ-Abu-HMC; 2b)

The synthesis using 4-methylumbelliferone (7-hydroxy-4-methylcoumarin, HMC; 0.22 g) yielded 0.31 g (55%) of **2b** as a white solid. R_f=0.11 (petrolether/ethyl acetate 1:1); m.p. 166-168.5°C; **^{1}H-NMR (DMSO-d_6):** δ=8.09 (t, ^3J=5.7 Hz, 1H, NH of γ-Abu), 7.82 (d, ^3J=8.7 Hz, 1H, H–5 of coumarin), 7.53 (d, ^3J=8.5 Hz, 1H, NH of Phe), 7.36–7.13 (m, 12H, H_{Phenyl} and H–6,8 of coumarin), 6.39 (d, ^4J=1.2 Hz, 1H, H–3 coumarin), 5.00–4.87 (m, 2H, CH_2O of Z), 4.27–4.14 (m, 1H, $C_\alpha H$ of Phe), 3.25–3.09 (m, 2H, $C_\gamma H_2$ of γ-Abu), 2.97 (dd, ^2J=13.6 Hz, ^3J=5.0 Hz, 1H, $C_\beta H$*H* of Phe), 2.78 (dd, ^2J=13.5, ^3J=9.9 Hz, 1H, C_β*H*H of Phe), 2.57 (t, ^3J=7.3 Hz, 2H, $C_\alpha H_2$ of γ-Abu), 2.44 (d, ^4J=1.1 Hz, 3H, CH_3), 1.79–1.68 (m, 2H, $C_\beta H_2$ of γ-Abu); **^{13}C-NMR (DMSO-d_6):** δ=171.44 (CO), 171.14 (CO), 159.62 (C–2 of coumarin), 155.82 (CO of Z), 153.53, 152.97, 152.92, 138.05, 137.00, 129.18, 128.25, 128.04, 127.66, 127.45, 126.41, 126.24, 118.43, 117.49, 113.71, 110.09, 65.21 (CH_2O of Z), 56.36 (C_α of Phe), 37.65, 37.48, 30.65 (C_α of γ-Abu), 24.19 (C_β of γ-Abu), 18.17 (CH_3); ESI-MS (ESI+) *m/z*: calc. for $C_{31}H_{31}N_2O_7$ $[M+H]^+$, 543.20, found 543.7; Elemental analysis: calc. for $C_{31}H_{30}N_2O_7$, C, 68.62; H, 5.57; N, 5.16; found C, 68.73; H, 5.63; N, 5.26.

Synthesis of 7-(4-(*N*-benzyloxycarbonyl-L-phenylalanylamino)-butanoyl)amino-4-methylcoumarin (Z-Phe-γ-Abu-AMC; 2c)

A solution of **1** (0.40 g, 1.04 mmol, 1 equiv.) in THF (10 mL) was cooled to -25 °C by a mixture of isopropanol and liquid nitrogen. Then, NMM (114 µL, 1.04 mmol, 1 equiv.) and IBCF (136 µL, 1.04 mmol, 1 equiv.) were added. After stirring for 1 min, a solution of 7-amino-4-methylcoumarin (AMC; 0.27 g, 1.56 mmol, 1.5 equiv.) in THF/DMF (13 mL, 12:1) was added. Cooling was stopped and the reaction mixture was stirred until the temperature reached 10 °C (approx. 5 h). Then, the solvent was evaporated and the residuum suspended in 1 M HCl (10 mL). The resulting solid was filtered off and washed with 1 M HCl, water, saturated $NaHCO_3$ and finally with water and dried *in vacuo* over P_2O_5 for 24 h. Then, the white solid was extensively washed with ethyl acetate and exposed to oil pump vacuum to obtain 0.38 g (68%) of **2c**. R_f=0.07 (CH_2Cl_2/CH_3OH 80:1); m.p. 223-226°C; **^{1}H-NMR (DMSO-d_6):** δ=10.33 (s, 1H, NH of coumarin), 8.06 (t, ^3J=5.4 Hz, 1H, NH of γ-Abu), 7.78 (d, ^4J=1.9 Hz, 1H, H–8 of coumarin), 7.70 (d, ^3J=8.7 Hz, 1H, H–5 of coumarin), 7.51–7.45 (m, 2H, NH of Phe and H–6 of coumarin), 7.36–7.14 (m, 10H, H_{Phenyl}), 6.25 (d, ^4J=1.1 Hz, 1H, H–3 of coumarin), 5.00–4.87 (m, 2H, CH_2O of Z), 4.24–4.15 (m, 1H, $C_\alpha H$ of Phe), 3.18–3.05 (m, 2H, $C_\gamma H_2$ of γ-Abu), 2.96 (dd, ^2J=13.6 Hz, ^3J=4.5 Hz, 1H, $C_\beta H$*H* of Phe), 2.76 (dd, ^2J=13.6 Hz, ^3J=10.3 Hz, 1H, C_β*H*H of Phe), 2.39 (s, 3H, CH_3), 2.38–2.33 (m, 2H, $C_\alpha H_2$ of γ-Abu), 1.77–1.66 (m, 2H, $C_\beta H_2$ of γ-Abu); **^{13}C-NMR (DMSO-d_6):** δ=171.67 (CO), 171.36 (CO), 160.05 (C–2 of coumarin), 155.80 (CO of Z), 153.69, 153.11, 142.58, 138.10, 137.03, 129.15, 128.26, 128.01, 127.64, 127.43, 126.21, 125.88, 115.05, 114.79, 112.10, 105.43, 65.18 (CH_2O of Z), 56.29 (C_α of Phe), 38.13, 37.71, 33.82 (C_α of γ-Abu), 24.77 (C_β of γ-Abu), 17.97 (CH_3); ESI-MS (ESI+) *m/z*: calc. for $C_{31}H_{31}N_3NaO_6$

$[M+Na]^+$, 564.21, found 564.8; Elemental analysis: calc. for $C_{31}H_{31}N_3O_6$, C, 68.75; H, 5.77; N, 7.76; found C, 68.73; H, 5.77; N, 7.71.

A) 4-(4-(*N*-Benzyloxycarbonyl-L-phenylalanylamino)-butanoylamino)-butyric acid (1a)

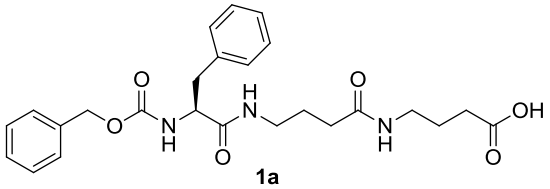

1a

0.43 g (19%) of **1a** as a white solid were obtained. R_f=0.0 (petrolether/ethyl acetate 1:1 + 0.1 acetic acid). **^{1}H-NMR (DMSO-*d*$_6$):** δ=8.09 (t, ^3J=5.4 Hz, 1H, NH), 7.89 (t, ^3J=5.3 Hz, 1H, NH), 7.55 (d, ^3J=8.6 Hz, 1H, NH of Phe), 7.36–7.12 (m, 10H, H_{Phenyl}), 4.99–4.87 (m, 2H, CH_2O of Z), 4.22– 4.13 (m, 1H, $C_\alpha H$ of Phe), 3.10–2.99 (m, 4H, 2×$C_\gamma H_2$ of γ-Abu), 2.95 (dd, ^2J=13.7 Hz, ^3J=4.7 Hz, 1H, $C_\beta H$*H* of Phe), 2.76 (dd, ^2J=13.5 Hz, ^2J=10.3 Hz, 1H, C_β*H*H of Phe), 2.15 (t, ^3J=7.3 Hz, 2H, $C_\alpha H_2$ of γ-Abu), 2.03 (t, ^3J=7.3 Hz, 2H, $C_\alpha H_2$ of γ-Abu), 1.65–1.54 (m, 4H, 2×$C_\beta H_2$ of γ-Abu); **^{13}C-NMR (DMSO-*d*$_6$):** δ=174.93 (COOH), 171.58 (CO), 171.27 (CO), 155.78 (CO of Z), 138.15, 137.06, 129.17, 128.25, 128.00, 127.62, 127.39, 126.18, 65.13 (CH_2O of Z), 56.38 (C_α of Phe), 38.25 (2C), 37.73, 32.79 (C_α of γ-Abu), 32.30 (C_α of γ-Abu), 25.30 (C_β of γ-Abu), 24.97 (C_β of γ-Abu); ESI-MS (ESI+) *m/z*: calc. for $C_{25}H_{32}N_3O_6$ $[M+H]^+$, 470.23, found 470.7.

Figure S1

gpTGase 2-catalysed aminolyses of the acyl donors 2a and 2b at pH=8.0 over a broad range of concentrations

Plots of v_{0total}=f([acyl donor]) where a drop of v_{0total} occurs at acyl donor concentrations <10 µM due to beginning formation of precipitates. Data (●) shown are mean values of at least 2 separate experiments, each performed in triplicate. When not apparent, error bars are smaller than the symbols. Conditions: pH=8.0, 30 °C, 5% DMSO, 500 µM DTT, 400 µM aminoacetonitrile, 2 µg/mL gpTGase 2.

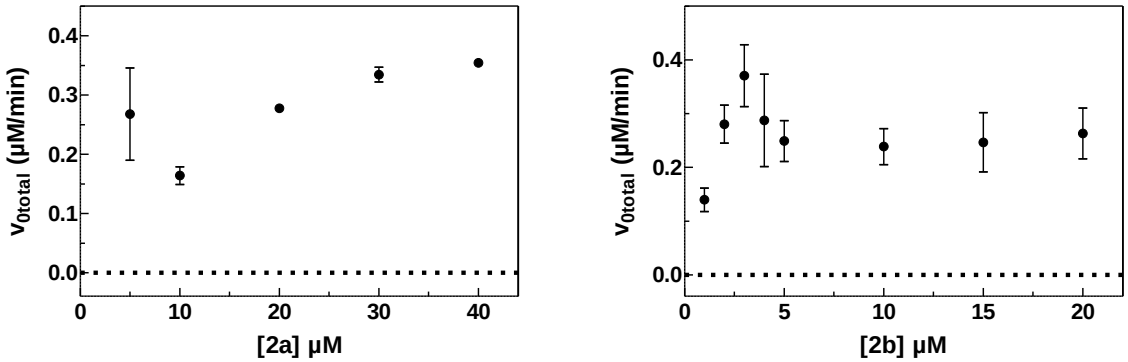

Figure S2

Solubility of the γ-aminobutyric acid-derived acyl donors 2a and 2b

It should be emphasised that precipitation is a strongly time-dependent process. This is demonstrated by the progress curves for spontaneous reaction of the γ-Abu derivatives, for which at higher concentrations (≥10 µM) a gradual bending of the curves can be observed (see below). Therefore, simultaneous measurements of different compound concentrations in a 96-well plate format might lead to different results for the limits of the solubility compared to single measurements in cuvettes.[1b] Noteworthy, in the presence of TCEP as alternative antioxidant, both the extent of spontaneous disintegration (see below) and the solubility decrease significantly (<5 µM). With regards to the influence of methyl substitution at the fluorophore on solubility, **2a** seems to be slightly more favourable over its HMC-based counterpart **2b**. The solubility of both compounds was even lower when DMF was used instead of DMSO. As it is also known that DMSO is superior to DMF in maintaining the activity of the TGase 2 enzyme, we finally decided to use DMSO instead of DMF as organic co-solvent for all further experiments.[4]

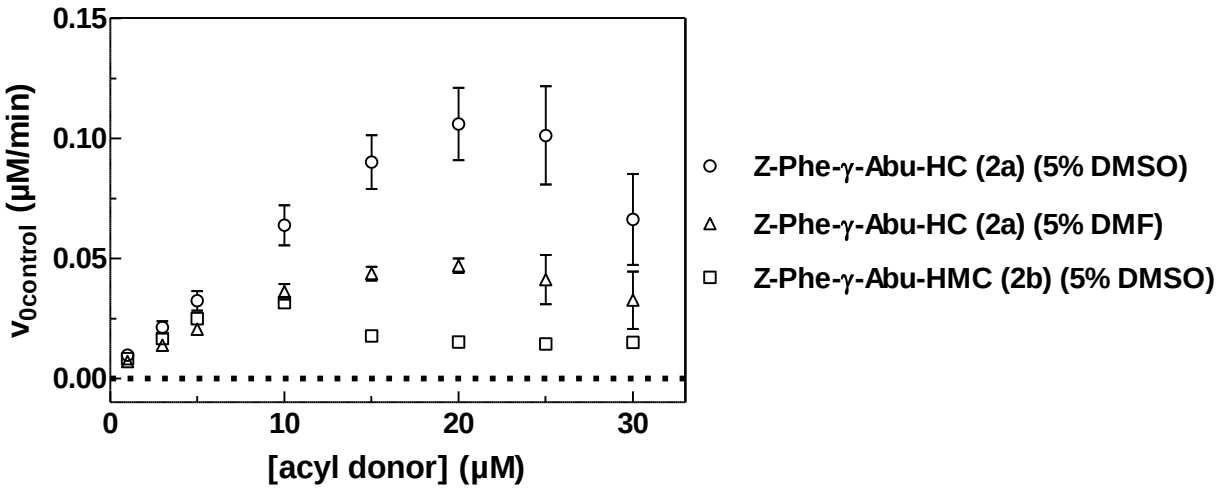

Plots of $v_{0control}$=f([acyl donor]) at pH=8.0 and 30 °C in the presence of 500 µM DTT and either 5% DMSO or 5% DMF. Data shown are mean values ± SEM of 2 separate experiments, each performed in duplicate. When not apparent, error bars are smaller than the symbols.

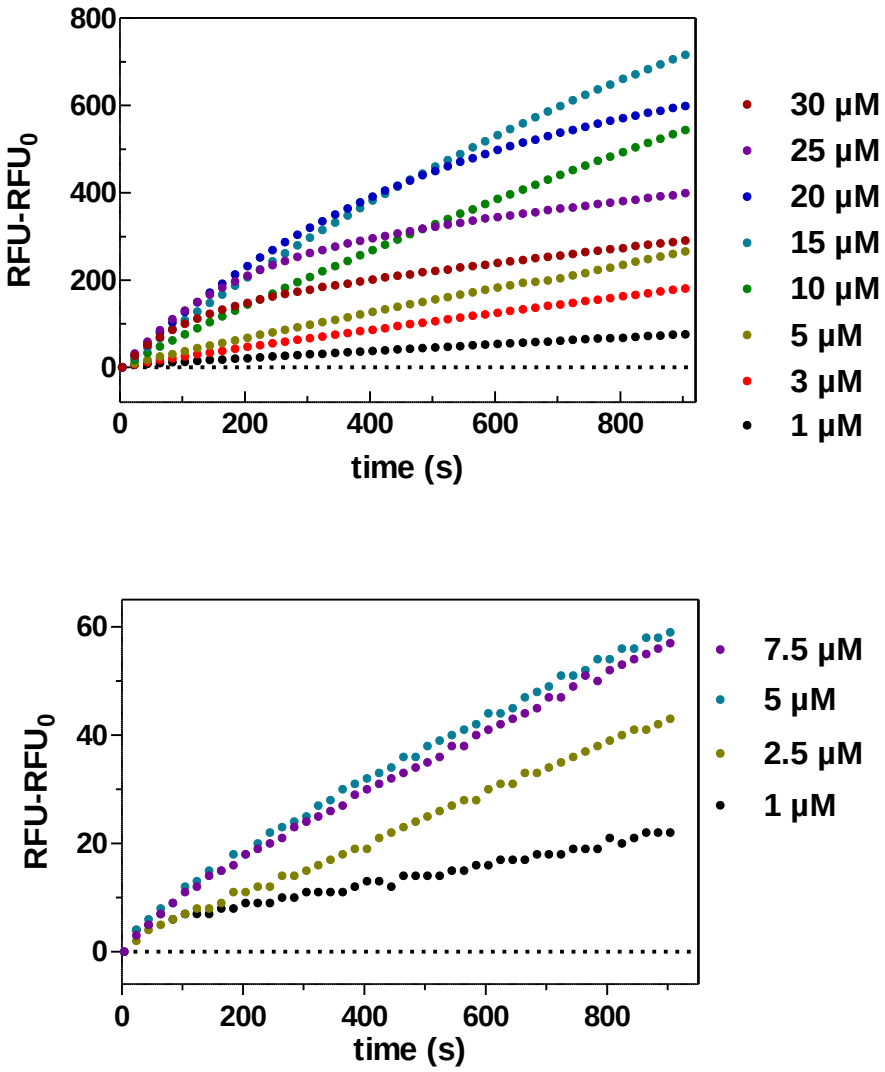

Progress curves for the spontaneous reaction of compound **2a** in the presence of 5% DMSO and 500 µM DTT (Top) and 500 µM TCEP (bottom).

Figure S3

gpTGase 2 catalysed hydrolysis of γ-Abu-derived acyl donors 2a and 2b in consideration of their limits of solubility

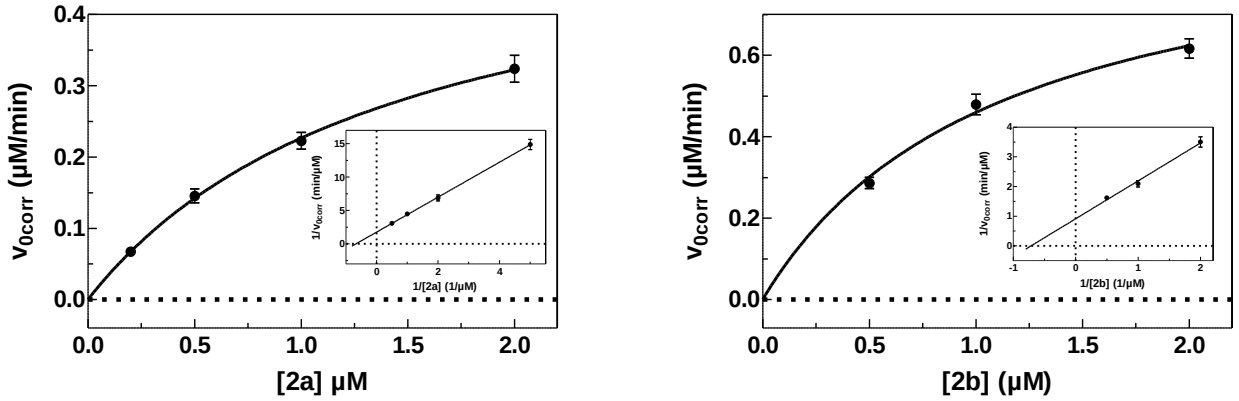

Plots of v_{0corr}=f([acyl donor]) for compounds **2a** and **2b** with nonlinear regression (—) using the Michaelis-Menten equation III. Insets show plots of $1/v_{0corr}$=f(1/[acyl donor]) (linearisation method according to Lineweaver and Burk). Data (●) shown are mean values ± SEM of 3 separate experiments, each performed in duplicate. When not apparent, error bars are smaller than the symbols. Conditions: pH=8.0, 30 °C, 5% DMSO, 500 µM TCEP, 3 µg/mL gpTGase 2.

Discussion S2: Attempts for the esterification reactions on resin using carbodiimides

General remarks

Initially, the conditions for the esterification reaction in solution, as described for the γ-aminobutyric acid-derived acyl donors using DCC and DMAP, were applied for the esterification reactions on resin. Surprisingly, analytical HPLC and ESI-MS analyses of the crude products obtained by HFIP-mediated cleavage of a small resin sample (referred to as minicleavage herein) revealed the formation of the desired esters in significantly lower extent compared to the syntheses in solution independent of the used carbodiimide (DCC or DIC; data not shown). Since microwave-assisted synthesis is a common procedure for the assembling of peptides on resin, which can provide excellent results for challenging couplings,[5] the influence of microwave irradiation was studied next. Surprisingly, even for long coupling cycles of 1200 s at 25 W and 75 °C in the presence of different combinations of coupling agents (DIC/DMAP, DIC/N-methylimidazole) only minor amounts of the desired esters were formed as detected by analysing the crude products obtained after minicleavages. It should be mentioned that in contrast to the synthesis without microwave irradiation in which the starting materials were mainly unaffected, the respective *N*-acyl ureas (ureides) were observed as major products under microwave irradiation (exemplarily shown for the ureide **4a** of Z-Phe-Glu-OH below). Since no satisfying results had been obtained for the esterification on resin by using carbodiimides, another coupling agent had to be identified for that purpose.

Ureide formation during microwave-assisted esterification by the use of DIC/DMAP, exemplarily shown for compound 4a

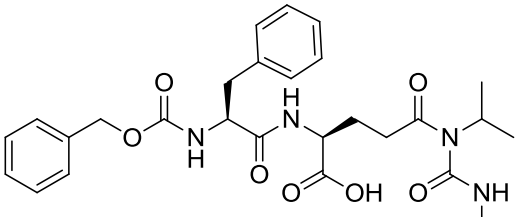

4a

The synthesis was accomplished using a modified protocol of the CEM Liberty 12-channel peptide synthesizer. The peptidyl resin (0.5 mmol Z-Phe-Glu-OH, 1 equiv.) was swollen in DMF (5 mL) for 30 min outside the peptide synthesizer. After transfer to the reaction vessel, the resin was swollen in CH_2Cl_2/DMF (1:1, 20 mL) for another 15 min. Coupling was performed with two solutions: 0.38 M DIC in DMF (4 mL, 3 equiv.) and 0.3 M DMAP in DMF (2 mL). HMC was applied as 0.2 M solution in DMF. 10 mL (4 equiv.) of this solution were taken for the coupling step (1200 s at 25 W and 75 °C). The peptidyl resin was then washed with DMF (60 mL) and outside the peptide synthesizer with ethanol (4×5 mL) and

CH_2Cl_2 (4×5 mL). Release of the peptide from the resin was performed as outlined in the main article (→Full-cleavage, see below in Discussion S4). The crude product was purified via preparative RP-HPLC. The microwave-assisted synthesis yielded 51 mg (18%) of **4a** as a yellow oil t_R=20.5 min, **^{1}H-NMR (DMSO-*d*$_6$):** δ=8.33 (d, ^3J=7.7 Hz, 1H, NH), 8.18 (d, ^3J=8.0 Hz, 1H, NH), 7.42 (d, ^3J=8.8 Hz, 1H, NH of Phe), 7.36–7.16 (m, 10H, H_{Phenyl}), 4.96–4.87 (m, 2H, CH_2O of Z), 4.36–4.26 (m, 2H), 4.25–4.16 (m, 1H), 3.82–3.70 (m, 1H, CH), 3.01 (dd, ^2J=13.9 Hz, ^3J=3.1 Hz, 1H, $C_\beta H$*H* of Phe), 2.71 (dd, ^2J=13.9 Hz, ^3J=11.2 Hz, 1H, C_β*H*H of Phe), 2.42–2.31 (m, 2H, $C_\gamma H_2$ of Glu), 2.09–1.97 (m, 1H, $C_\beta H$*H* of Glu), 1.94–1.79 (m, 1H, C_β*H*H of Glu), 1.14 (d, ^3J=6.8 Hz, 6H, 2×CH_3), 1.09 (d, ^3J=6.6 Hz, 6H, 2×CH_3); **^{13}C-NMR (DMSO-*d*$_6$):** δ=173.11, 171.66, 169.24, 155.74, 153.34, 138.09, 136.98, 129.18, 128.26, 128.00, 127.64, 127.40, 126.21, 65.14, 55.89, 51.51, 45.07, 42.41, 37.51, 30.70, 26.84, 21.67, 21.63, 20.34, 20.27. ESI-MS (ESI+) *m/z*: calc. for $C_{29}H_{39}N_4O_7$ $[M+H]^+$, 555.28, found 555.6.

Analytical HPLC run and ESI(+) mass spectrum of the crude product after esterification

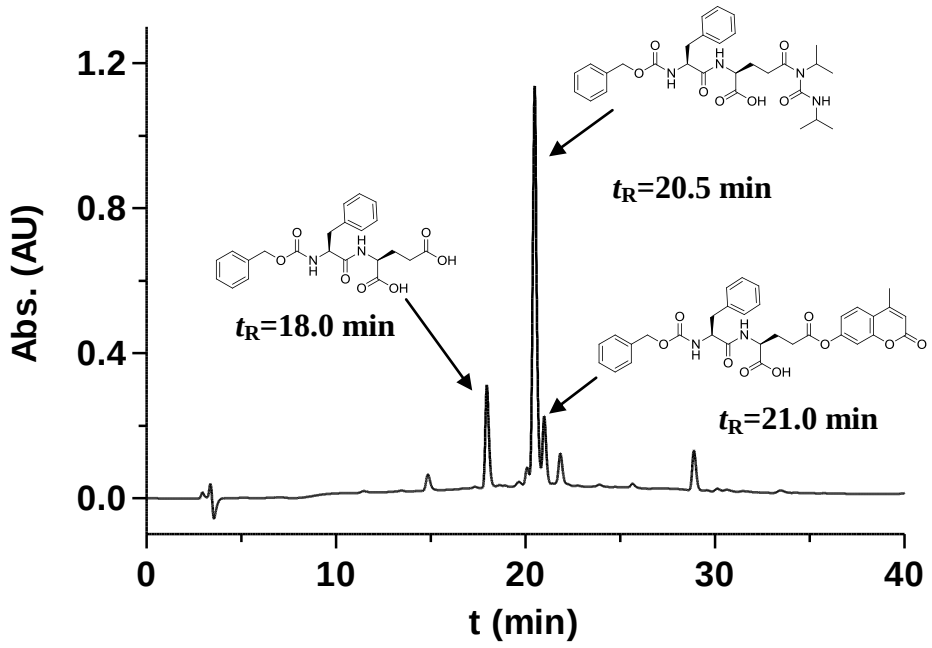

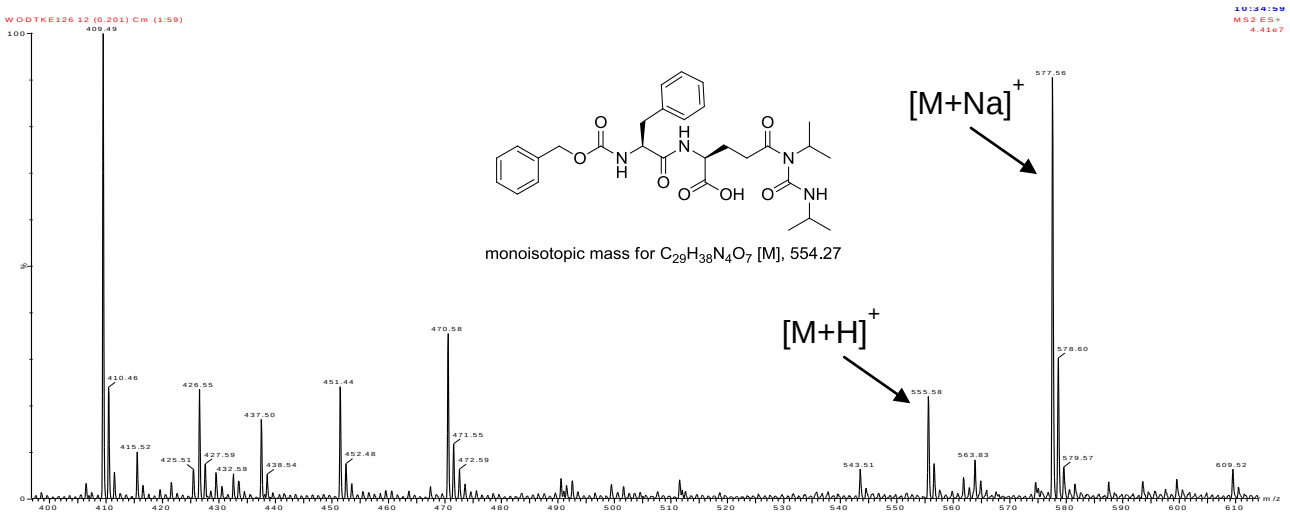
WODTKE126 12 (0.201) Cm (1:59)
MS2 ES+
4.41e7
100
%
0
409.49
410.46
415.52
425.51
426.55
427.59
432.58
437.50
438.54
451.44
452.48
470.58
471.55
472.59
543.51
555.58
563.83
577.56
578.60
579.57
609.52
400
410
420
430
440
450
460
470
480
490
500
510
520
530
540
550
560
570
580
590
600
610
m/z
[M+Na]+
[M+H]+
monoisotopic mass for C29H38N4O7 [M], 554.27

Discussion S3: Successful esterification on resin by the use of HATU

Twibanire and Grindley have reported on the esterification of carboxylic acids with both aromatic and aliphatic alcohols by exploiting uronium salt-based coupling agents, *i.e.*, TBTU, TATU and COMU, which resulted in excellent yields for the desired esters at room temperature.[6] Inspired by this study, we tried to transfer the described procedure for esterification in solution to polymeric support by using the similar uronium-based coupling agent HATU and DIPEA as base. After the required activation (20 min) of the acid by the coupling agent, HMC or HC were added and the reaction mixture was agitated for 3 h. Minicleavages followed by HPLC and ESI-MS analyses clearly showed a complete conversion of the γ-carboxylic acid precursors into the corresponding esters (exemplarily shown for compound **4** below), which emphasises the excellent properties of uronium-based coupling agents for esterification reactions not only in solution but also on resin.

Analytical HPLC runs of the crude products prior to (black) and after (red) esterification using HATU, exemplarily shown for compound 4

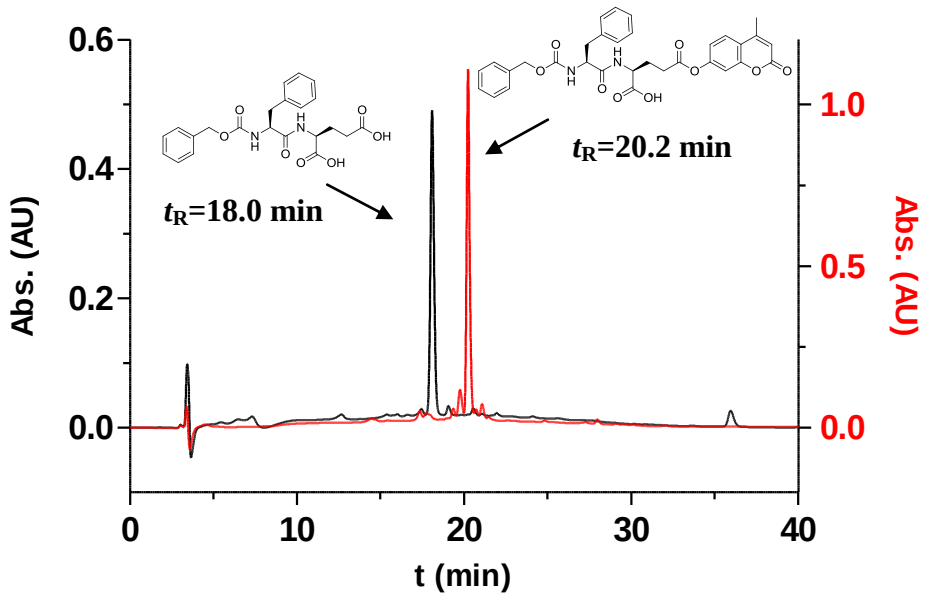

ESI(+) mass spectra of the crude products prior (top) and after (bottom) esterification

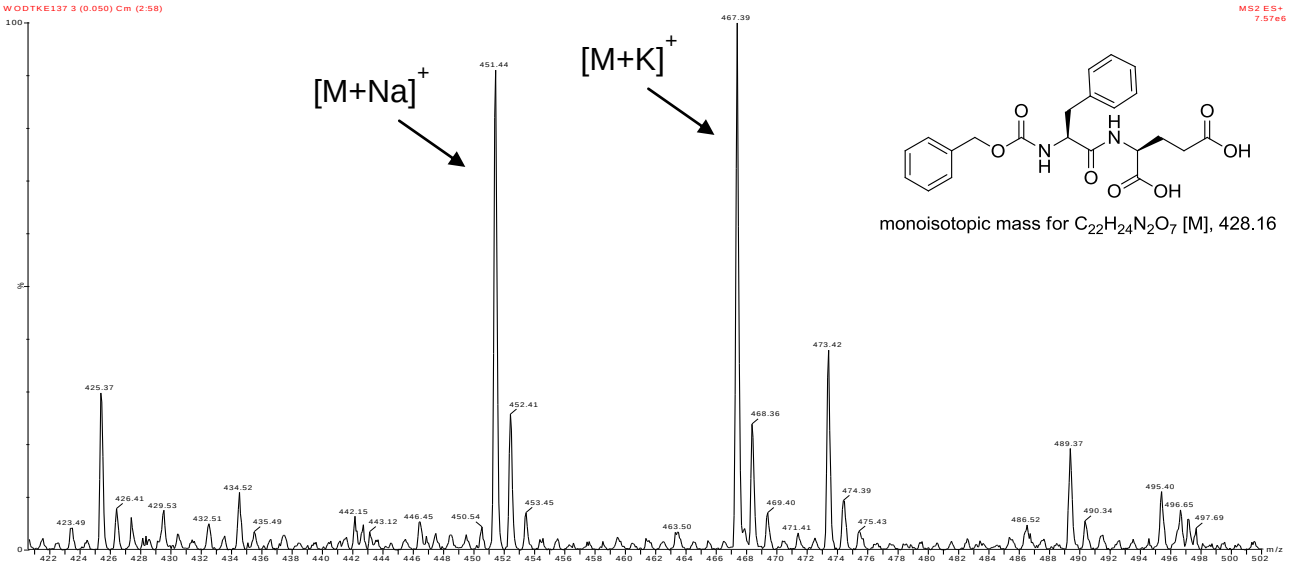

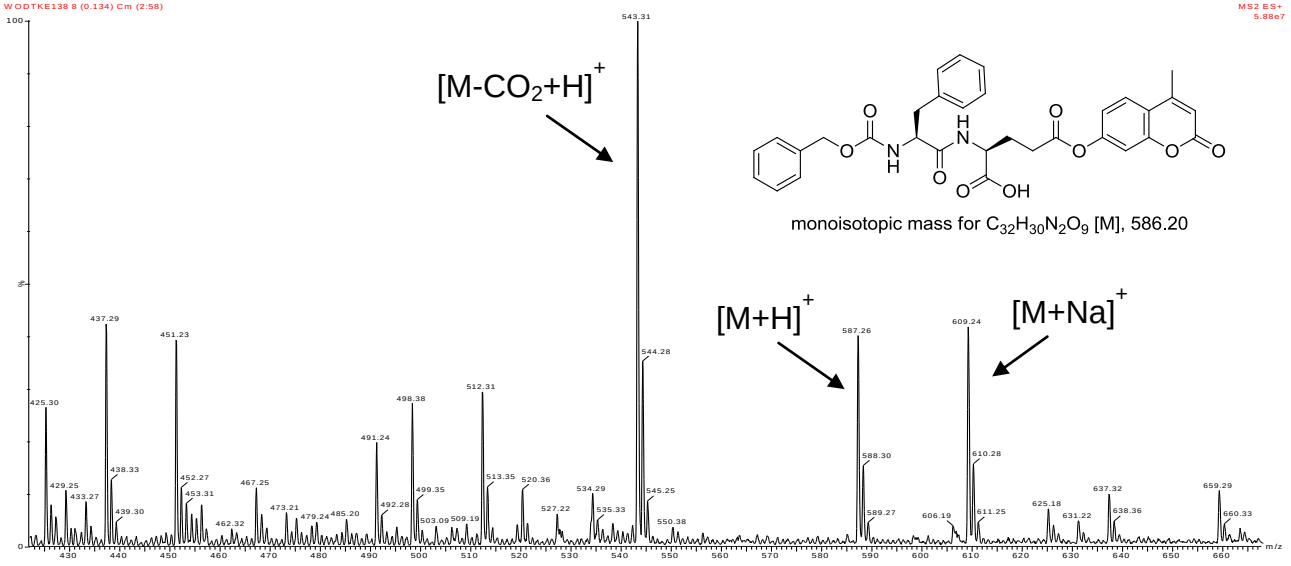

Discussion S4: Solid-phase syntheses of the fluorogenic acyl donors

Loading of Fmoc-Gly-OH / Fmoc-L-Glu(OAll)-OH onto 2-ClTrtCl resin

The synthesis was accomplished according to Barlos *et al*.[7] A solution of Fmoc-Gly-OH (I) or Fmoc-L-Glu(OAll)-OH (II) (1 mmol, 0.65 equiv.) and DIPEA (523 µL, 3 mmol, 1.95 equiv.) in CH_2Cl_2 (5 mL) was added to the pre-swollen (5 mL, CH_2Cl_2, 30 min) 2-ClTrtCl resin (1.0 g, 1.55 mmol, 1 equiv., 1.55 mmol/g) in a PP filter vessel. The PP filter vessel was sealed and agitated for 5 h at room temperature. Afterwards, the resin was successively washed with DMF (4 mL, 4×1 min), CH_2Cl_2 (4 mL, 4×1 min), CH_2Cl_2/CH_3OH/DIPEA (17:1:2, 4 mL, 3×2 min) and finally with CH_2Cl_2 (4 mL, 4×1 min) again. The resin was dried *in vacuo* overnight. The loading yields were determined by photometric quantitation of the Fmoc groups according to Gude *et al*.[8] Maximum loading yields were always achieved as calculated on the basis of the corresponding amino acid (Loading (I)=0.79 mmol/g, Loading (II)=0.74 mmol/g).

Removal of the Fmoc protecting group from 2-ClTrtCl resin loaded with Fmoc-L-Glu(OAll)-OH within the synthesis of Z-L-Glu(HMC)-OH (3)

The loaded resin (0.5 mmol Fmoc-L-Glu(OAll)-OH, 1 equiv.) was swollen in DMF (6 mL) for 30 min and then treated with 20% piperidine in DMF (5 mL, 4×10 min). Subsequently, the resin was washed with DMF (5 mL, 4×1 min), 5% DIPEA in DMF (5 mL, 4×1 min), DMF (5 mL, 4×1 min) and CH_2Cl_2 (5 mL, 4×1 min). The resin was dried *in vacuo* overnight.

Synthesis of the peptidic scaffolds

The peptides were assembled on the 2-ClTrtCl resin loaded with Fmoc-Gly-OH / Fmoc-L-Glu(OAll)-OH by microwave-assisted solid-phase peptide synthesis using the CEM Liberty 12-channel peptide synthesizer with integrated microwave reactor following a standard Fmoc protocol. The resin (0.5 mmol amino acid, 1 equiv.) was swollen in DMF (5 mL) for 30 min outside the peptide synthesizer. After transfer into the reaction vessel, the resin was swollen in CH_2Cl_2/DMF (1:1, 20 mL) for further 15 min. Removal of the Fmoc groups was performed by using a solution of 20% piperidine in DMF (1×15 mL for 30 s and 1×15 mL for 180 s, both at 35 W and 75 °C). After each treatment, the resin was washed with DMF (5+60 mL). Coupling of each amino acid was performed by combining two solutions: 0.45 M HBTU in DMF (4 mL, 3.6 equiv.) and 2 M DIPEA in NMP (2 mL). The amino acids were applied as 0.2 M solutions in DMF. 10 mL (4 equiv.) of these solutions were taken for the coupling steps (300 s at 25 W and 75 °C). After each coupling step, the peptidyl resin was washed with DMF (60 mL). After completed

synthesis and final Fmoc deprotection, the resin was washed with ethanol (4×5 mL) and CH_2Cl_2 (4×5 mL) outside the peptide synthesizer.

Procedure for Z protection

The synthesis was accomplished according to Mahoney *et al.*[9] The peptidyl resin (0.5 mmol peptide, 1 equiv.) was swollen in CH_2Cl_2 (4 ml) for 30 min followed by addition of DIPEA (183 µL, 1.05 mmol, 2.1 equiv.) in CH_2Cl_2 (2.5 mL) and Z-OSu (262 mg, 1.05 mmol, 2.1 equiv.) in CH_2Cl_2 (2.5 mL). The resulting suspension was agitated for 16 h at room temperature. The peptidyl resin was washed with DMF (5 mL, 4×1 min) and CH_2Cl_2 (5 mL, 4×1 min) and dried *in vacuo* overnight.

Removal of Allyl protecting group

The peptidyl resin (0.5 mmol peptide, 1 equiv.) was swollen in CH_2Cl_2 (6 mL) for 30 min and then suspended in CH_2Cl_2/NMM/CH_3COOH (8:2:1, 6 mL). After 2 min of degassing with Ar, $Pd(PPh_3)_4$ (173 mg, 0.15 mmol, kept under Ar atmosphere) was added to the mixture and the formed yellow suspension was degassed for further 2 min with Ar. The PP filter vessel was sealed and agitated for 4 h. The suspension was filtered and the peptidyl resin was successively washed with CH_2Cl_2 (5 mL, 4×1 min), DMF (5 mL, 4×1 min), 0.5% w/v sodium diethyldithiocarbamate in DMF (5 mL, 6×1 min) and, finally, with DMF (5 mL, 5×1 min) again and dried *in vacuo* overnight.

Coupling of coumarin derivatives

The on-resin esterification was accomplished according to the method of Twibanire and Grindley[6] for esterification in solution. The peptidyl resin (0.5 mmol peptide, 1 equiv.) was swollen in DMF (6 mL) for 30 min followed of degassing with Ar for another 5 min. Then, DIPEA (226 µL, 1.3 mmmol, 2.6 equiv.) and HATU (247 mg, 0.65 mmol, 1.3 equiv.) were added and the resulting suspension was agitated for 20 min. After that, the coumarin derivative (0.65 mmol, 1.3 equiv.) dissolved in DMF (1.5 mL) was added. The mixture was agitated for 3 h at room temperature. The peptidyl resin was washed with DMF (5 mL, 4×1 min) and CH_2Cl_2 (5 mL, 4×1 min) and dried *in vacuo* overnight.

Cleavage of resin bond

TFA-Minicleavage

The cleavage was accomplished according to Seebach *et al*.[10]. The synthesis steps after assembly of the peptides, except the couplings of coumarin derivatives, were monitored by subjecting small portions to cleavage from resin after each step and analysis by ESI-MS. For this purpose, the dry peptidyl resin

was suspended in 1 mL of a solution of TFA/TES/H_2O (95:2.5:2.5) for 30 min. After filtering, the resin was washed with TFA (2×1 mL) and the combined filtrates were evaporated in a N_2 stream.

HFIP-Minicleavage

The cleavage was accomplished according to Bollhagen *et al.*[11] The couplings of the coumarin derivatives were monitored by subjecting small portions to cleavage from resin and analysis by ESI-MS. For this purpose, the dry peptidyl resin was swollen in CH_2Cl_2 (2 mL) for 30 min, followed by repetitive treatments with a solution of HFIP/CH_2Cl_2 (1:4, 1 mL, 3×10 min). The filtrates were collected and evaporated in a N_2 stream.

Full-cleavage

The cleavage was accomplished according to Bollhagen *et al.*[11] The dry peptidyl resin was swollen in CH_2Cl_2 (5 mL) for 30 min, followed by repetitive treatments with a solution of HFIP/CH_2Cl_2 (1:4, 5 mL, 3×10 min). The filtrates were collected and evaporated in a N_2 stream and the obtained crude products were purified by preparative RP-HPLC.

Discussion S5: Investigations on the formation of compound 5c under different coupling conditions

To increase the yield for obtaining coumarinyl amide **5c**, an attractive alternative appeared to be the use of *N*,*N*'-carbonyldiimidazole (CDI) as coupling reagent in the presence of imidazole•HCl as acid catalyst, which was recently described by Woodman *et al.*[12] for the coupling of aromatic amines. Noteworthy, neither formation of the desired product nor side products could be observed (**B**). Recently, Vendrell *et al.*[13] demonstrated the successful amidation of the side chain carboxylic group of resin-bound glutamate with aromatic amines by using the strong activating agent *N*,*N*'-tetramethylchloroformamidinium chloride (TMUCl Cl), which even allowed for amide coupling with weakly nucleophilic amines such as *p*-nitroaniline. Indeed, application of these conditions for the amidation with AMC led to the formation of compound **5c**, but, similar to the coupling procedure with HATU, only minor amounts of **5c** were obtained (3%), despite formation of side products was less pronounced (**C**). Surprisingly, the amount of crude product after HFIP-mediated cleavage from resin was significantly lower than expected, which indicates undesired cleavage of peptide during the amidation procedure. Since the 2-chlorotrityl ester is highly acid-labile, HCl released from TMUCl Cl upon reaction with the carboxylic group might lead to partial cleavage of this bond. To prove this assumption, Z-Glu-Gly-OH was assembled at Wang resin followed by amidation using TMUCl Cl and AMC. However, instead of coumarinyl amide **5c**, the respective glutarimide **5d** of Z-Glu-Gly-OH was observed as main product which was not formed during amidation on 2-ClTrtCl-resin (**D**). In consequence, it might be more advantageous to use the respective Fmoc/Z-Glu(AMC)-OH building block for the synthesis of Z-Glu(AMC)-Gly-OH (**5c**) than performing the amidation reaction on resin.[14] However, the amounts of **5c** obtained by the synthetic methods outlined above were sufficient for initial investigations concerning its behaviour towards TGase 2.

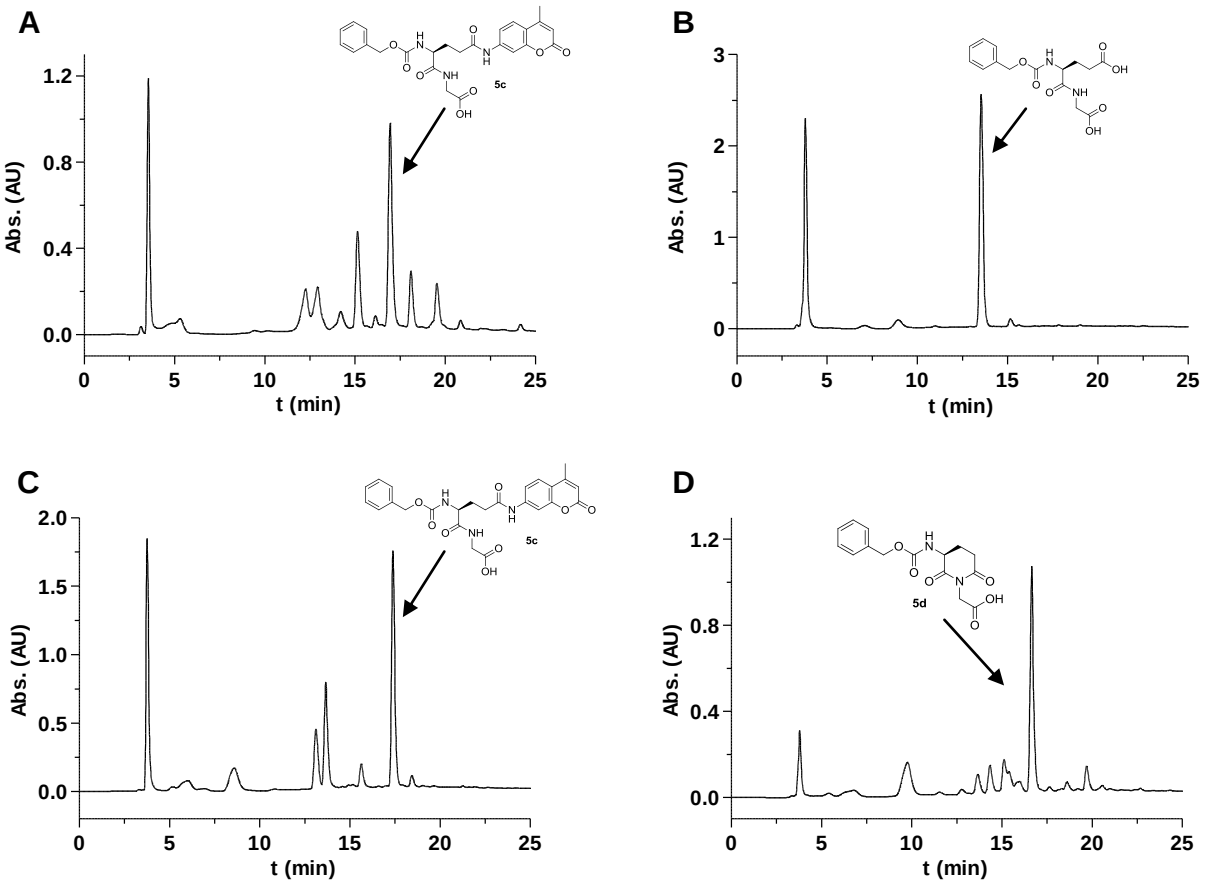

HPLC profiles (214 nm) of the crude products obtained by coupling of AMC to Z-Glu-Gly-O-resin under different conditions. **A**) Z-Glu-Gly-O-2ClTrtCl resin, HATU, DIPEA, DMF, 5 h; 7.3 mg (3%) of compound **5c** were obtained. **B**) Z-Glu-Gly-O-2ClTrtCl resin, CDI, imidazole•HCl, NMP, 4 h; only starting material Z-Glu-Gly-OH could be identified. **C**) 1. Z-Glu-Gly-O-2ClTrtCl resin, TMUCl Cl, DIPEA, CH_2Cl_2/DMF (1:2.5, v/v), 30 min, 2. AMC, DMF, 3 h; 4.5 mg (3%) of compound **5c** were obtained. **D**) 1. Z-Glu-Gly-O-Wang resin, TMUCl Cl, DIPEA, CH_2Cl_2, 30 min, 2. AMC, CH_2Cl_2/DMF (1:2.5, v/v), 3 h; 8.1 mg (13%) of glutarimide **5d** were obtained.

Figure S4

Solubility of the glutamate-derived acyl donors 3-6

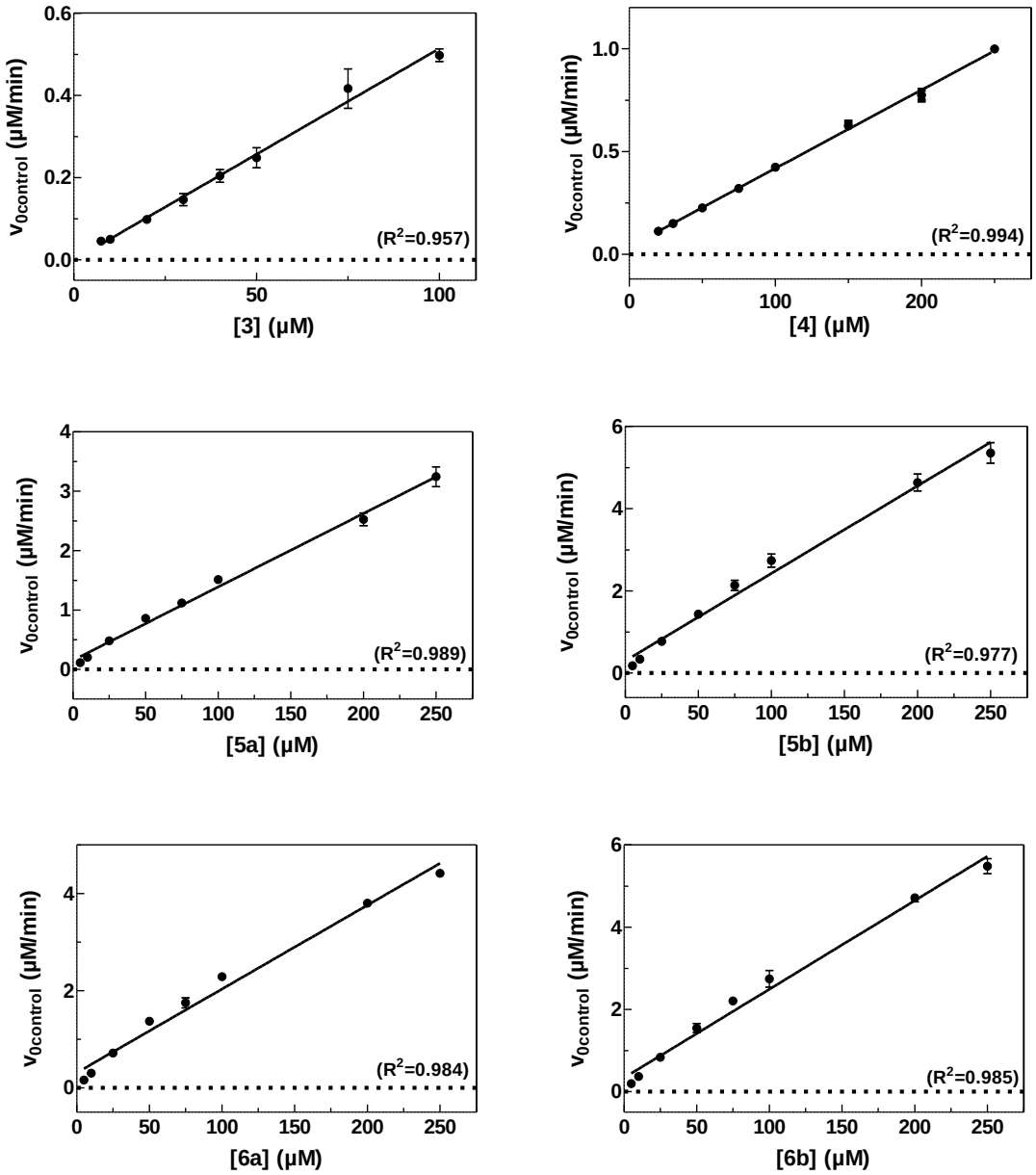

Plots of $v_{0control}$=f([acyl donor]) at pH=8.0 and 30 °C in the presence of 5% DMSO and 500 µM DTT with the respective regression coefficients for the linear regressions (—) to the experimental data. Data (●) shown are mean values of at least 2 separate experiments, each performed in duplicate. When not apparent, error bars are smaller than the symbols.

Figure S5

Determination of pseudo-first-order rate constants (k_{obs}) for the spontaneous reactions of compounds 2-6

Plots of $v_{0control}$=f([acyl donor]) with the respective k_{obs} values (mean values ± SEM) obtained by linear regression (—) to the data. Data points (●) are mean values of two or three independent measurements each performed in duplicate. When not apparent, error bars are smaller than the symbols. Conditions: pH=8.0, 30 °C, 5% DMSO, 500 µM DTT (**left column**) or 500 µM TCEP (**right column**).

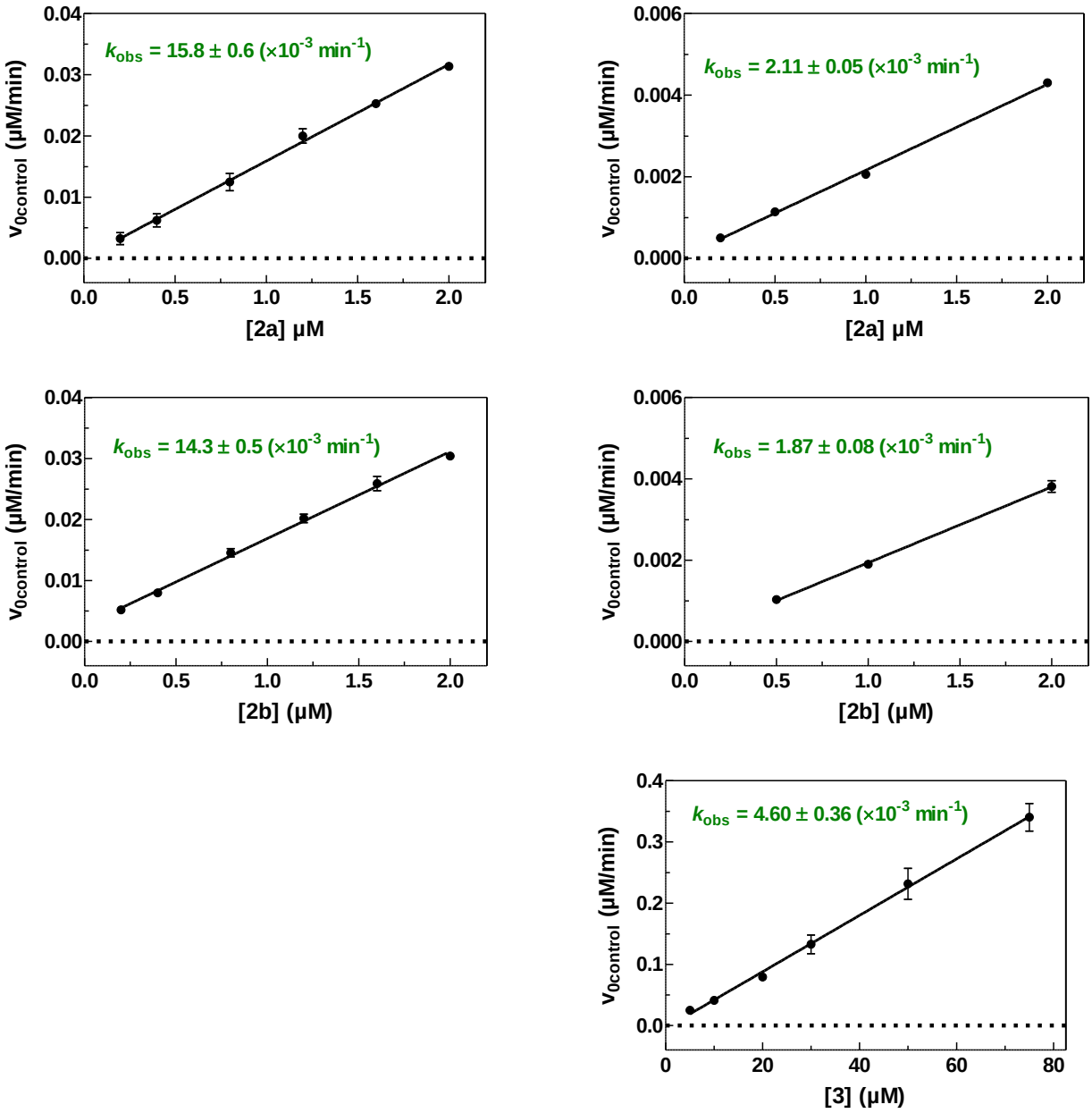

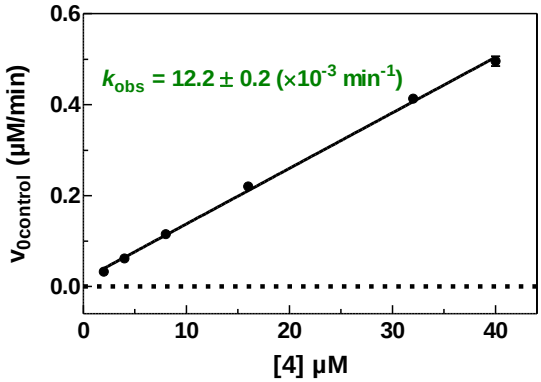
k_{obs} = 12.2 ± 0.2 (×10^{-3} min^{-1})
$v_{0control}$ (μM/min)
[4] μM

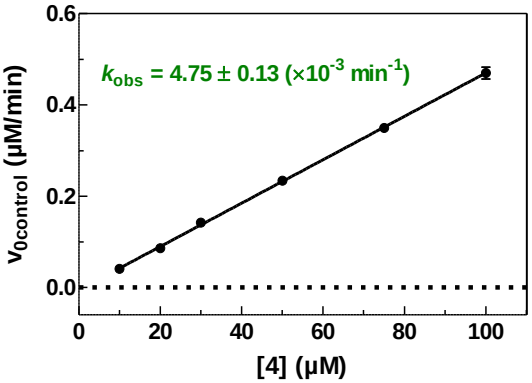
k_{obs} = 4.75 ± 0.13 (×10^{-3} min^{-1})
$v_{0control}$ (μM/min)
[4] (μM)

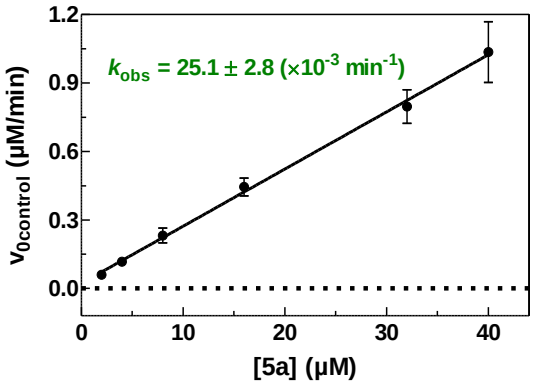
k_{obs} = 25.1 ± 2.8 (×10^{-3} min^{-1})
$v_{0control}$ (μM/min)
[5a] (μM)

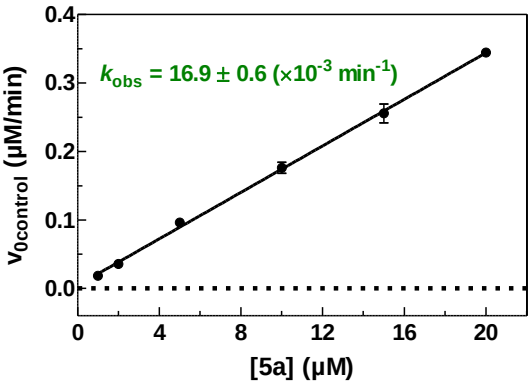
k_{obs} = 16.9 ± 0.6 (×10^{-3} min^{-1})
$v_{0control}$ (μM/min)
[5a] (μM)

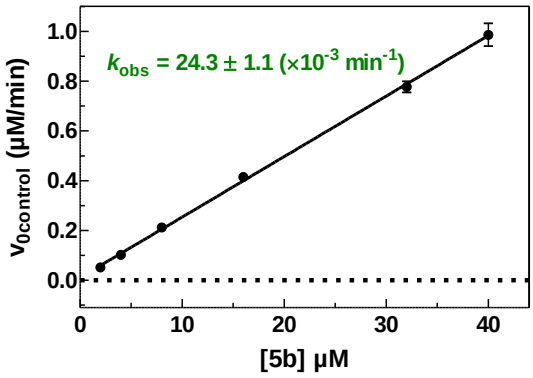
k_{obs} = 24.3 ± 1.1 (×10^{-3} min^{-1})
$v_{0control}$ (μM/min)
[5b] μM

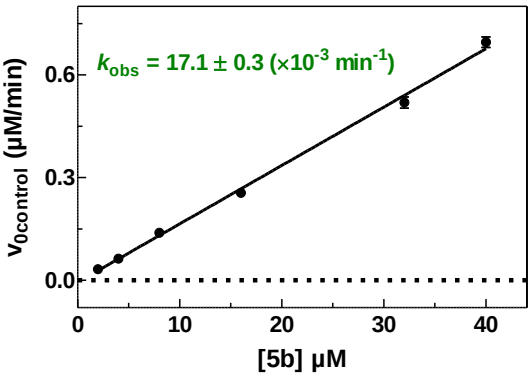
k_{obs} = 17.1 ± 0.3 (×10^{-3} min^{-1})
$v_{0control}$ (μM/min)
[5b] μM

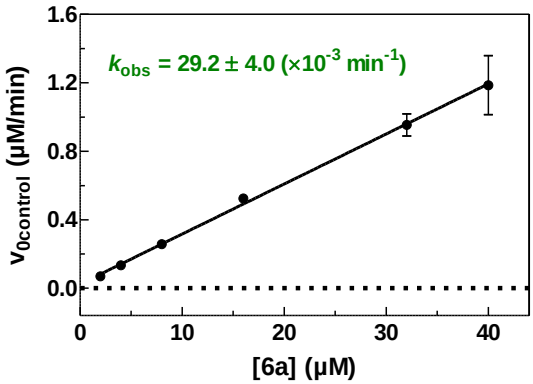
k_{obs} = 29.2 ± 4.0 (×10^{-3} min^{-1})
$v_{0control}$ (μM/min)
[6a] (μM)

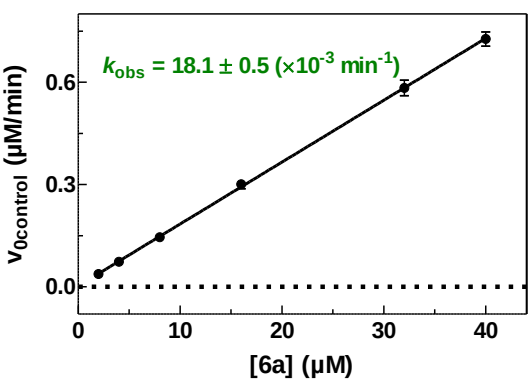
k_{obs} = 18.1 ± 0.5 (×10^{-3} min^{-1})
$v_{0control}$ (μM/min)
[6a] (μM)

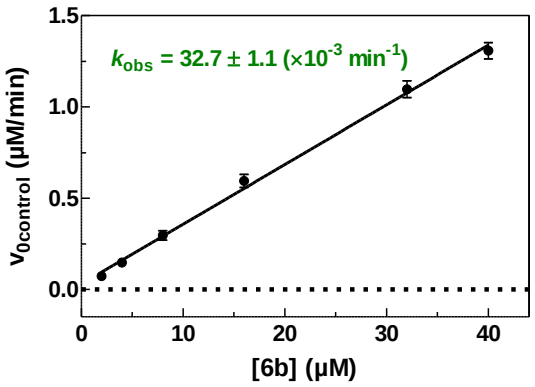

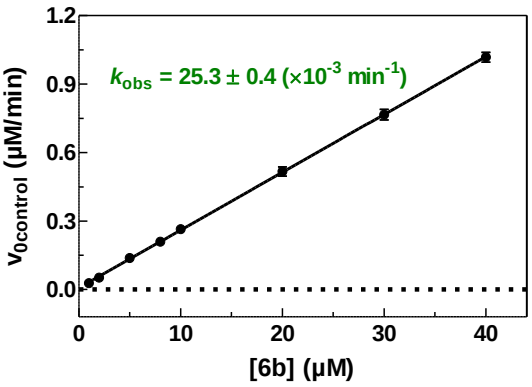

Postulated mechanistic model to explain the high tendency for spontaneous decay of compounds with C-terminal glycine residue

Hypothetic 11-membered ring intermediate composed of acyl donor **5b** and one water molecule which might support the deprotonated carboxylic group to act as intramolecular general base in substrate compounds with C-terminal glycine residue. Analogous structures for the compounds with a C-terminal glutamate residue might be less favoured due to conformational strain (11- *vs* 8-membered ring).

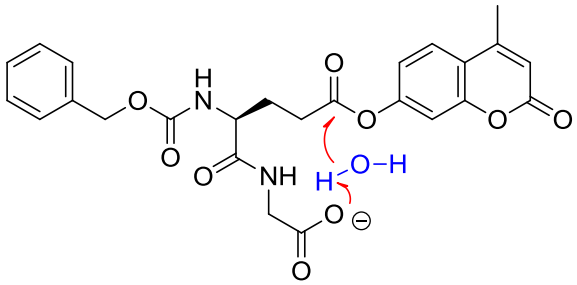

Figure S6

Determination of retention times of 5b and potential reaction products

To determine the retention time of **5b** in the HPLC system described in the main article, 50 µL of a solution of the compound in acetonitrile (2 mM) were injected into the HPLC apparatus. To identify the retention time of the **5b**-derived hydrolysis product, a solution of **5b** (2 mM) in a mixture of acetonitrile and 0.1 M NaOH (1:1, v/v) was incubated for 1 h at room temperature. An aliquot of 50 µL was withdrawn and subjected to HPLC analysis. Independent of MS analysis, the glutarimide product (**5d**) arising from cyclisation of **5b** was identified by injecting a 2 mM solution of the authentic compound **5d** in acetonitrile into the HPLC device. To quantitatively determine the extent of cyclisation under assay conditions, aliquots of 5 to 50 µL of that solution were injected and the peak areas were correlated to the amount of substance by linear regression (see inset of **B**).

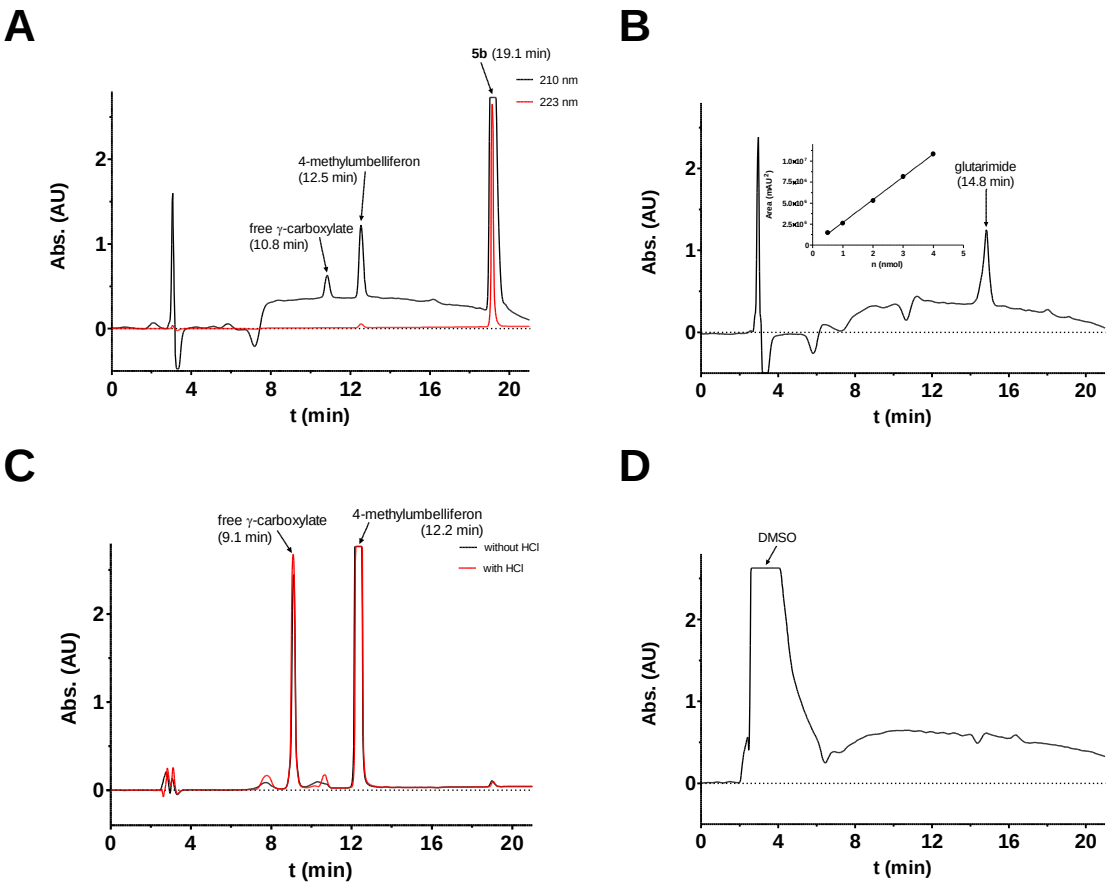

HPLC profiles (210 nm) for investigations of authentic compounds in the HPLC system used to detect products of spontaneous and enzymatic reactions of **5b** for identification of retention times. **A**) Compound **5b**. Compared to detection at 223 nm, the hydrolysis products that are formed in tiny amounts during purification of **5b** are clearly visible at 210 nm. **B**) Glutarimide **5d**. The inset shows the calibration diagram for the peak area *vs.* the amount of **5d**. The chromatogram corresponds to the injection of 4 nmol of **5d** (40 µL of a 100 µM solution in acetonitrile). **C**) Analysis of **5b** after total hydrolysis (2 mM **5b** in 0.1 M NaOH/acetonitrile 1:1 after 1h at room temperature). The difference in the retention time of more than 1 min for the free γ-carboxylic acid derived from **5b** in **A** and **C** is probably caused by different solvents: while an aqueous solution was injected in **C**, **5b** was dissolved in acetonitrile in **A** (also compare Figures S7A and C and Figures S7B and D). **D**) HPLC analysis of assay buffer (100 mM MOPS pH=8.0, 3 mM $CaCl_2$, 50 µM EDTA) containing 5% DMSO.

Figure S7

Reaction of 5b with DTT in acetonitrile

Reactivity towards thiols and tendency of cyclisation were investigated by incubating a solution of **5b** (2 mM) and triethylamine (2 mM) in acetonitrile at room temperature in the absence or presence of DTT (20 mM), respectively. After different times (see below) aliquots of 50 µL were withdrawn and subjected to HPLC analysis. Eluate solutions corresponding to peaks, which represented components of interest, were collected and analysed by ESI-MS. The DAD-recorded chromatograms were analysed by extracting profiles at a wavelength of 210 nm. UV/Vis spectra were retrieved for peaks of interest.

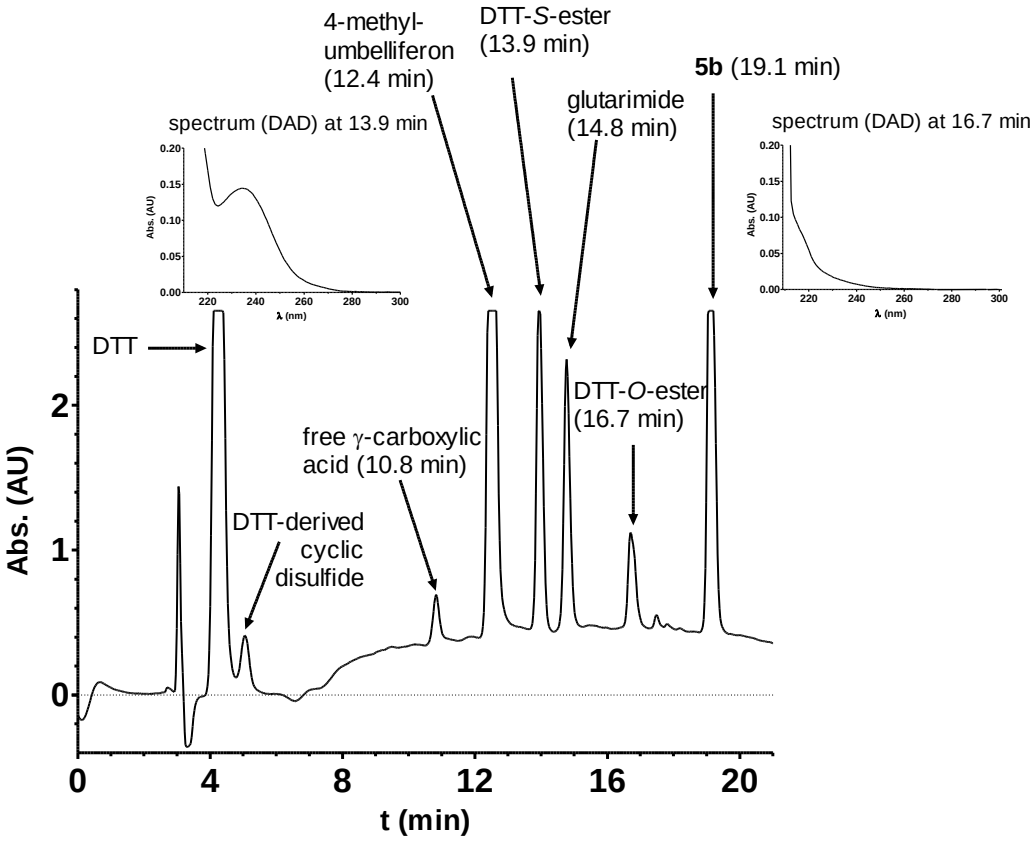

HPLC profile (210 nm) of the mixture for the reaction of **5b** (2 mM) with DTT (20 mM) in the presence of triethylamine (2 mM) in acetonitrile after 5 h at room temperature. The peaks were identified on the basis of authentic compounds (**5b**, 4-methylumbelliferon and glutarimide) and by ESI-MS analysis of the collected eluate. The peaks of the isomeric DTT-*S*- and -*O*-esters were unequivocally assigned by considering their DAD-recorded UV/Vis spectra (see insets). The thioester functionality causes absorption in the range of 230-240 nm[15], which can only be observed for the peak at 13.9 min, while the isomeric peak at 16.7 min is devoid of the shoulder in that range. The detected DTT-*O*-ester arises from *S*→*O* acyl migration of the corresponding thioester according to studies by Gates *et al.* who investigated the formal hydrolysis of peptide thioesters by mercaptoethanol and DTT. The DTT-*O*-ester can form the free carboxylic acid by intramolecular nucleophilic attack of the thiol sulphur at C-2 of the DTT moiety under thiirane ring formation.[16]

Figure S8

Reactivity of 5b under assay conditions in the absence and presence of DTT

To detect products of spontaneous reactions under assay conditions, a solution of **5b** (400 µM) and DTT (500 µM, **C**) or TCEP (500 µM, **D**) in assay buffer pH=8.0 containing 5% DMSO was incubated at 30 °C. After 1 h, an aliquot of 50 µL was withdrawn and subjected to HPLC analysis.

The results confirm the reactivity of the coumarinyl ester-based substrates towards DTT and thus a considerable contribution of thiolysis to the overall rates of the spontaneous reactions. In general, TCEP as antioxidant bears the advantages of higher stability at pH>7.5 and greater reduction potential at pH<8 compared to DTT.[17] Glutarimide formation from **5b** under assay conditions was unexpected, however, this kind of cyclisation has been occasionally observed during solid-phase synthesis of glutamate-containing peptides using the Fmoc strategy.[18] Glutarimides have, furthermore, been identified as intermediates during the deamidation of glutamine-containing peptides under physiological conditions.[19] Glutarimide formation may potentially account for the observed higher rates of spontaneous disintegration of the glycine containing substrates. When **5b** is subjected to assay conditions in the absence of TGase 2, the calculated concentration of the glutarimide allowed for the conclusion that only 3% of the substrate is transformed by cyclisation (see below).

HPLC analyses towards the spontaneous reactivity of **5b** in acetonitrile (**A**, **B**) and under assay conditions (**C**, **D**) in the presence (**A**, **C**) and absence (**B**, **D**) of DTT. The black trace in **A** is identical to Figure S7 **B)** HPLC profiles (210 nm) of the mixture for the reaction of **5b** (2 mM) in the presence of triethylamine (2 mM) in acetonitrile after 5 h and 21 h at room temperature. **C)** HPLC profiles (210 nm) of the mixture of **5b** (400 µM) dissolved in DTT-containing assay medium (100 mM MOPS pH=8.0, 3 mM $CaCl_2$, 50 µM EDTA, 500 µM DTT) after 0 and 1 h at 30 °C. On the basis of the k_{obs} value (24.3×10^{-3} min^{-1}, see **Table 1** in the main article), it can be calculated that a concentration of 306.9 µM of **5b** has been consumed after 1 h (equation SI). From the area under the peak representing glutarimide **5d** a concentration of 9.3 µM was calculated, which corresponds to 3.0% of the total concentration of **5b**-derived reaction products. Under the simplified assumption of a first-order process without parallel reactions (not correct in reality) for the cyclisation of **5b** to glutarimide **5d**, a rate constant of 3.9×10^{-4} min^{-1} can be calculated for the cyclisation reaction (equation SII). Thus, glutarimide formation does only contribute to a minor extent to the increased susceptibility of the glycine-containing substrates to spontaneous disintegration. **D)** HPLC profile (210 nm) of the mixture of **5b** (400 µM) dissolved in TCEP-containing assay medium (100 mM MOPS pH=8.0, 3 mM $CaCl_2$, 50 µM EDTA, 500 µM TCEP) after 1 h. According to the k_{obs} value of 17.1×10^{-3} min^{-1} (see **Table 1** in the main article) a concentration of 256.6 µM of **5b** has been consumed after 1 h. From the area under the peak representing glutarimide

5d a concentration of 14.3 µM was calculated, which corresponds to 5.6% of the total concentration of **5b**-derived reaction products.

$$c = c_0 \cdot e^{-k_{obs}t} \qquad \text{(SI)}$$

$$c = c_\infty(1 - e^{-k_{obs}t})$$

$$k_{cycl} = -\frac{ln\frac{c_\infty - c}{c_\infty}}{t} \qquad \text{(SII)}$$

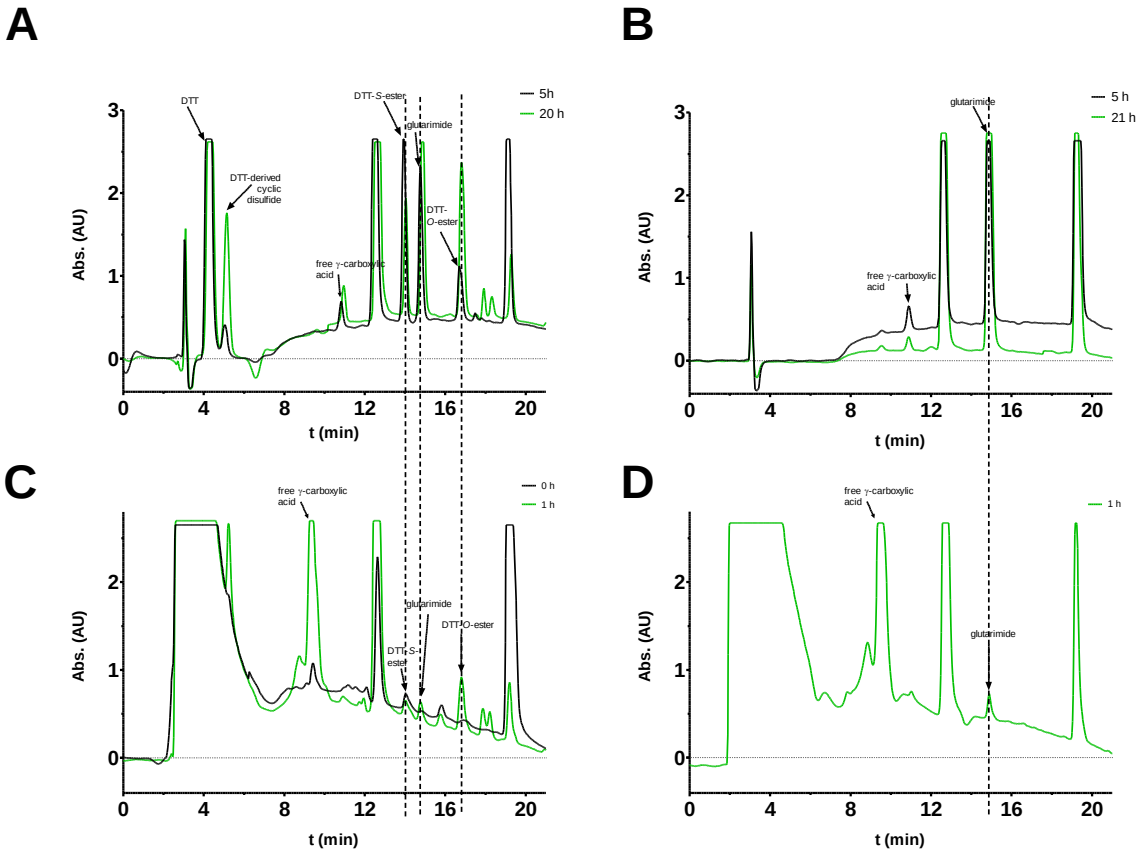

Figure S9

Selwyn test for gpTGase 2 by measurement of enzymatic hydrolysis

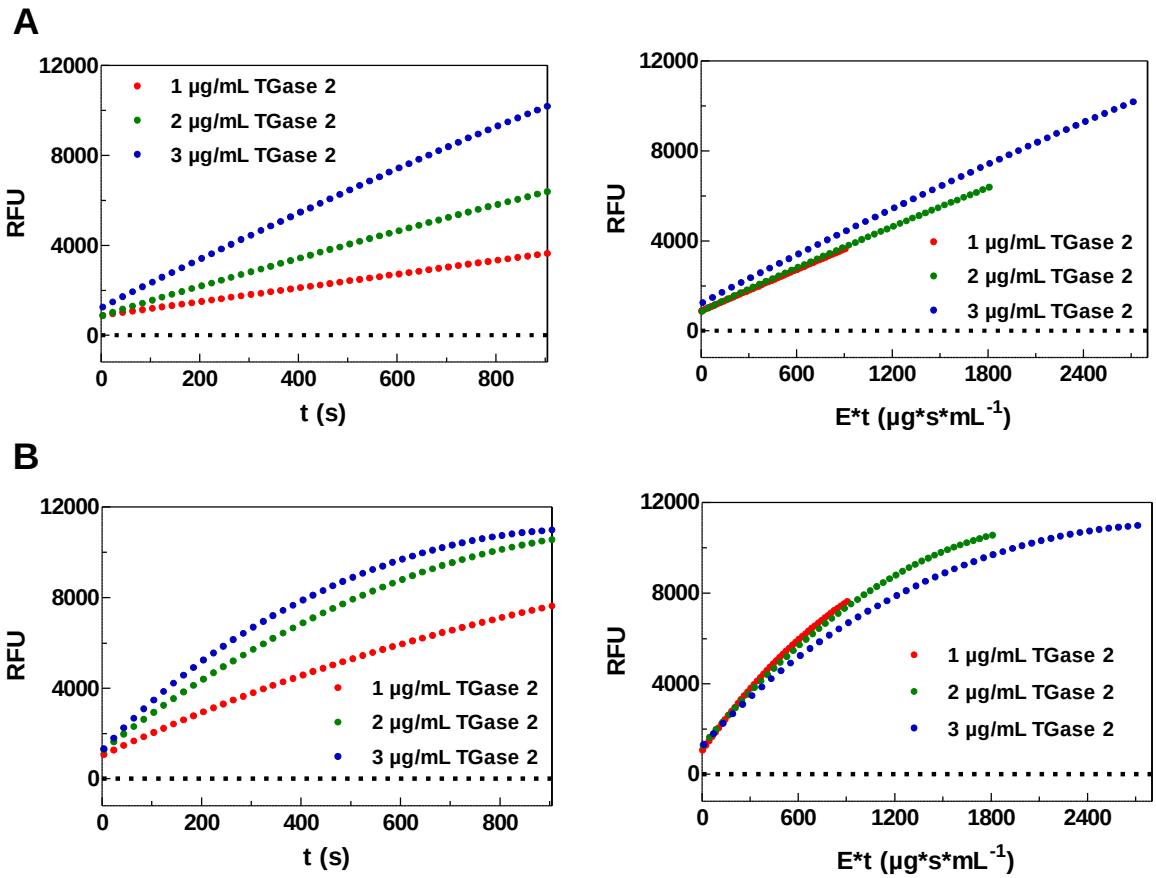

A) pH=6.5, 30 °C, 5% DMSO, 500 µM TCEP with compound **5b** (25 µM) as acyl donor; **B)** pH=8.0, 30 °C, 5% DMSO, 500 µM TCEP with compound **5b** (25 µM) as acyl donor. The data reveal that enzyme inactivation does not occur, neither at pH=6.5 nor pH=8.0, over 900 s as the plots of RFU=f(E*t) show no increasing slope with higher enzyme concentrations but almost a single trace.

Figure S10

Comparison of enzymatic and spontaneous rates at different concentrations of gpTGase 2

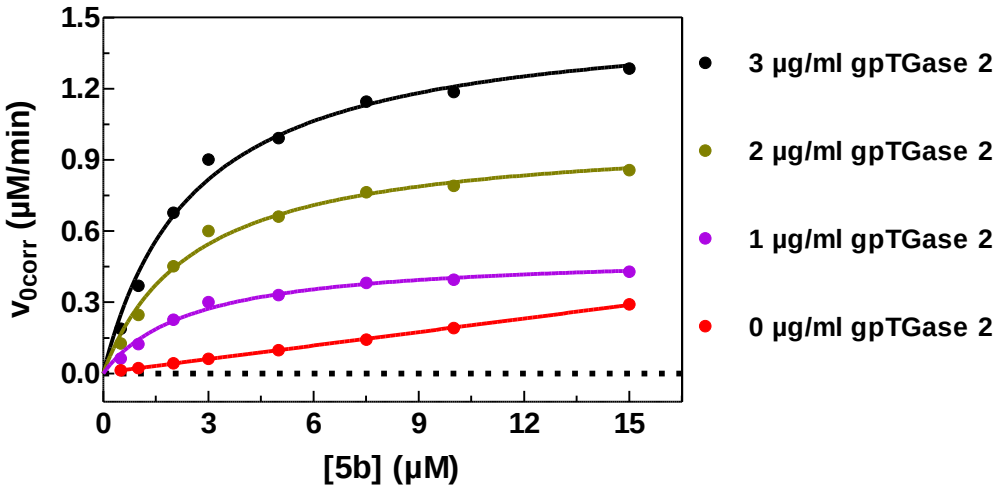

Plots of v_{0corr}=f([**5b**]) at different concentrations of gpTGase 2. Data shown for 0 and 3 µg/ml gpTGase 2 are mean values of three independent measurements each performed in duplicate. When not apparent, error bars are smaller than the symbols. Data shown for 1 and 2 µg/ml gpTGase 2 were calculated on the basis of the data for 3 µg/ml gpTGase 2. Conditions: pH=8.0, 30 °C, 5% DMSO, 500 µM DTT.

Figure S11

gpTGase 2-catalysed hydrolyses of the acyl donors 3-6 at pH=8.0

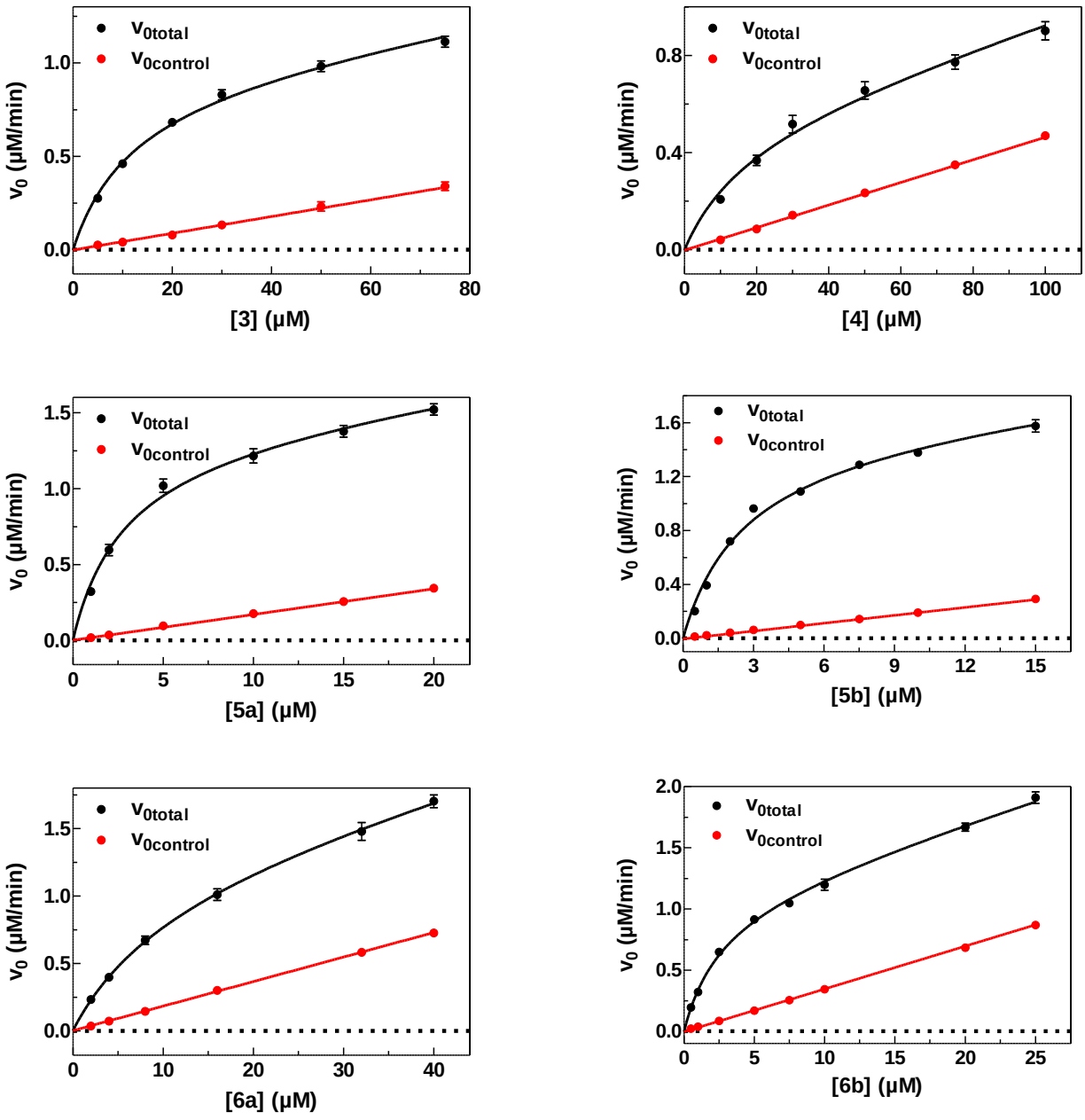

Plots of v_{0total}=f([acyl donor]) and $v_{0control}$=f([acyl donor]) with the results of a regression according to the global fit model to determine the kinetic parameters of the enzymatic hydrolyses. Data shown are mean values of three independent measurements each performed in duplicate. When not apparent, error bars are smaller than the symbols. Conditions: pH=8.0, 30 °C, 5% DMSO, 500 µM DTT (for **5b** and **6b**) or 500 µM TCEP (for **3**, **4**, **5a** and **6a**), 3 µg/mL gpTGase 2.

Figure S12

hTGase 2-catalysed hydrolyses of the acyl donors 5a, 5b and 6b at pH=8.0

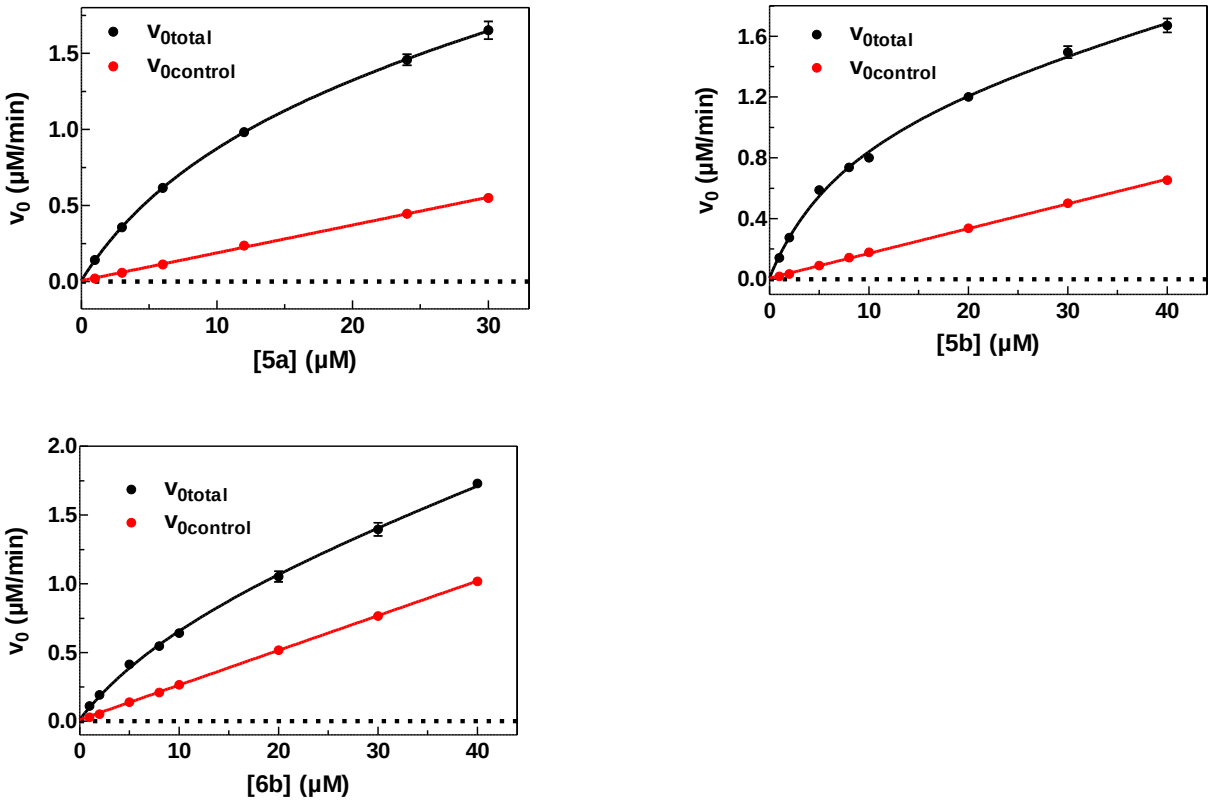

Plots of v_{0total}=f([acyl donor]) and $v_{0control}$=f([acyl donor]) with the results of a regression according to the global fit model to determine the kinetic parameters of the enzymatic hydrolyses. Data shown are mean values of three independent measurements each performed in duplicate. When not apparent, error bars are smaller than the symbols. Conditions: pH=8.0, 30 °C, 5% DMSO, 500 µM TCEP, 3 µg/mL hTGase 2.

Figure S13

Alignment of the protein sequences for the TGase 2 orthologues from *Cavia cutleri* and *Homo sapiens*. Identical positions are denoted by asterisks, similar positions by dots and different positions by colons. Colour coding of amino acids is according to aliphatic, aromatic, positively and negatively charged residues. Identical residues are present in 575 positions, which corresponds to 83.2% of sequence identity.

The alignment was done by using the Clustal Omega programme, as implemented in the web-based portal of the UniProt database[1], using the UniProt identifier codes P08587 (gpTGase 2) and P21980 (hTGase 2).

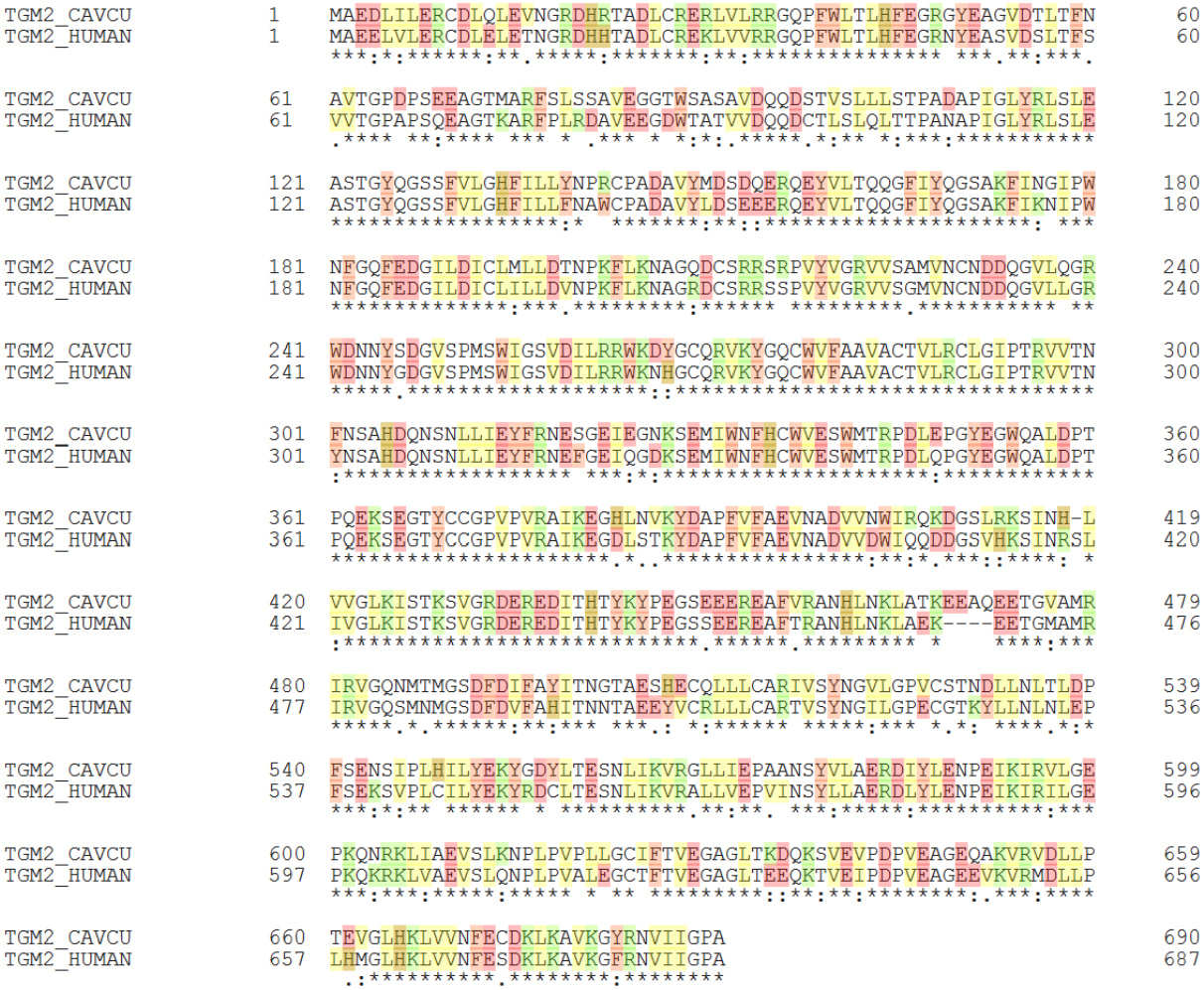

[1] *www.uniprot.org*

Discussion S6: Investigations on coumarinyl amide 5c

Initial investigations with respect to enzymatic and nonenzymatic conversions of 5c

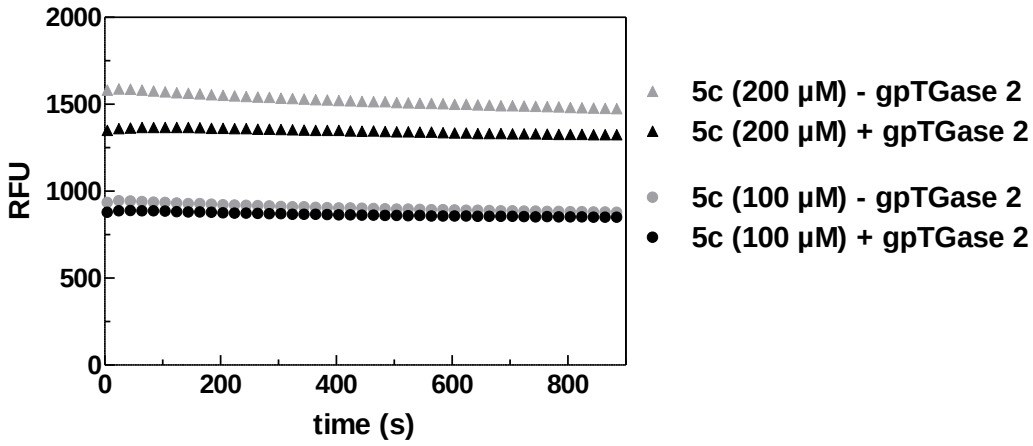

Plots of RFU=f(t) for two different concentrations of **5c** at pH=8.0 and 30 °C in the presence of 5% DMSO, 500 µM TCEP, 400 µM aminoacetonitrile and 3 µg/mL gpTGase 2 or enzyme buffer. Obviously, there is neither spontaneous nor enzymatic release of AMC over the period of 900 s.

Hydrolysis of acyl donor 5b in the presence of 5c

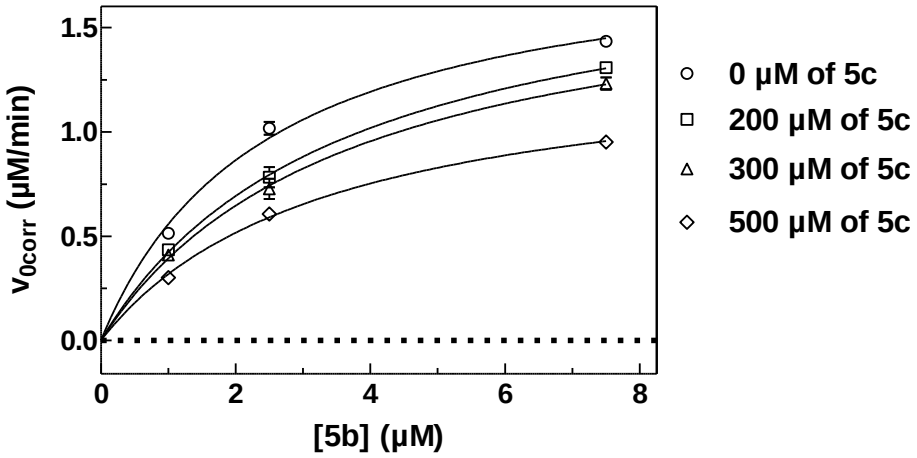

Plot of v_{0corr}=f([**5b**]) in the presence of different fixed concentrations of **5c** with nonlinear regressions using equation III (Michaelis-Menten). Data shown are mean values of one experiment which was performed in duplicate. Conditions: pH=8.0, 30 °C, 5% DMSO, 500 µM TCEP, 3 µg/mL gpTGase 2.

Analysis of the inhibitory behaviour of 5c

Double reciprocal plots ($1/v_{0corr}$ *versus* 1/[**5b**]) at different fixed concentrations of coumarinyl amide **5c** gave a family of lines which intersect to the left of the $1/v_{0corr}$-axis (**A**). As the replots of the obtained slopes and $1/v_{0corr}$ intercepts from the double reciprocal plots *versus* the concentration of **5c** appear linear and exhibit different intercepts on the abscissa (**B**), the coumarinyl amide seems most likely to act as a linear (β=0) mixed, predominantly specific ($1<\alpha<\infty$) inhibitor according to the systematic classification of enzyme-modifier interactions suggested by Baici[20] [2] (**D**). This is further supported by the Dixon plot which showed linear curves at all substrate concentrations with a shared interception point above the abscissa (**C**).[21] Analysis of the Dixon plot revealed a K_i value of 583 µM for compound **5c**. This in turn means that all concentrations of **5c** studied are below its respective K_i value. However, investigations at higher inhibitor concentrations are restricted due to inherent solubility of **5c**. For this reason, it cannot be completely proven whether the ternary enzyme-substrate-inhibitor complex (ESI) is indeed inactive (β=0) or shows residual catalytic activity ($0<\beta<1$). In general, the proposed mixed inhibition type for $\alpha>1$ and β=0 implicates binding of the inhibitor to the substrate binding site and in addition binding to a distinct site at the enzyme-substrate complex with less affinity. The reason for the aberrant kinetic behavior of **5c** compared to the natural amide substrates for TGase 2 might be due to the increased sterical demand of the chromene moiety, which prevents acylation of the enzyme. This seems to be contradictory to the results for the coumarinyl esters in this study which require a similar spatial demand but were all efficiently converted by TGase 2. However, their high acylation potential might arise from their high intrinsic reactivity as aliphatic coumarinyl esters can be considered as active esters.

Based on the structural analogy of **5c** and **5b**, the K_i value of the former compound should correlate with the K_d value (*i.e.*, the affinity of the Michaelis complex) of the latter one (**D**). At a first glance, this high K_d value seems to be contradictory to the low K_m value determined for **5b** (2.53 µM). However, for enzymes such as TGase 2 that pass through an acyl enzyme intermediate adhering to the kinetic model shown in **Scheme 5** in the main article, K_m has the following significance according to Wilson and Alexander[22]:

$$K_{\mathrm{m}} = \frac{k_{-1}+k_{\mathrm{acyl}}}{k_1*(1+\frac{k_{\mathrm{acyl}}}{k_{\mathrm{deacyl}}})} \qquad \text{(SIII)}$$

Given that $K_d=k_{-1}/k_1$ and assuming that $k_{acyl}<<k_{-1}$, this equation can be simplified according to Hillman and Mautner[23] as follows:

$$K_{\mathrm{d}} = K_{\mathrm{m}} * \left(1+\frac{k_{\mathrm{acyl}}}{k_{\mathrm{deacyl}}}\right) \qquad \text{(SIV)}$$

[2] According to that system for classification of enzyme-modifier interactions, competitive inhibition is referred to as specific inhibition whereas noncompetitive inhibition is referred to as catalytic inhibition.

Moreover, as both k_{cat} and K_m of **5b** (and also the other acyl donors) increase in the presence of aminoacetonitrile (see below), the rate for acylation must be greater than that for deacylation ($k_{acyl}>k_{deacyl}$),[24] which in turn leaves to conclude that $K_d>K_m$ or even $K_d>>K_m$.

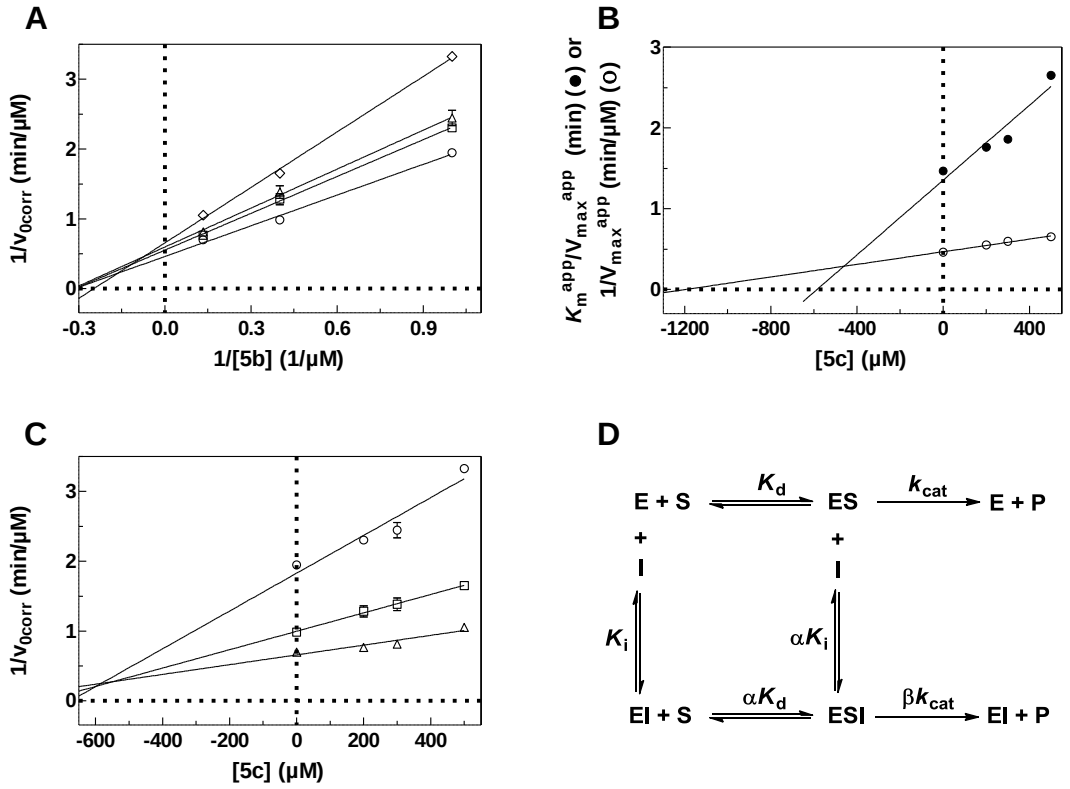

Kinetic investigations on the coumarinyl amide **5c**. Based on the kinetic data and analyses, coumarinyl amide **5c** most likely acts as linear mixed-type inhibitor with α>1 and β=0.[20] **A**) Plot of $1/v_{0corr}=f(1/[\mathbf{5b}])$ in the presence of different fixed concentrations of **5c** (0 µM (○), 200 µM (□), 300 µM (△) and 500 µM (◇)) and linear regressions (—) to the data. **B**) Replots of slope (K_m^{app}/V_{max}^{app}) and $1/v_{0corr}$ intercepts ($1/V_{max}^{app}$) of curves in **A** *versus* [**5c**] and linear regressions (—) to the data. According to the inhibition type mentioned above, K_i was determined from the abscissa intercept ($X=-K_i$) of the former replot to be 585 µM. Using the K_i value and the [**5c**] intercept of the latter replot, α was determined to be 2.0. **C**) Plot of $1/v_{0corr}=f([\mathbf{5c}])$ (Dixon plot) at different fixed concentrations of acyl donor **5b** (1 µM (○), 2.5 µM (□) and 7.5 µM (△)) and linear regressions to the data. According to the inhibition type mentioned above, K_i was independently determined from the intercepts of all lines ($x=-K_i$) to be 583 µM (median value from three intercepts) which is in accordance with the determined value from the replot of $K_m^{app}/V_{max}^{app}=f([\mathbf{5c}])$ in **B**. **D**) Kinetic model for mixed-type inhibition. For the case that α>1 and β=0 the model represents linear mixed, predominantly specific inhibition according to Baici.[20]

Discussion S7: Investigations on the interdependence of acyl donor 5b and aminoacetonitrile

It should be emphasised that changing the acyl acceptor substrate from water, which is present in high invariant concentration, to a primary amine will shift the pseudo-one substrate kinetics of the TGase 2-catalysed hydrolysis to the more complex scenario of an enzymatic reaction that involves two substrates. Given that TGase 2 follows a ping-pong mechanism passing an acyl enzyme intermediate,[25] the corresponding Michaelis-Menten equation reads as follows:

$$v = \frac{V_{max}[A][B]}{K_{mB}[A]+K_{mA}[B]+[A][B]} \qquad \text{(SV)}$$

If A stands for the respective acyl donor substrate and B for aminoacetonitrile, variation of the concentration of A in the presence of B at constant concentration will allow for the determination of the apparent kinetic parameters K_{mA}^{app} and V_{maxA}^{app}.[26] These values relate to the true kinetic parameters as follows:

$$K_{mA}^{app} = \frac{K_{mA}[B]}{K_{mB}+[B]} \qquad \text{(SVI)}$$

$$V_{maxA}^{app} = \frac{V_{max}[B]}{K_{mB}+[B]} \qquad \text{(SVII)}$$

To determine K_m^{app} and k_{cat}^{app} of the synthesised acyl donors for their TGase 2-catalysed aminolyses, aminoacetonitrile was chosen as primary amine due to its low pK_a value (5.6) of its conjugate ammonium ion.[27]

To gain insights into the true Michaelis constant of aminoacetonitrile, K_m^{app} values were determined at four different concentrations of the fluorogenic acyl donor **5b**, which concomitantly provided insight into the true K_m value of **5b**. The original Michaelis-Menten plots of the velocities against the concentrations of each substrate are shown in **Figure I** (below). True values of V_{max} and the Michaelis constants for each substrate were derived from replots of the determined V_{max}^{app} values against the concentrations of **5b** and aminoacetonitrile, respectively (see **Figure II** below). Notably, plotting the ratios V_{max}^{app}/K_m^{app} for each substrate against the concentrations of the respective second substrate revealed their independence of substrate concentration. This finding is in agreement with the established ping-pong mechanism of transglutaminases[25] and confirms that the performance constants in **Table 3** in the main article represent true values. The independence of V_{max}/K_m from substrate concentration is also reflected by the appearance of the transformed plots according to Lineweaver-Burk and Hanes-Woolf, which displayed lines that are approximately parallel or intersected in proximity to the ordinate, respectively (see **Figure III below**).[28] Furthermore, results obtained from data analysis according to the formalism of

Dalziel are consistent with the constant V_{max}/K_m ratio (**Figure IV**).[29] The true Michaelis constants obtained by data analysis shown in **Figure II** are 138 µM and 78.5 µM for **5b** and aminoacetonitrile, respectively. The true K_m of aminoacetonitrile is roughly twice as high as the apparent value in **Table 4** in the main article, which is due to fact that the employed concentration of **5b** was in the range of its K_m value. From the determined true maximum velocity a true catalytic constant of 54.7 s^{-1} was calculated.[3] When calculating the ratios between these true kinetic parameters of substrate **5b** on gpTGase 2 (K_m=138 µM, k_{cat}=54.7 s^{-1}) and the corresponding apparent values included in **Table 3** in the main article, quotients of 0.88 and 0.96 were yielded, respectively. These ratios are close to the quotient of $[B]/(K_{mB}+[B])=0.84$ (see equations SVI and SVII), which is obtained by applying the true Michaelis constant for aminoacetonitrile (K_{mB}=78.5 µM). These results suggest that the apparent kinetic parameters of the acyl donor substrates on gpTGase 2 listed in **Table 3** in the main article might be only marginally lower than their respective true values. The true V_{max} values that were obtained from replotting the apparent maximum velocities against the concentrations of **5b** and aminoacetonitrile, respectively, as well as the k_{cat} values derived thereof are not significantly different from each other, as one would expect from equation SV (**Figure II**).

[3] Mean value of the two catalytic constants obtained by analysing the apparent maximum velocities in dependence of [**5b**] and [aminoacetonitrile].

I) Primary plots for the gpTGase 2-catalysed conversion of the substrate pair 5b and aminoacetonitrile

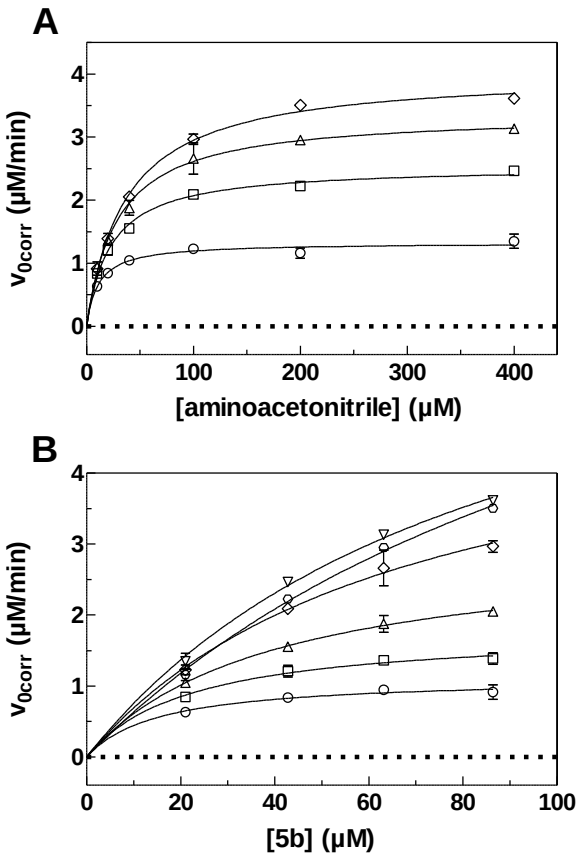

A) Plots of v_{0corr}=f([aminoacetonitrile]) in the presence of fixed concentrations of acyl donor **5b** (21 µM (○), 42.8 µM (□), 63.2 µM (△) and 86.4 µM (◇)) with nonlinear regressions using Michaelis-Menten equation III. **B**) For the same data as in **A**, plots of v_{0corr}=f([**5b**]) in the presence of fixed concentrations of aminoacetonitrile (10 µM (○), 20 µM (□), 40 µM (△), 100 µM (◇), 200 µM (⬭) and 400 µM (▽)) with nonlinear regressions using Michaelis-Menten equation III. Data shown are mean values ±SD of one experiment, which was performed in duplicate. When not apparent, error bars are smaller than the symbols. Conditions: pH=8.0, 30 °C, 5% DMSO, 500 µM TCEP, 0.3 µg/mL gpTGase 2.

II) Secondary plots for the gpTGase 2-catalysed conversion of the substrate pair 5b and aminoacetonitrile

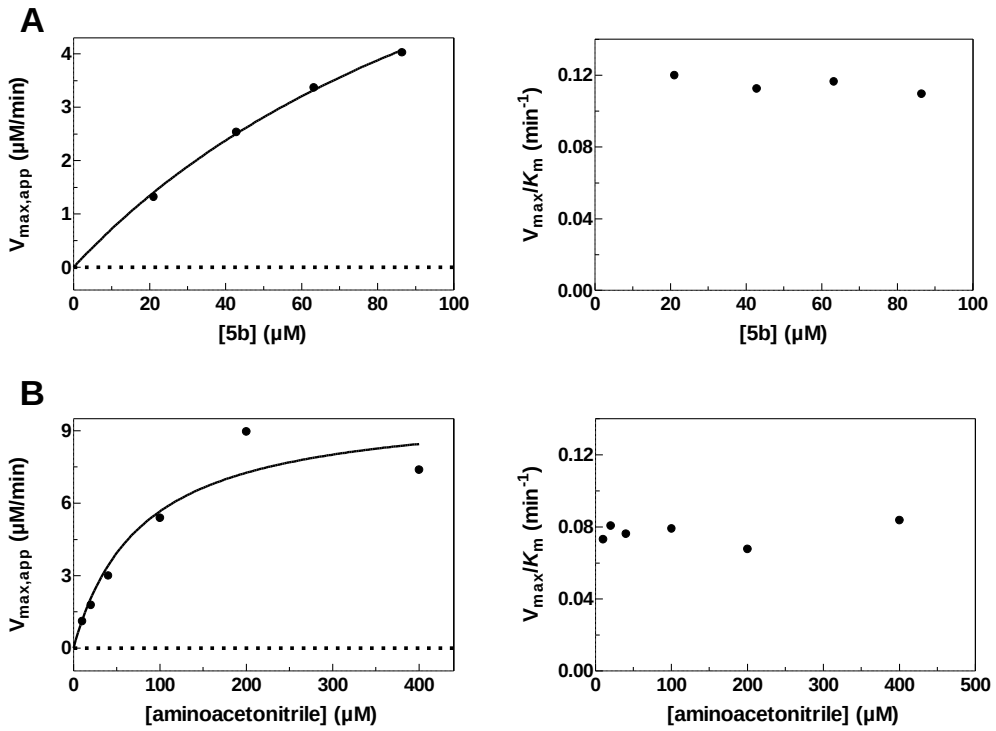

A) Replots of V_{max}^{app} and V_{max}/K_m *versus* [**5b**] with nonlinear regression for the former plot using the Michaelis-Menten equation III. K_m, k_{cat} and k_{cat}/K_m values derived thereof are 138 µM, 55.9 s^{-1} and 405,000 $M^{-1}s^{-1}$, respectively. **B**) Replots of V_{max}^{app} and V_{max}/K_m *versus* [aminoacetonitrile] with nonlinear regression for the former plot using the Michaelis-Menten equation III. K_m and k_{cat} and k_{cat}/K_m values derived thereof are 78.5 µM, 53.4 s^{-1} and 680,000 $M^{-1}s^{-1}$, respectively.

III) Reciprocal plots for the gpTGase 2-catalysed conversion of the substrate pair 5b and aminoacetonitrile

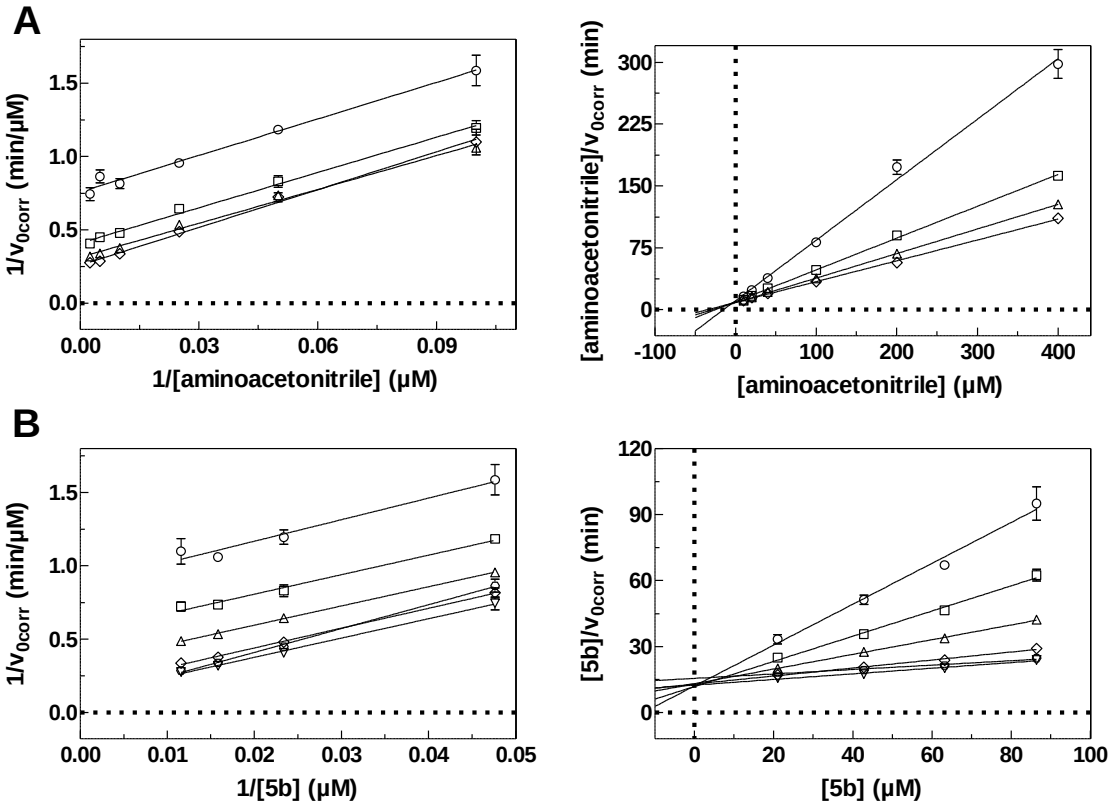

A) Plots of $1/v_{0corr}$=f([aminoacetonitrile]) and [aminoacetonitrile]/v_{0corr}=f([aminoacetonitrile]) in the presence of fixed concentrations of acyl donor **5b** (21 µM (○), 42.8 µM (□), 63.2 µM (△) and 86.4 µM (◇)) with linear regressions (—) to the data. Data shown are of one experiment which was performed in duplicate. **B**) For the same data as in **A**, plots of $1/v_{0corr}$=f([**5b**]) and [**5b**]/v_{0corr}=f([**5b**]) in the presence of fixed concentrations of aminoacetonitrile (10 µM (○), 20 µM (□), 40 µM (△), 100 µM (◇), 200 µM (⬡) and 400 µM (▽)) with linear regressions (—) to the data are shown. According to the known ping-pong mechanism of the TGase 2-catalysed acyl transfer, Lineweaver-Burk plots in **A** and **B** (left) revealed a family of parallel lines while in the Hanes-Woolf plots (right) the lines share an interception point on the y-axis.[28]

IV) Dalziel transformation for the gpTGase 2-catalysed conversion of the substrate pair 5b and aminoacetonitrile

A) For the same data as above, plots of E_0/v_{0corr}=f([substrate]) (Dalziel Transformation[29a], equation SVIII) in the presence of fixed concentrations of the other substrate with linear regressions (—) to the data are shown. **B**) Replots of the E_0/v_{0corr} intercepts and slopes of curves in **A** *versus* the respective fixed concentrations of substrate. According to the known ping-pong mechanism of the TGase 2-catalysed acyl transfer, the former replots gave a linear correlation as the y-intercept relates to ϕ_0 and the slope to $\phi_{\mathbf{5b}}$ or $\phi_{aminoacetontrile}$ while the latter replots showed essentially parallel lines to the x-axis as the values relates to $\phi_{aminoacetonitrile}$ or $\phi_{\mathbf{5b}}$.[29a,30] The initial rate parameters ϕ can be transformed into the more familiar Michaelis-Menten parameters by comparison of equations SIX and SX according to Dickinson [30]:

$$\frac{[E_0]}{v} = \phi_0 + \frac{\phi_A}{[A]} + \frac{\phi_B}{[B]} \qquad \text{(SVIII)}$$

$$\frac{v}{E_0} = \frac{[A][B]}{\phi_0[A][B]+\phi_A[B]+\phi_B[A]+\phi_{AB}} \qquad \text{(SIX)} \qquad \frac{v}{E_0} = \frac{V_{max}[A][B]}{K_{mB}[A]+K_{mA}[B]+[A][B]} \qquad \text{(SX)}$$

$\phi_0=1/k_{cat}$ $K_{m,\mathbf{5b}}=\phi_{\mathbf{5b}}/\phi_0$ $K_{m,aminoacetonitrile}=\phi_{aminoacetontrile}/\phi_0$

Based on these relations, the determined kinetic parameters are as follows:

k_{cat}=56.7 s^{-1} $K_{m,\mathbf{5b}}$=82.6 µM $K_{m,aminoacetonitrile}$=86.9 µM

These parameters are reasonably comparable to those obtained by nonlinear regression according to Michaelis-Menten equation III (see **Figure II** above).

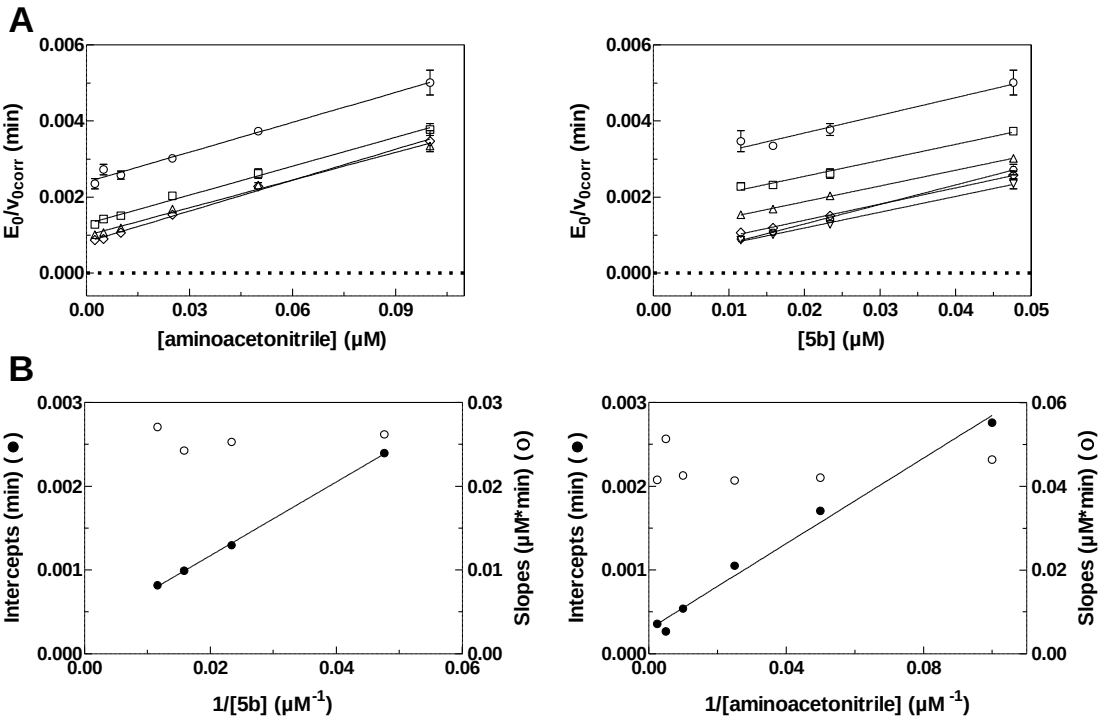
A
0.006
0.004
0.002
0.000
E_0/v_{0corr} (min)
0.00
0.03
0.06
0.09
[aminoacetonitrile] (μM)
0.006
0.004
0.002
0.000
E_0/v_{0corr} (min)
0.00
0.01
0.02
0.03
0.04
0.05
[5b] (μM)
B
0.003
0.002
0.001
0.000
Intercepts (min) (●)
0.03
0.02
0.01
0.00
Slopes (μM*min) (○)
0.00
0.02
0.04
0.06
1/[5b] (μM^{-1})
0.003
0.002
0.001
0.000
Intercepts (min) (●)
0.06
0.04
0.02
0.00
Slopes (μM*min) (○)
0.00
0.04
0.08
1/[aminoacetonitrile] (μM^{-1})

Figure S14

gpTGase 2-catalysed aminolyses of the acyl donors 3-6 at pH=8.0

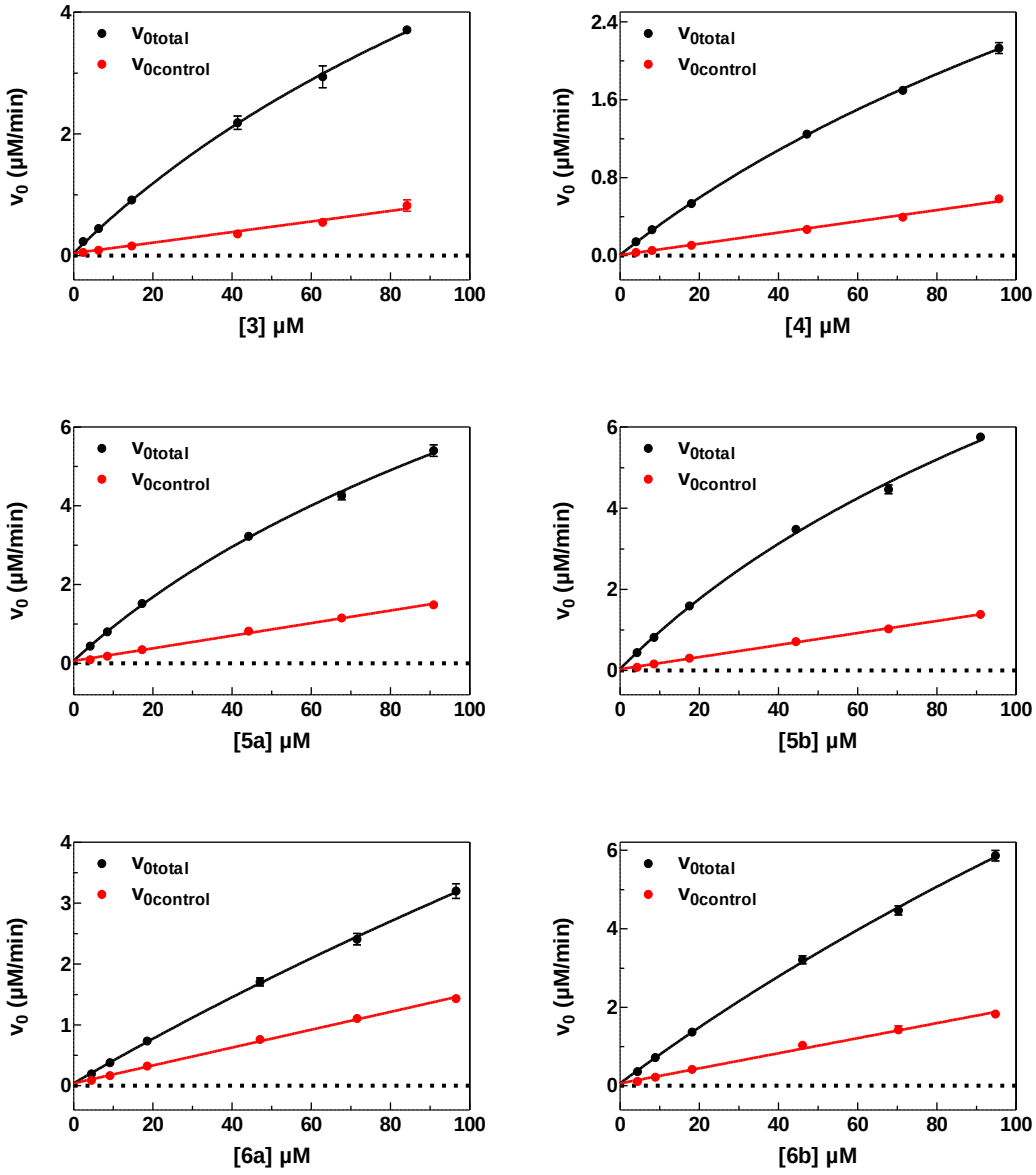

Plots of v_{0total}=f([acyl donor]) and $v_{0control}$=f([acyl donor]) for the global fit model of the enzymatic aminolyses. Data shown are mean values ±SEM of 3 separate experiments, each performed in duplicate. When not apparent, error bars are smaller than the symbols. Conditions: pH=8.0, 30 °C, 5% DMSO, 500 µM TCEP, 400 µM aminoacetonitrile, 0.3 µg/mL (**5a**, **5b**, **6a** and **6b**) or 2 µg/mL (**3** and **4**) gpTGase 2.

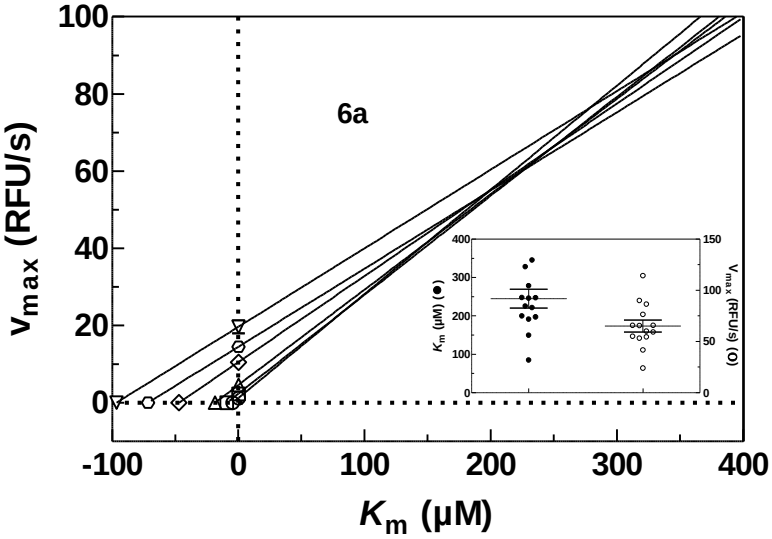

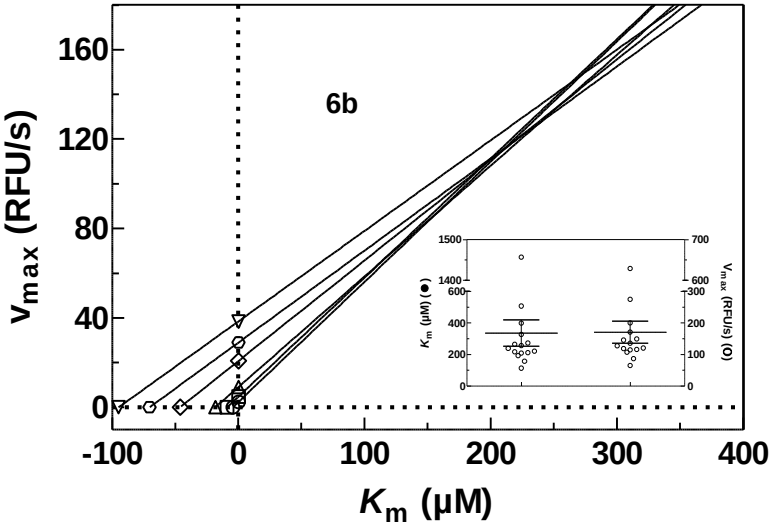

Direct linear plots of V_{max} against K_m according to Cornish-Bowden & Eisenthal to estimate the values for V_{max}^{app} and K_m^{app} of **6a** and **6b** towards gpTGase 2 as the medians from the series of interception points. The insets show the distribution of the V_{max}^{app} and K_m^{app} values including the lines for the respective medians and percentiles of 25% and 75%.

Figure S15

hTGase 2-catalysed aminolysis of acyl donor 5b at pH=8.0

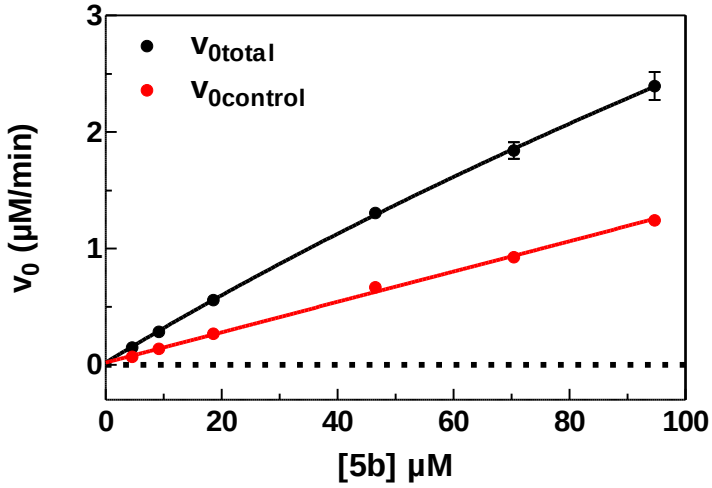

Plots of v_{0total}=f([**5b**]) and $v_{0control}$=f([**5b**]) for the global fit model of the enzymatic aminolyses. Data shown are mean values ± SEM of 3 separate experiments, each performed in duplicate. When not apparent, error bars are smaller than the symbols. Conditions: pH=8.0, 30 °C, 5% DMSO, 500 µM TCEP, 400 µM aminoacetonitrile, 0.3 µg/mL hTGase 2.

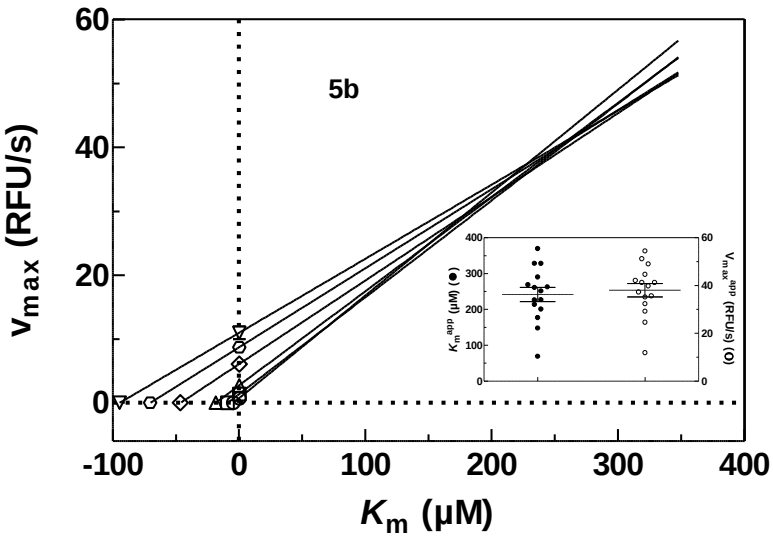

Direct linear plots of V_{max} against K_m according to Cornish-Bowden & Eisenthal to estimate the values for V_{max}^{app} and K_m^{app} of **5b** towards hTGase 2 as the medians from the series of interception points. The insets show the distribution of the V_{max}^{app} and K_m^{app} values including the lines for the respective medians and percentiles of 25% and 75%.

Figure S16

Confirmation of TGase 2-catalysed aminolysis of 5b by identification of reaction product

To confirm the formation of the aminolysis product, a solution (200 µL) of compound **5b** (400 µM), aminoacetonitrile (400 µM) and gpTGase 2 (0.3 µg/ml) in assay buffer pH=8.0 containing 5% DMSO was incubated at 30 °C. After 90 min, the reaction was stopped by adding 200 µL of 1% TFA/acetonitrile. The resulting solution was centrifuged at 6000 rpm for 5 min and an aliquot of 100 µL was subjected to HPLC analysis (see below). Eluate solutions corresponding to peaks which represented components of interest were collected and analysed by ESI-MS.

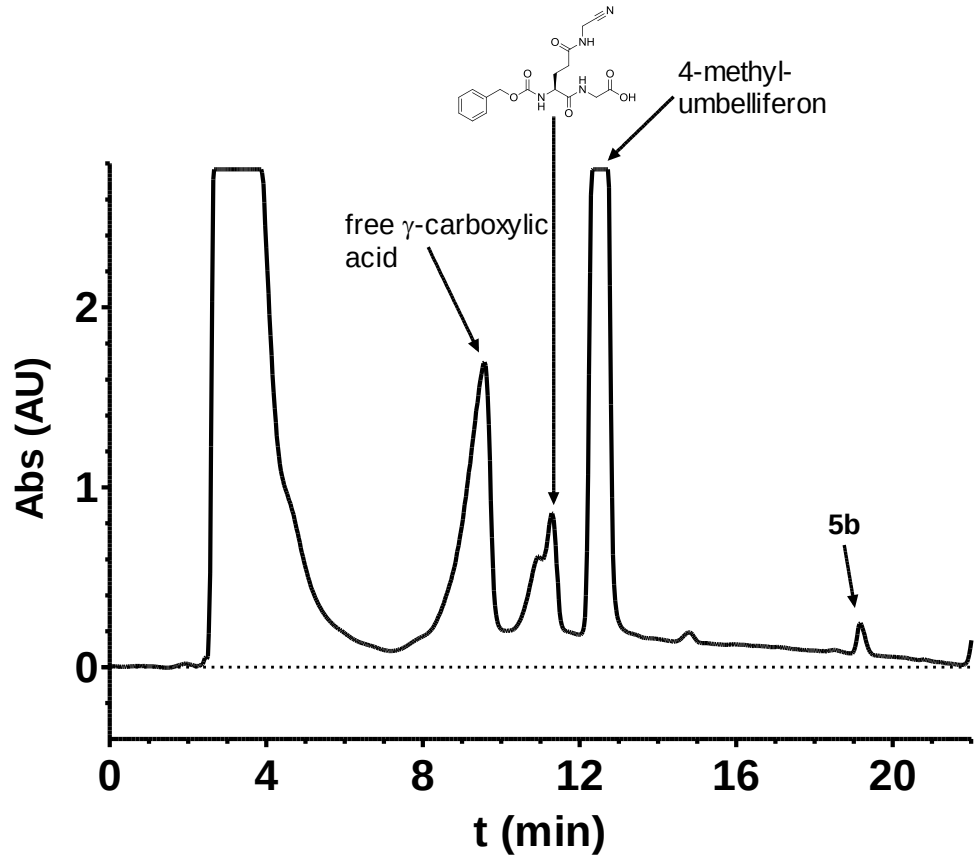

HPLC profile (210 nm) for TGase 2-catalysed conversion of **5b** after 90 min at 30 °C (400 µM **5b**, 400 µM aminoacetonitrile, 100 mM MOPS pH=8.0, 3 mM $CaCl_2$, 50 µM EDTA, 500 µM TCEP, 0.3 µg/mL gpTGase 2). The peaks were identified by ESI-MS analysis of the collected eluent and on the basis of comparison with other HPLC data.

Discussion S8: Synthesis of *N*-(biotinyl)cadaverine×TFA

General remarks

To ensure that biotinylation takes place just at one primary amino group, cadaverine was anchored to the 2-ClTrtCl resin according to a published procedure.[31] Afterwards, coupling of commercially available biotin was achieved by the use of PyBOP as coupling reagent and DIPEA as base. TFA-mediated release from the resin and purification by preparative RP-HPLC provided *N*-(biotinyl)cadaverine (**7**) in good yield (46%).

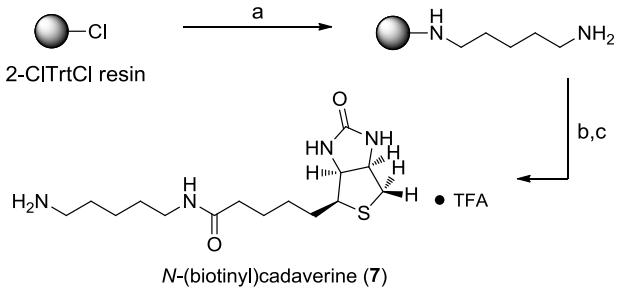

N-(biotinyl)cadaverine (**7**)

Solid phase synthesis of *N*-(biotinyl)cadaverine (**7**). Reagents and conditions: **a)** 1. cadaverine, CH_2Cl_2, 17 h, 2. CH_2Cl_2/CH_3OH/DIPEA (17:1:2); **b)** biotin, PyBOP, DIPEA, DMF, 6 h; **c)** TFA/TES/H_2O (95:2.5:2.5), 2 h.

Loading of cadaverine onto 2-ClTrtCl resin

The synthesis was accomplished according to Egner *et al*.[31] A solution of cadaverine (526 µL, 4.48 mmol, 4 equiv.) in CH_2Cl_2 (5 mL) was added to the pre-swollen (5 mL, CH_2Cl_2, 30 min) 2-ClTrtCl resin (0.7 g, 1.12 mmol, 1 equiv., 1.6 mmol/g) in a PP filter vessel. The PP filter vessel was sealed and agitated for 17 h at room temperature. Afterwards, the resin was successively washed with DMF (4 mL, 4×1 min), CH_2Cl_2 (4 mL, 4×1 min), CH_2Cl_2/CH_3OH/DIPEA (17:1:2, 4 mL, 3×2 min), MeOH (4 mL, 4×1 min), TEA/DMF (1:4, 4 mL, 3×1 min), MeOH (4 mL, 4×1 min) and, finally, with CH_2Cl_2 (4 mL, 4×1 min) again. The resin was dried *in vacuo* overnight. The loading yields were gravimetrically determined according to Bernecker *et al*.[32] using the following equation:

$$Loading(\frac{mol}{g}) = \frac{m_2 - m_1}{(MW - 36.461) * m_2}$$

with m_1, m_2, and MW being the weight of the unloaded resin, the weight of the loaded resin and the molecular mass of cadaverine in g/mol, respectively. A loading degree of 1.52 mmol/g was determined.

Biotinylation

The loaded resin (0.5 mmol cadaverine, 1 equiv.) was swollen in DMF (5 mL) for 30 min. A suspension of biotin (183 mg, 0.75 mmol, 1.5 equiv.) and DIPEA (392 µL, 2.25 mmol, 4.5 equiv.) in DMF (4 mL) was added. Afterwards, solid PyBOP (585 mg, 1.13 mmol, 2.25 equiv.) was added and the mixture was agitated for 6 h at room temperature. Then, the resin was washed with DMF (5 mL, 4×1 min) and CH_2Cl_2 (5 mL, 4×1 min) and dried *in vacuo* overnight.

Cleavage

The cleavage was accomplished according to Seebach *et al*.[10]

The dry resin was suspended in 5 mL of a solution of TFA/TES/H_2O (95:2.5:2.5) for 2 h. After filtering, the resin was washed with TFA (2×5 mL) and the combined filtrates were evaporated in a N_2 stream.

***N*-(Biotinyl)cadaverine×TFA (7)**

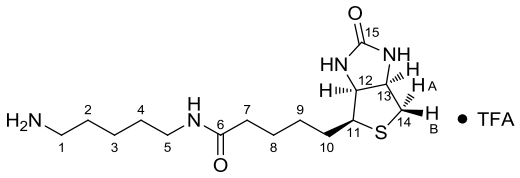

The synthesis yielded 101 mg (46%) of **7** as a slightly yellow solid. **^{1}H-NMR (DMSO-*d*$_6$):** δ=7.75 (t, ^3J=5.6 Hz, 1H, NH of amide), 7.69 (broad s, 3H, NH_3^+), 6.41 (s, 1H, NH of urea), 6.37 (s, 1H, NH of urea), 4.31 (dd, ^3J=7.7, 4.9 Hz, 1H, H–13), 4.12 (dd, ^3J=7.6, 4.5 Hz, 1H, H–12), 3.12–3.06 (m, 1H, H–11), 3.05–2.98 (m, 2H, H–5), 2.82 (dd, ^2J=12.4 Hz, ^3J=5.1 Hz, 1H, H–14A), 2.79–2.71 (m, 2H, H–1), 2.58 (d, ^2J=^3J=12.4 Hz, 1H, H–14B), 2.04 (t, ^3J =7.4 Hz, 2H, H–7), 1.66–1.20 (m, 12H, H–2,3,4,8,9,10); **^{13}C-NMR (DMSO-*d*$_6$):** δ=171.85 (C–6), 162,69 (C–15), 61.05 (C–12), 59.19 (C–13), 55.44 (C–11), 39.83 (C–14), 38.76, 38.04, 35.20, 28.63, 28.23, 28.06, 26.66, 25.32, 23.17; ^{19}F-NMR (DMSO-*d*$_6$): δ=-73.95 (s, CF_3); ESI-MS (ESI+) *m/z*: calc. for $C_{15}H_{29}N_4O_2S$ $[M+H]^+$, 329.20, found 329.1; Elemental analysis: calc. for $C_{15}H_{28}N_4O_8S×C_2HF_3O_2$, C, 46.04; H, 6.82; N, 12.63; S, 7.23 found C, 45.17; H, 6.41; N, 12.19; S, 6.85. Assignments of the ^{1}H-NMR spectrum and the ^{13}C-NMR spectrum for the biotin moiety were done according to literature data.[33]

Figure S17

Determination of the fluorescence coefficients of HC and HMC

To convert the measured arbitrary fluorescence units into concentrations of HMC and HC, the fluorescence coefficients of the fluorophores were determined on a monthly basis. For this purpose, the fluorescence intensities of eight different concentrations of the respective coumarin derivative (stock solutions in DMSO) ranging from 0 to 20 µM (10 µL) in buffer **A** or **B** (190 µL) were measured over 900 s (three independent measurements, each performed in duplicate). The average fluorescence intensities were determined as mean values between 300 and 600 s. Typical calibration curves for HMC at pH=8.0 and pH=6.5 are shown below.

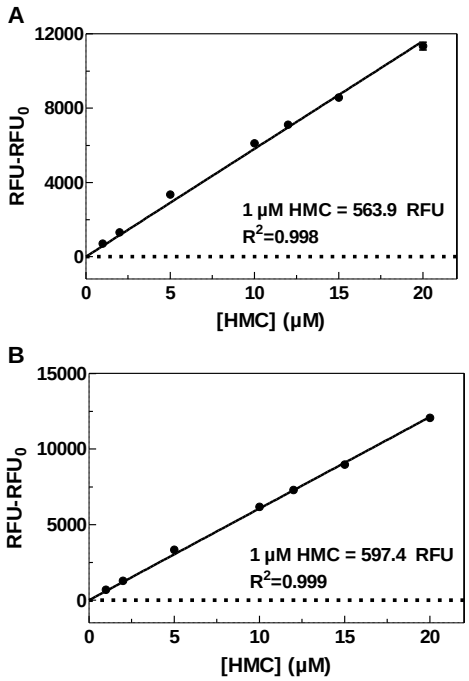

Typical calibration curves for HMC at pH=8.0 (**A**) and pH=6.5 (**B**) with the respective fluorescence coefficients. Data points (●) are mean values ±SEM of 3 separate experiments, each performed in duplicate. The regression coefficients were obtained by linear regression (—) to these data points. When not apparent, error bars are smaller than the symbols.

Figure S18

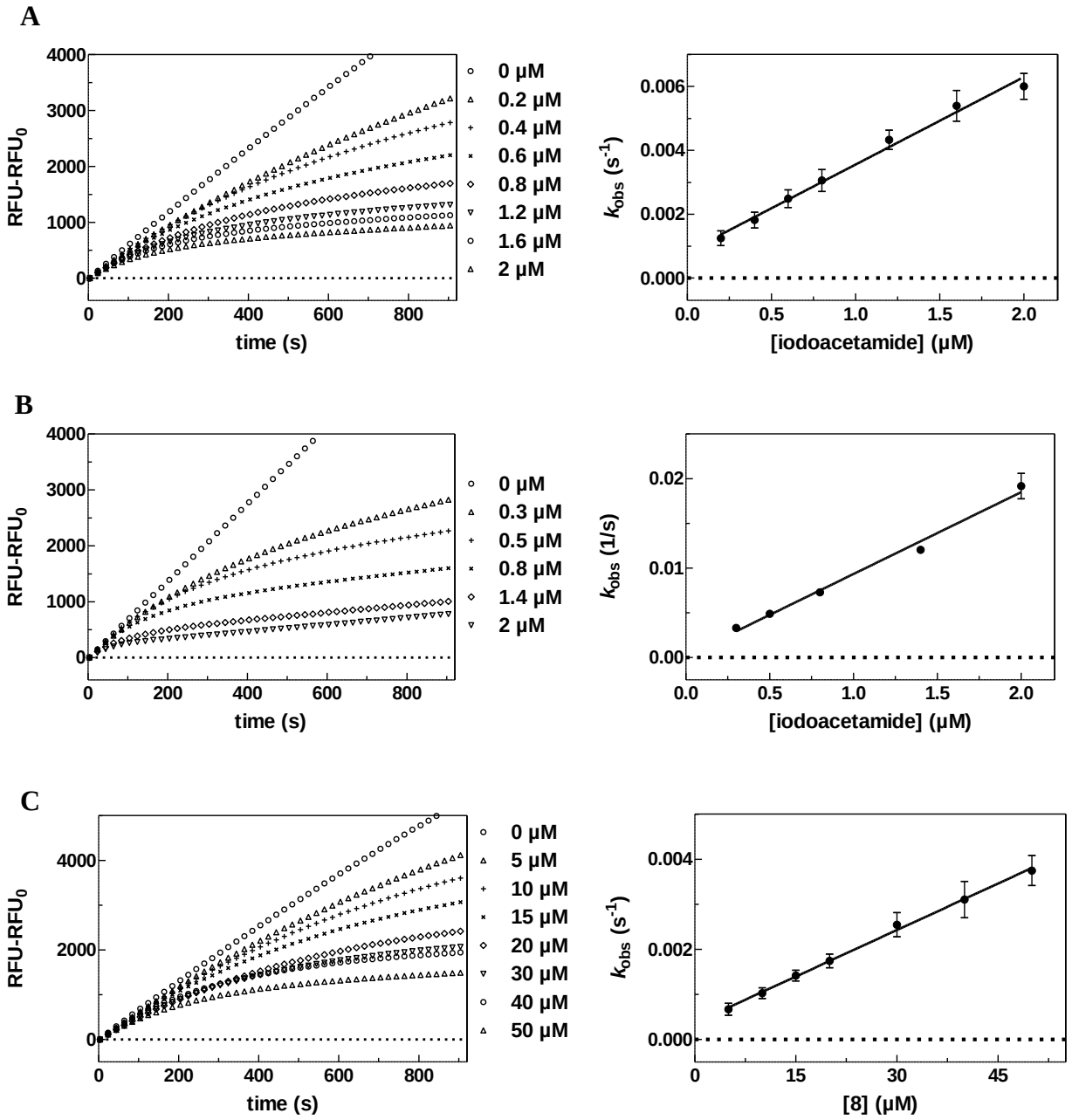

A) **Left**: Typical time courses at different concentrations of iodoacetamide in the presence of 25 µM (~10×K_m) of **5b** for the inhibition of acyl donor hydrolysis by gpTGase 2. **Right**: Plot of k_{obs}=f([iodoacetamide]) with linear regression to the data for the calculation of k_{obs}/[I]. Data (●) shown are mean values ±SEM of 3 separate experiments, each performed in duplicate. When not apparent, error bars are smaller than the symbols. **B**) As in **A**, but for inhibition of hTGase 2 by iodoacetamide at 30 µM (~4.5×K_m) of acyl donor **5b**. **C**) As in **A,** but for inhibition of gpTGase 2 by acrylamide **8** at 25 µM (~10×K_m) of acyl donor **5b**. Conditions: pH=6.5, 30 °C, 5% DMSO, 500 µM TCEP, 3 µg/mL gpTGase 2 or hTGase 2

Figure S19

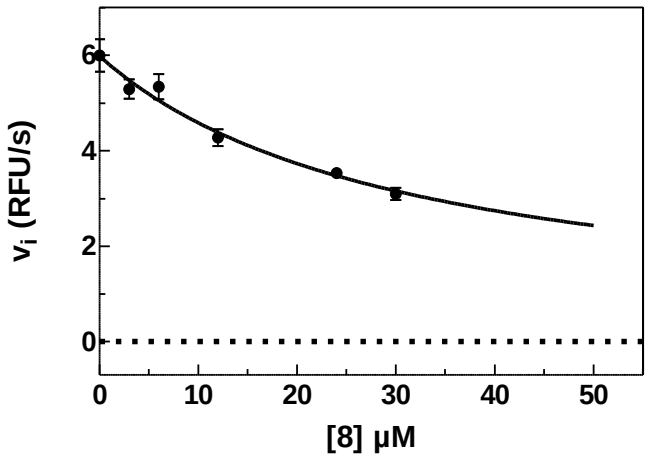

Plot of v_i=f([**8**]) with nonlinear regression using equation VIII for the determination of K_i;

NMR spectra of Products

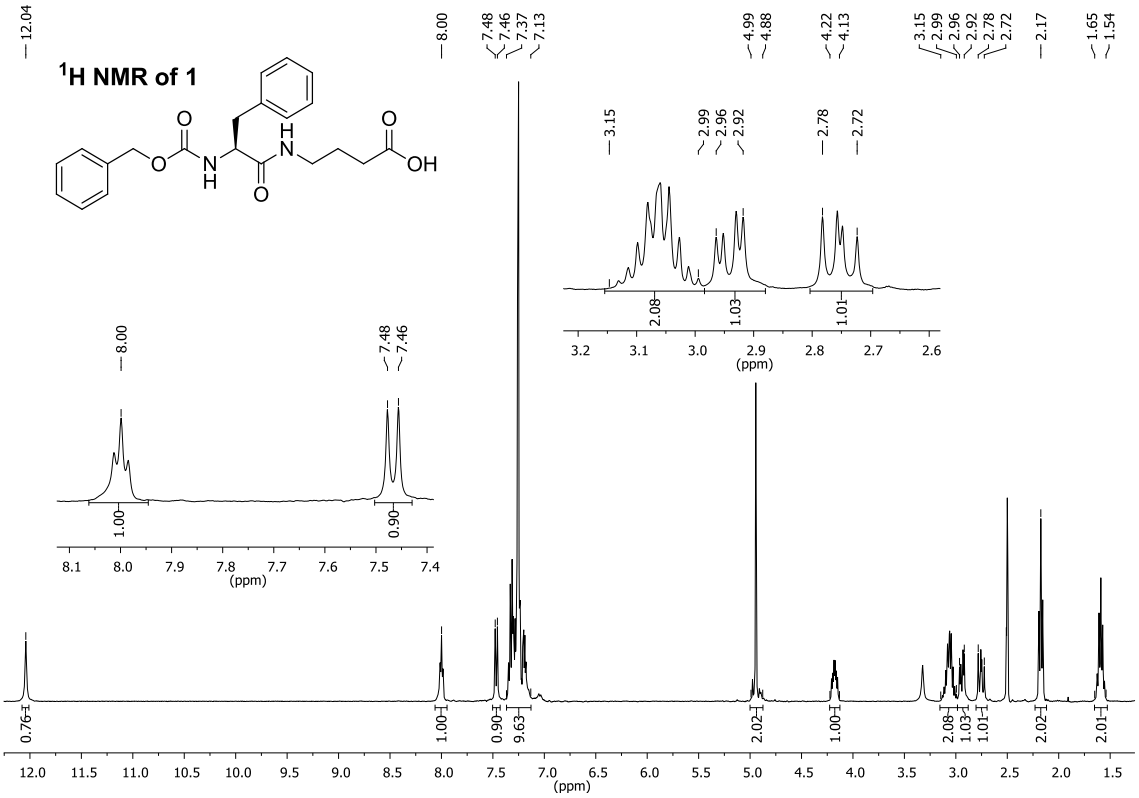

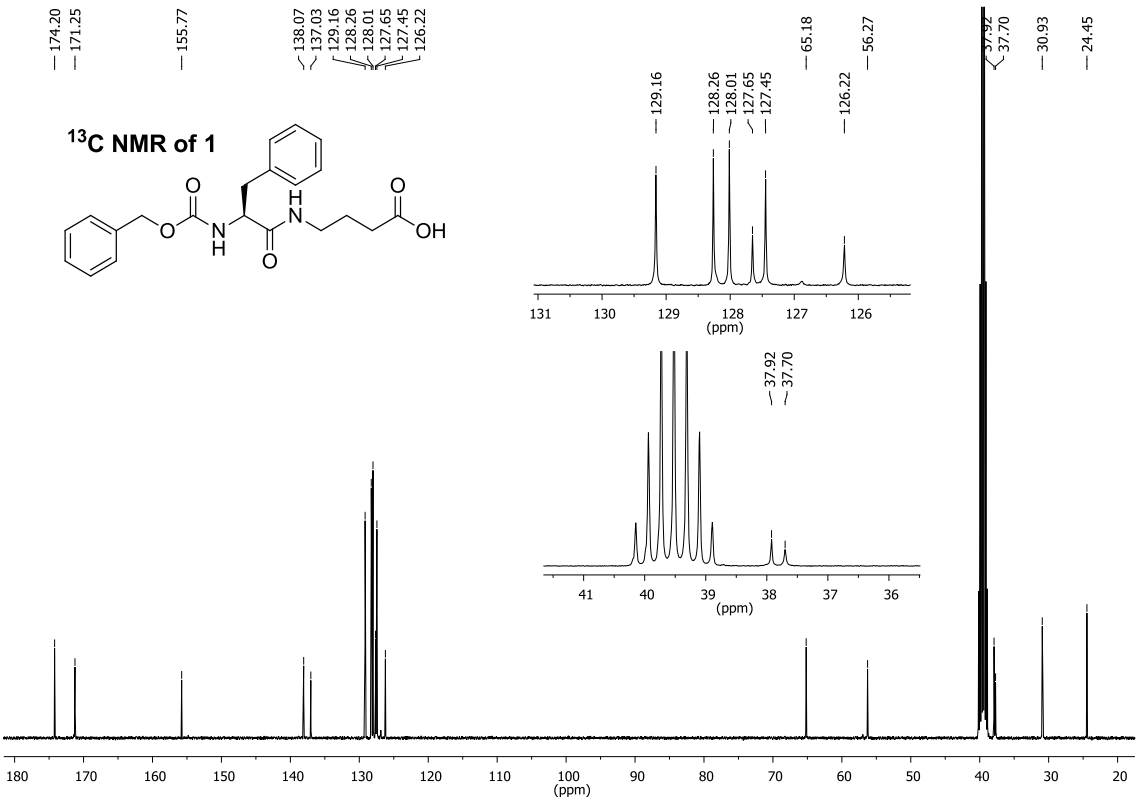

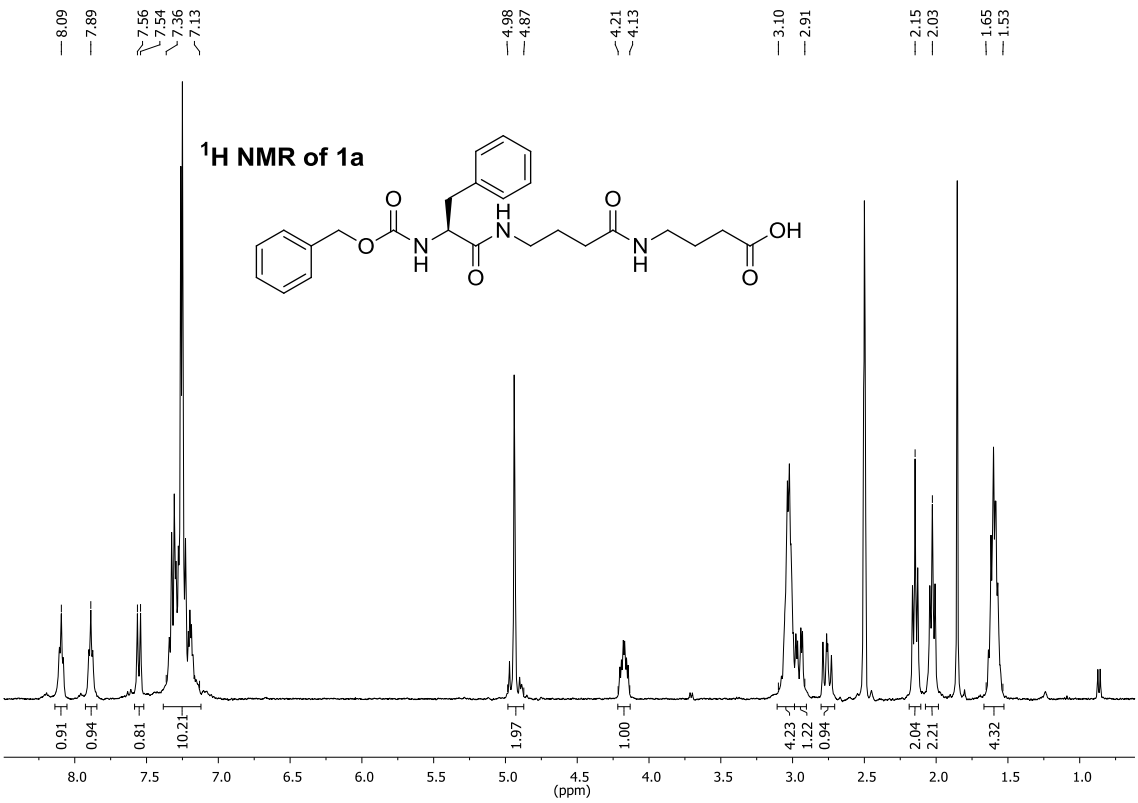
8.09
7.89
7.56
7.54
7.36
7.13
4.98
4.87
4.21
4.13
3.10
2.91
2.15
2.03
1.65
1.53
^{1}H NMR of 1a
OH
0.91
0.94
0.81
10.21
1.97
1.00
4.23
1.22
0.94
2.04
2.21
4.32
(ppm)

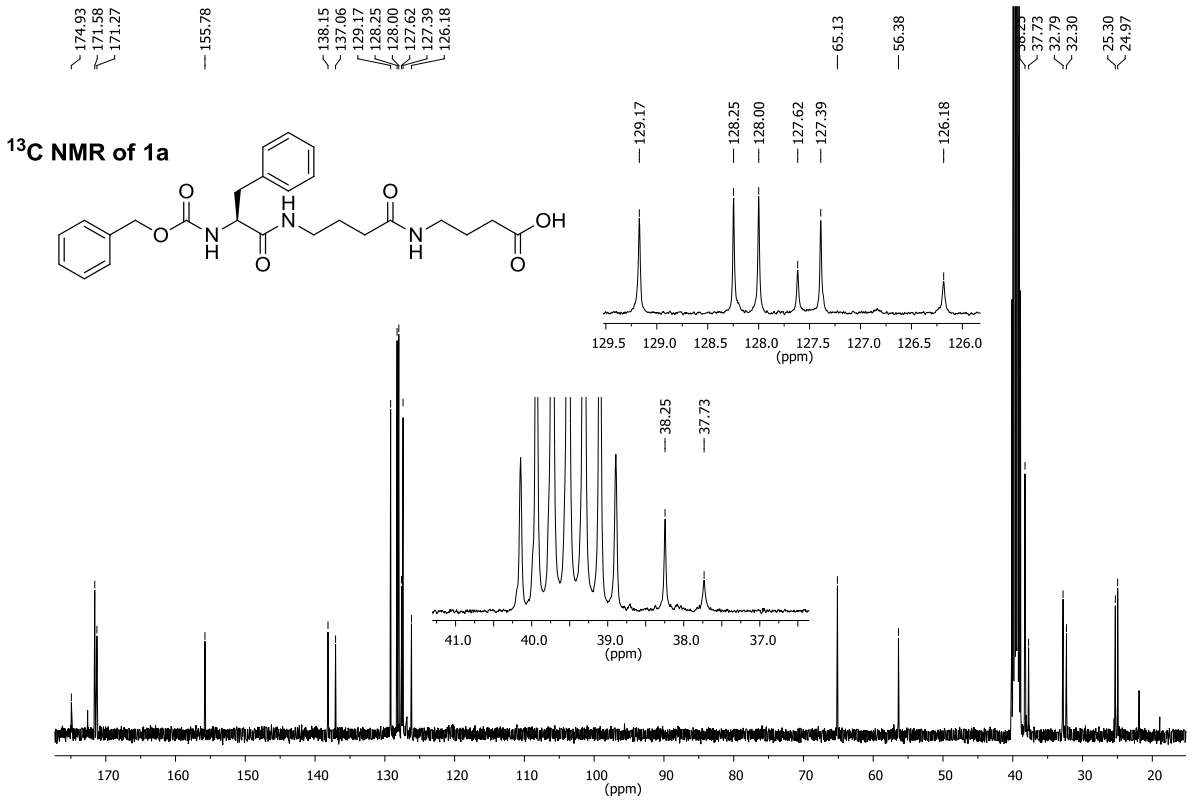
174.93
171.58
171.27
155.78
138.15
137.06
129.17
128.25
128.00
127.62
127.39
126.18
65.13
56.38
38.25
37.73
32.79
32.30
25.30
24.97
^{13}C NMR of 1a
OH
129.17
128.25
128.00
127.62
127.39
126.18
(ppm)
38.25
37.73
(ppm)
(ppm)

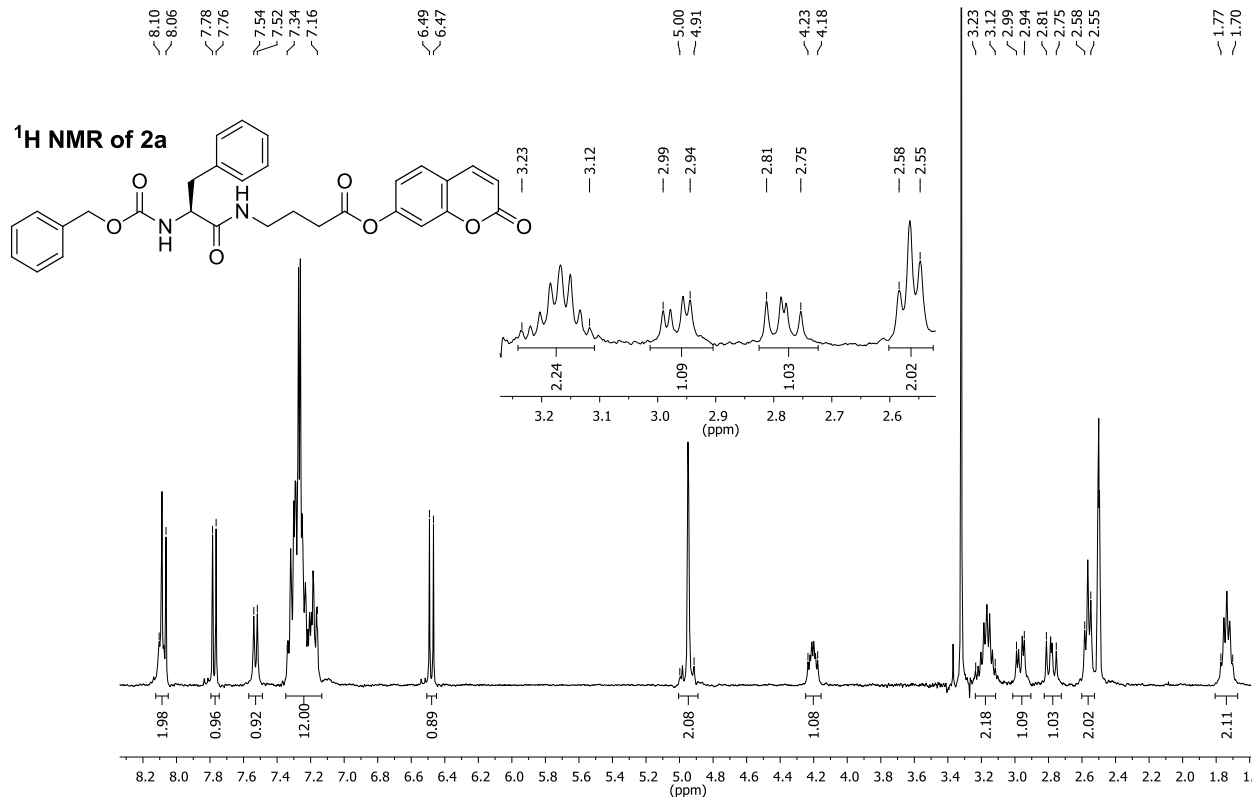
1H NMR of 2a
8.10
8.06
7.78
7.76
7.54
7.52
7.34
7.16
6.49
6.47
5.00
4.91
4.23
4.18
3.23
3.12
2.99
2.94
2.81
2.75
2.58
2.55
1.77
1.70
1.98
0.96
0.92
12.00
0.89
2.08
1.08
2.18
1.09
1.03
2.02
2.11
(ppm)

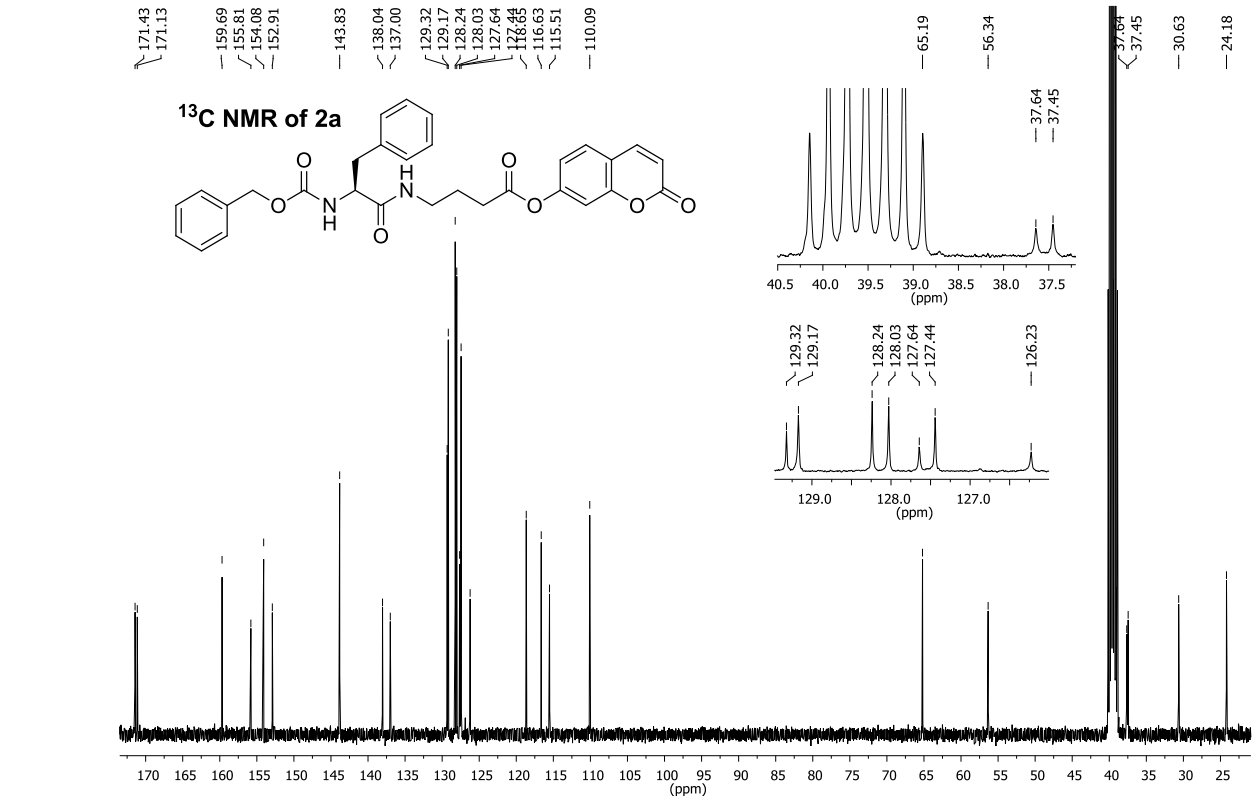
13C NMR of 2a
171.43
171.13
159.69
155.81
154.08
152.91
143.83
138.04
137.00
129.32
129.17
128.24
128.03
127.64
127.44
118.85
116.63
115.51
110.09
65.19
56.34
37.64
37.45
30.63
24.18
126.23
(ppm)

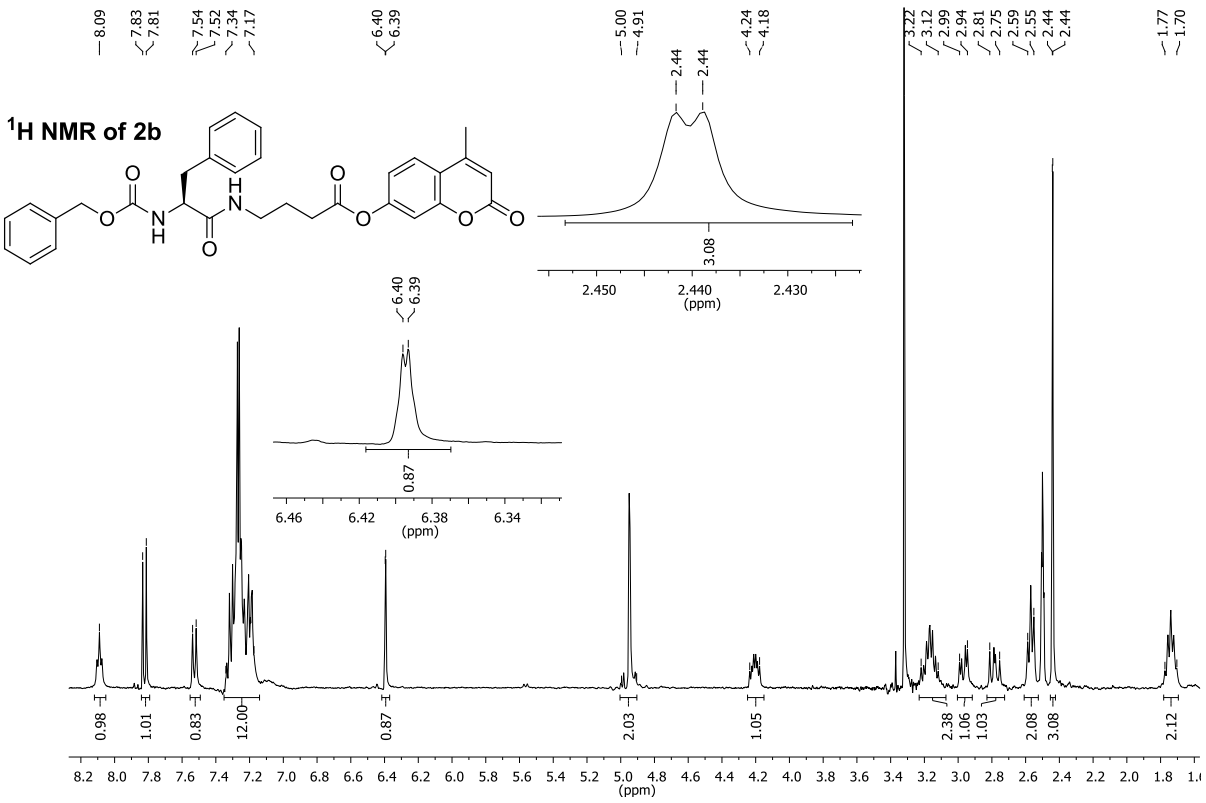
1H NMR of 2b
8.09
7.83
7.81
7.54
7.52
7.34
7.17
6.40
6.39
5.00
4.91
4.24
4.18
3.22
3.12
2.99
2.94
2.81
2.75
2.59
2.55
2.44
2.44
1.77
1.70
2.44
2.44
3.08
2.450
2.440
2.430
(ppm)
6.40
6.39
0.87
6.46
6.42
6.38
6.34
(ppm)
0.98
1.01
0.83
12.00
0.87
2.03
1.05
2.38
1.06
1.03
2.08
3.08
2.12
(ppm)

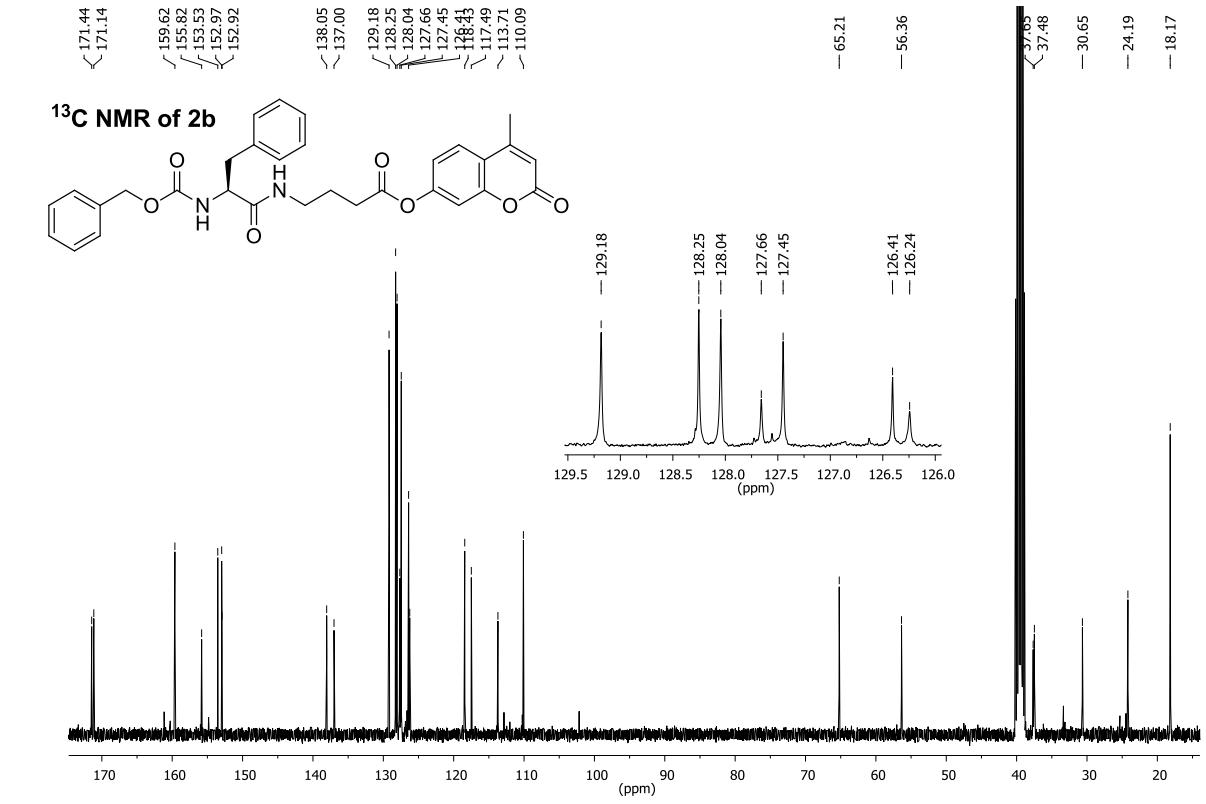
13C NMR of 2b
171.44
171.14
159.62
155.82
153.53
152.97
152.92
138.05
137.00
129.18
128.25
128.04
127.66
127.45
118.43
117.49
113.71
110.09
65.21
56.36
37.65
37.48
30.65
24.19
18.17
129.18
128.25
128.04
127.66
127.45
126.41
126.24
129.5
129.0
128.5
128.0
127.5
127.0
126.5
126.0
(ppm)
(ppm)

^{1}H NMR of 2c

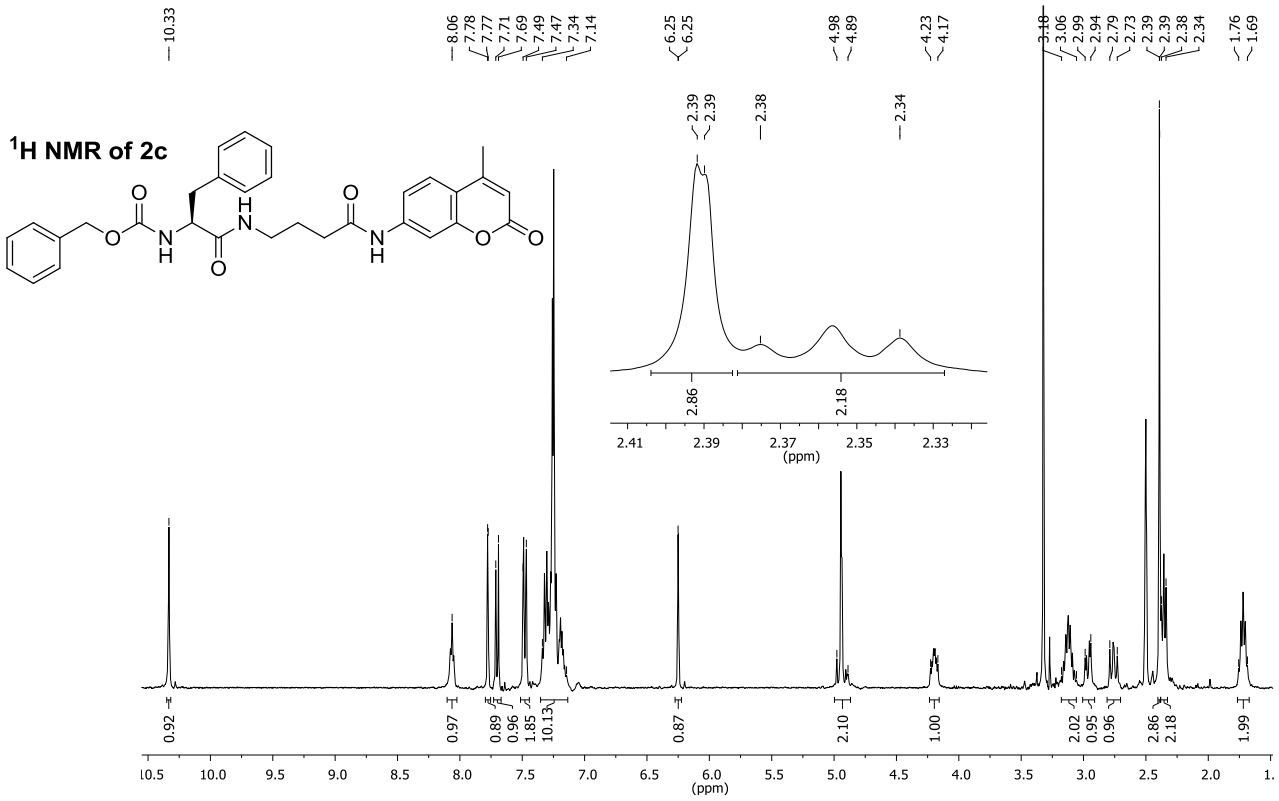

^{13}C NMR of 2c

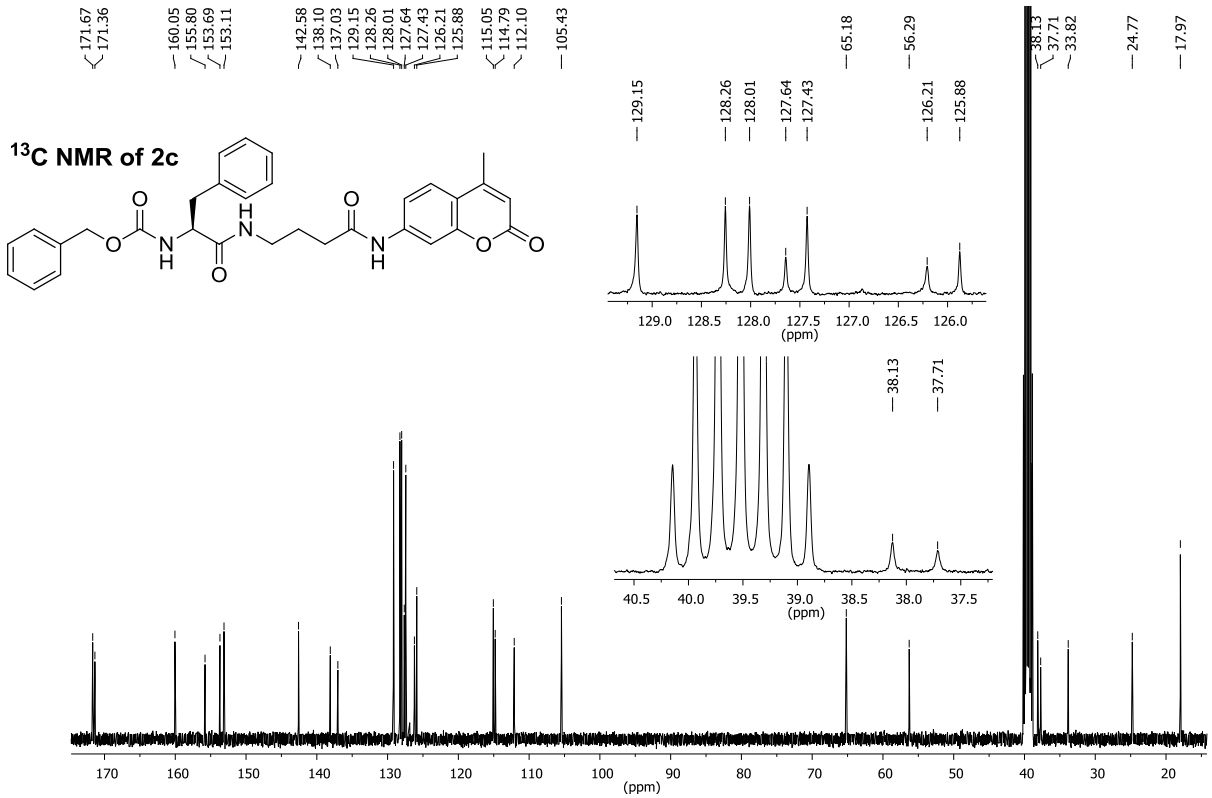

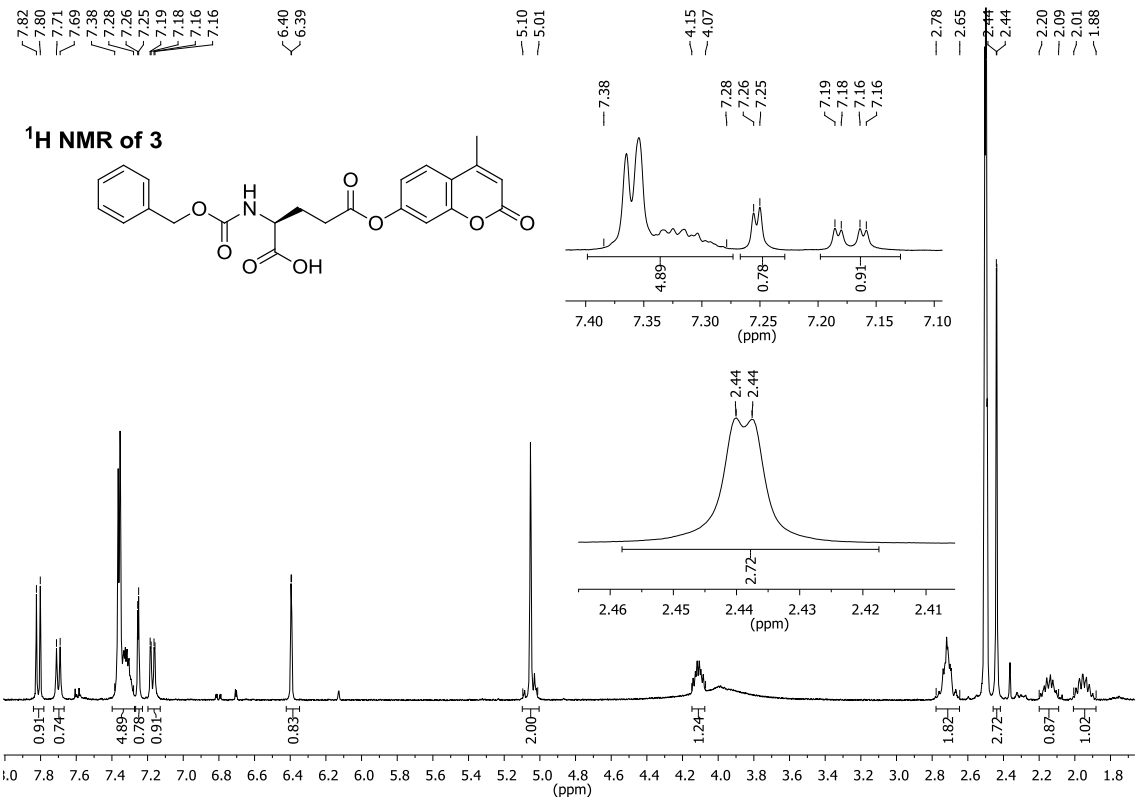
^{1}H NMR of 3
(ppm)

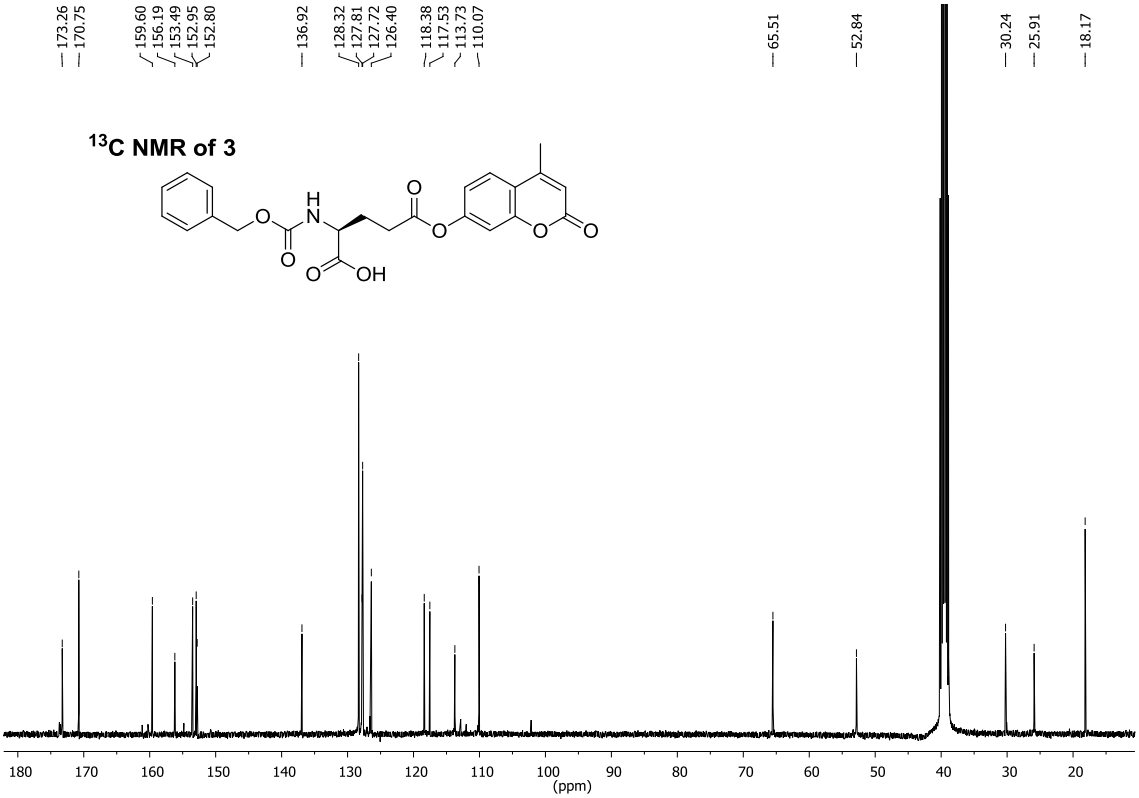
^{13}C NMR of 3
(ppm)

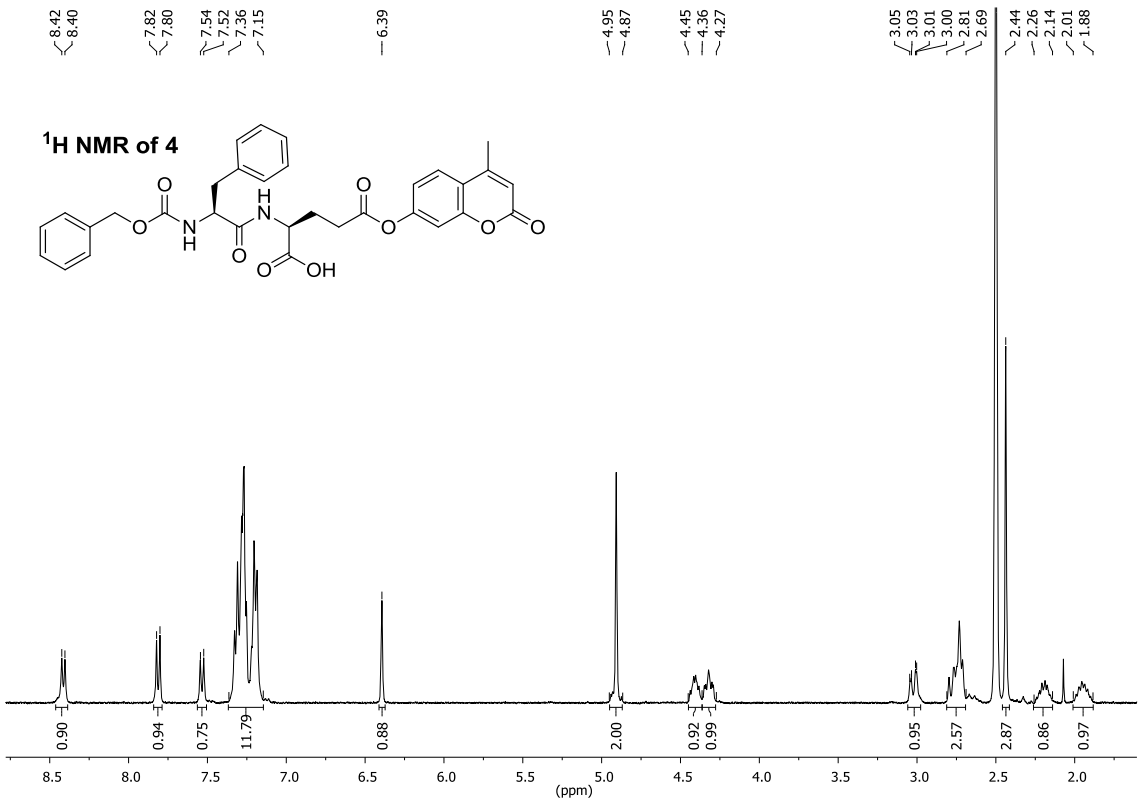

^{1}H NMR of 4

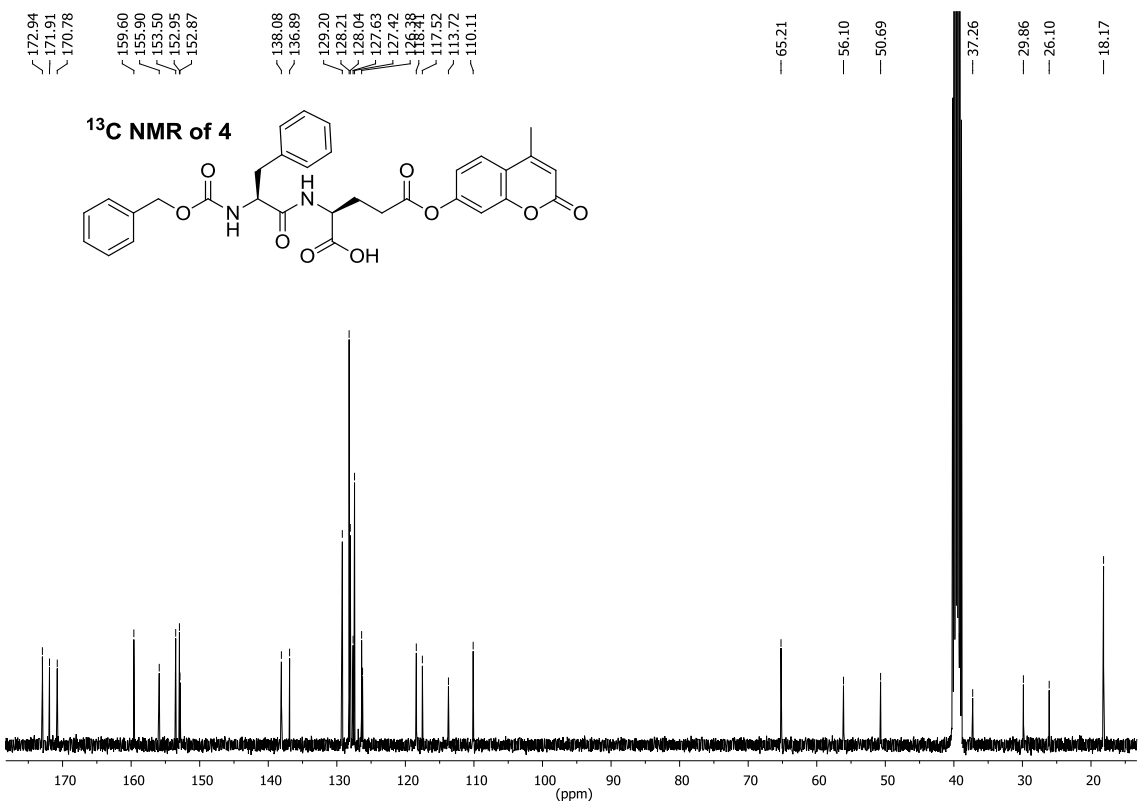

^{13}C NMR of 4

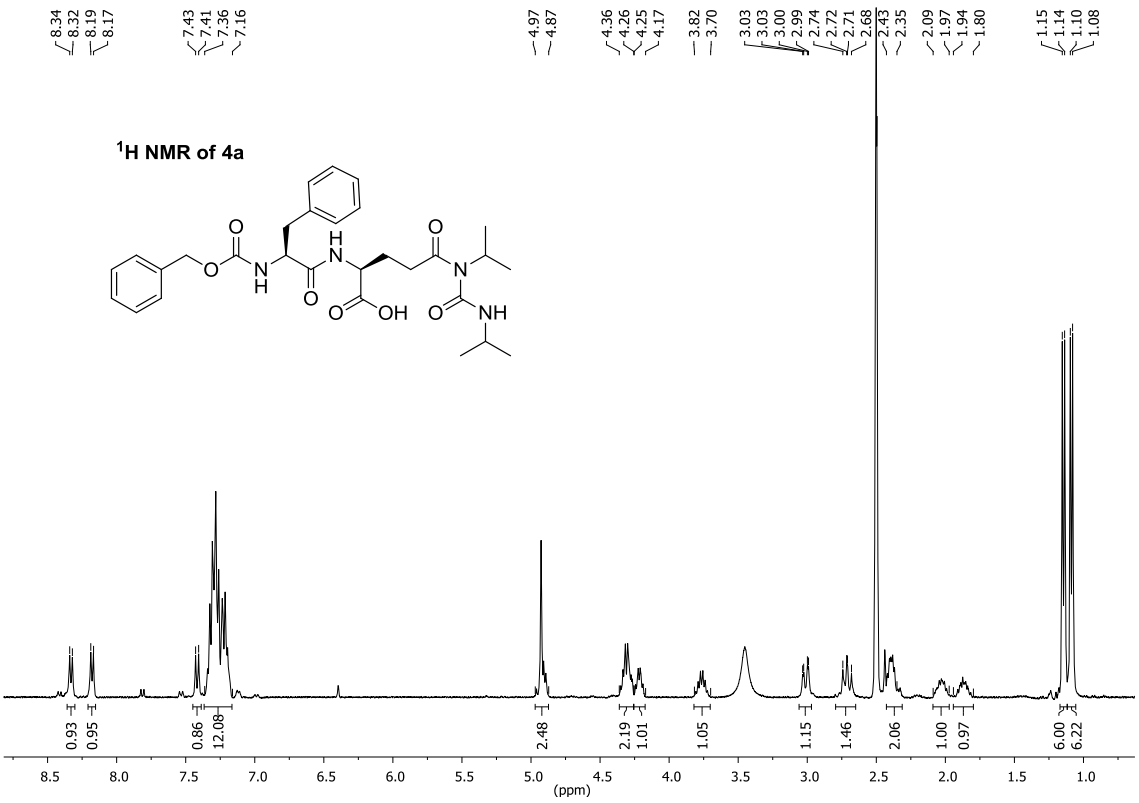

^{1}H NMR of 4a

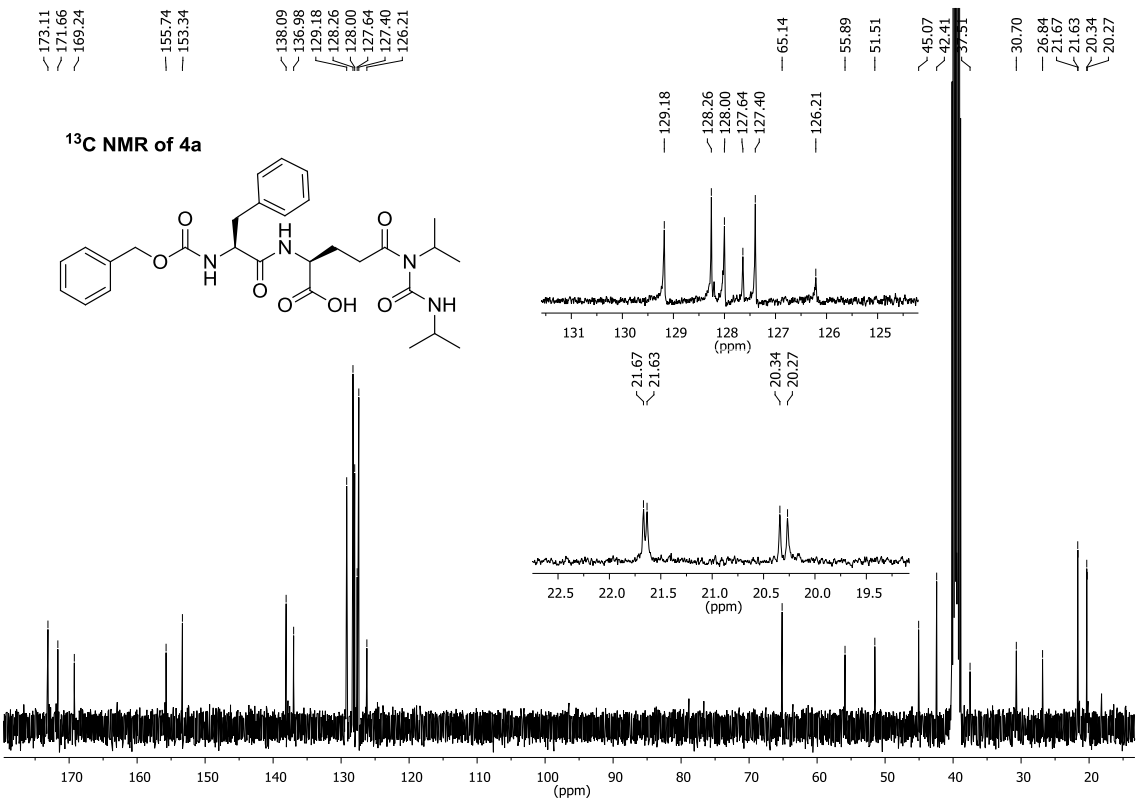

^{13}C NMR of 4a

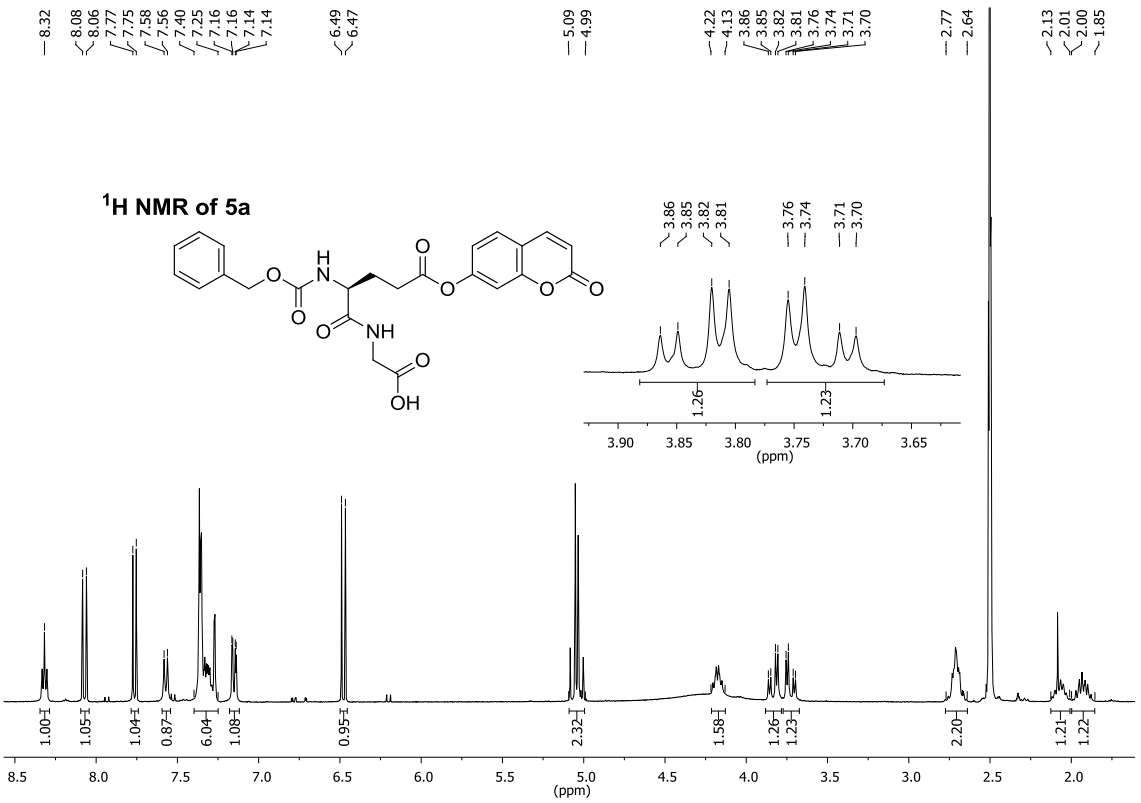
8.32
8.08
8.06
7.77
7.75
7.58
7.56
7.40
7.25
7.16
7.16
7.14
7.14
6.49
6.47
5.09
4.99
4.22
4.13
3.86
3.85
3.82
3.81
3.76
3.74
3.71
3.70
2.77
2.64
2.13
2.01
2.00
1.85
1H NMR of 5a
3.86
3.85
3.82
3.81
3.76
3.74
3.71
3.70
1.26
1.23
3.90 3.85 3.80 3.75 3.70 3.65
(ppm)
1.00
1.05
1.04
0.87
6.04
1.08
0.95
2.32
1.58
1.26
1.23
2.20
1.21
1.22
8.5 8.0 7.5 7.0 6.5 6.0 5.5 5.0 4.5 4.0 3.5 3.0 2.5 2.0
(ppm)

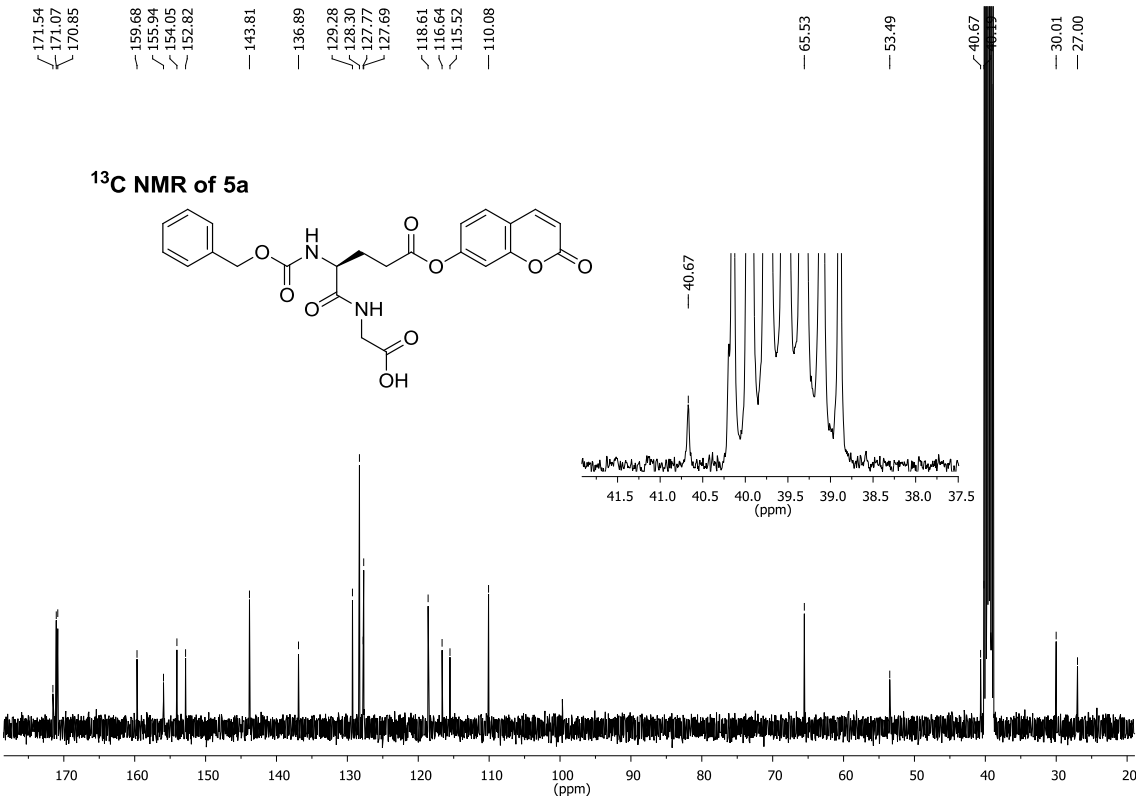
171.54
171.07
170.85
159.68
155.94
154.05
152.82
143.81
136.89
129.28
128.30
127.77
127.69
118.61
116.64
115.52
110.08
65.53
53.49
40.67
30.01
27.00
13C NMR of 5a
40.67
41.5 41.0 40.5 40.0 39.5 39.0 38.5 38.0 37.5
(ppm)
170 160 150 140 130 120 110 100 90 80 70 60 50 40 30 20
(ppm)

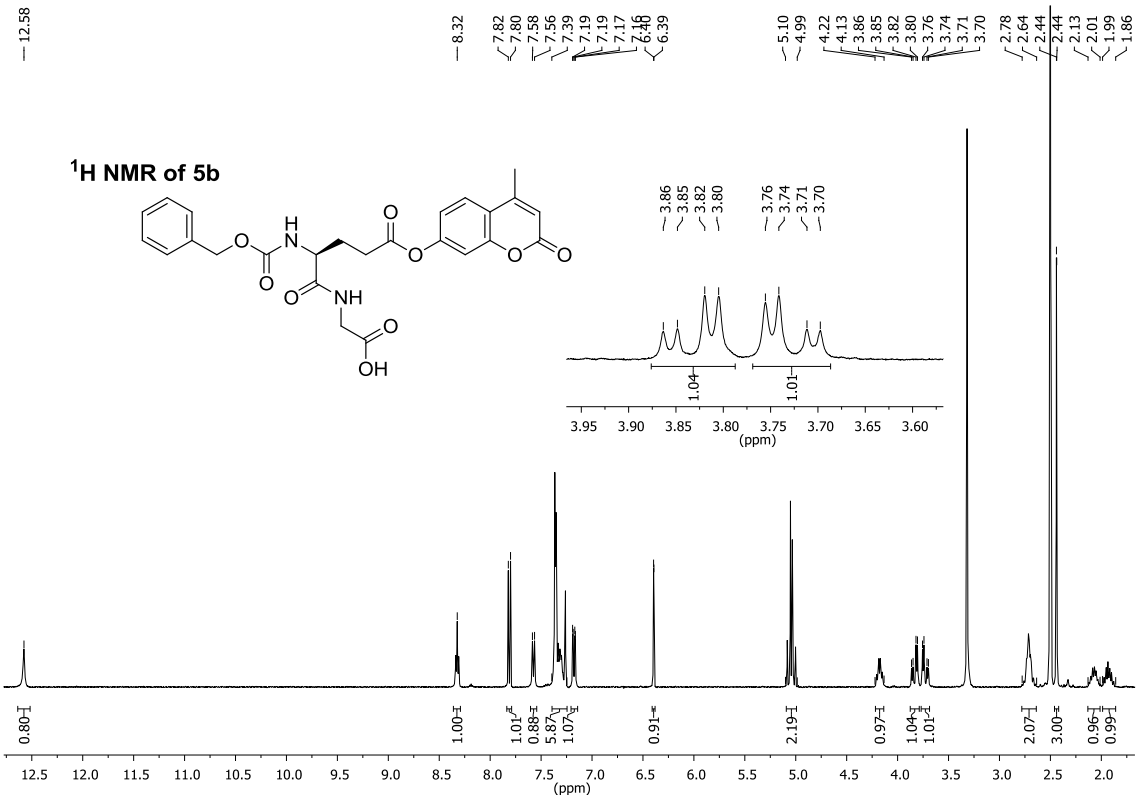
^{1}H NMR of 5b
12.58
8.32
7.82
7.80
7.58
7.56
7.39
7.19
7.19
7.17
7.16
6.40
6.39
5.10
4.99
4.22
4.13
3.86
3.85
3.82
3.80
3.76
3.74
3.71
3.70
2.78
2.64
2.44
2.44
2.13
2.01
1.99
1.86
1.04
1.01
(ppm)
0.80
1.00
1.01
0.88
5.87
1.07
0.91
2.19
0.97
1.04
1.01
2.07
3.00
0.96
0.99
(ppm)

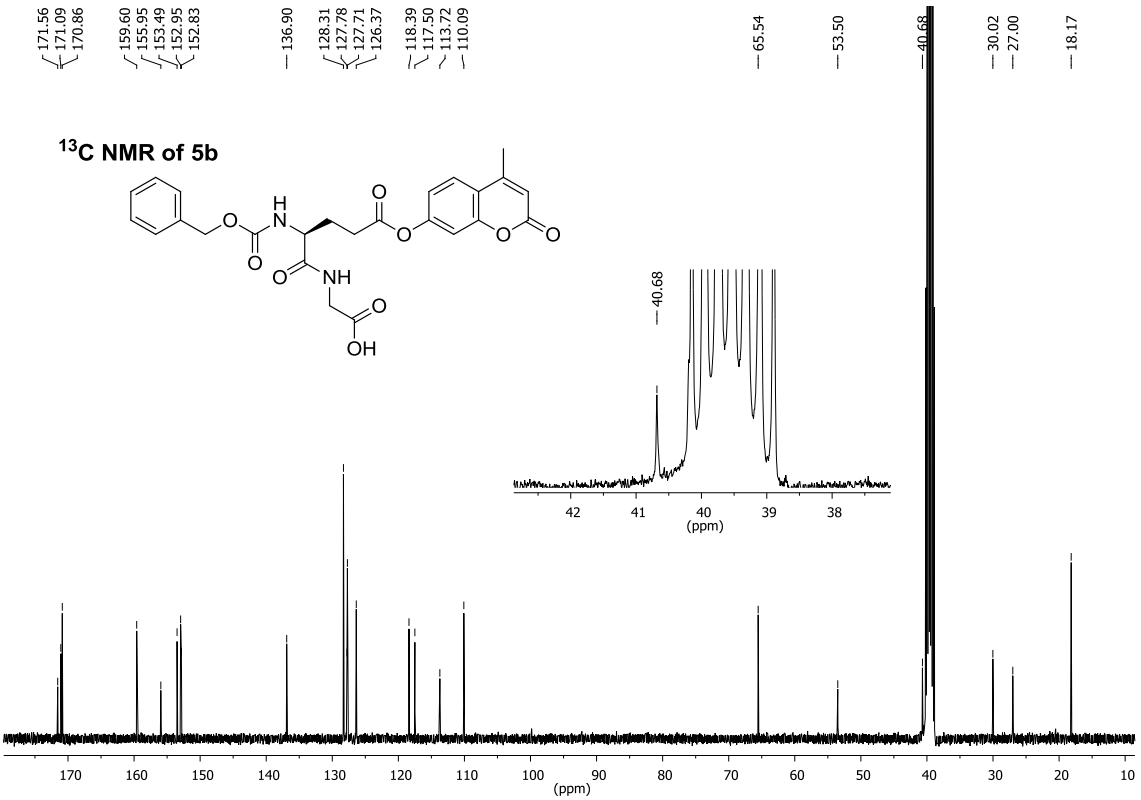
^{13}C NMR of 5b
171.56
171.09
170.86
159.60
155.95
153.49
152.95
152.83
136.90
128.31
127.78
127.71
126.37
118.39
117.50
113.72
110.09
65.54
53.50
40.68
30.02
27.00
18.17
40.68
(ppm)
(ppm)

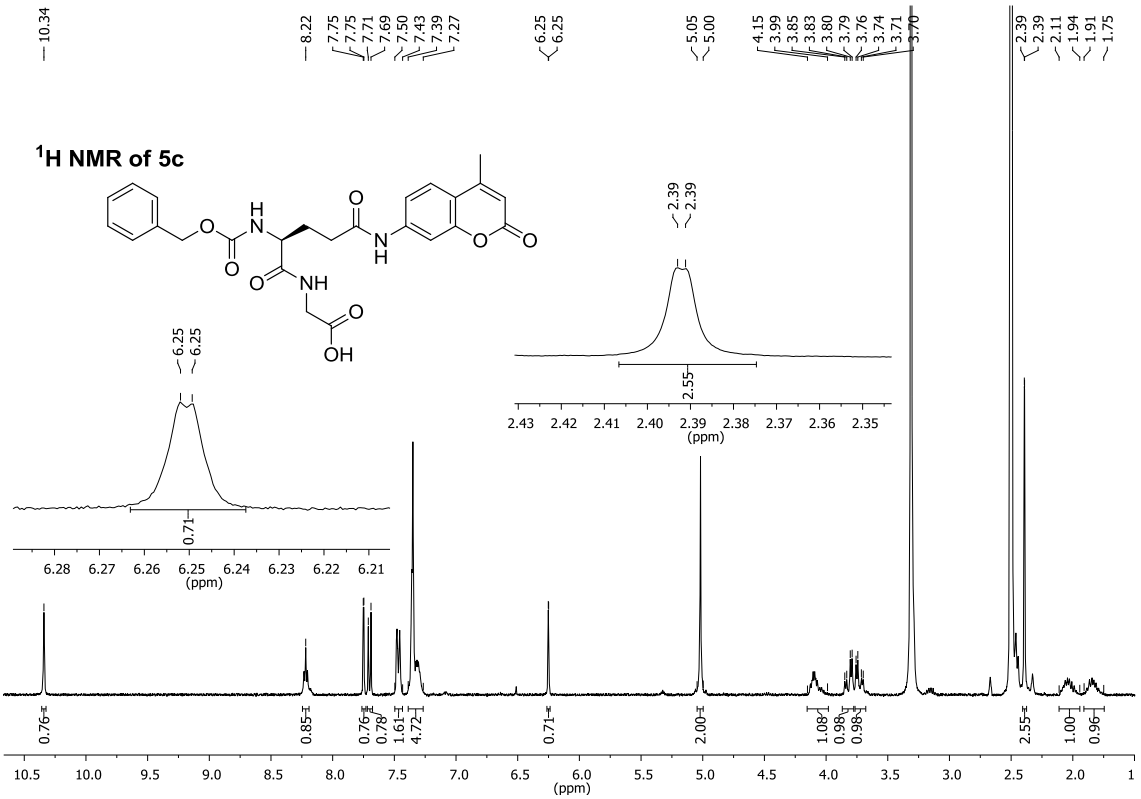
10.34
8.22
7.75
7.75
7.71
7.69
7.50
7.43
7.39
7.27
6.25
6.25
5.05
5.00
4.15
3.99
3.85
3.83
3.80
3.79
3.76
3.74
3.71
3.70
2.39
2.39
2.11
1.94
1.91
1.75
1H NMR of 5c
2.39
2.39
2.55
6.25
6.25
0.71
0.76
0.85
0.76
0.78
1.61
4.72
0.71
2.00
1.08
0.98
0.98
2.55
1.00
0.96
(ppm)

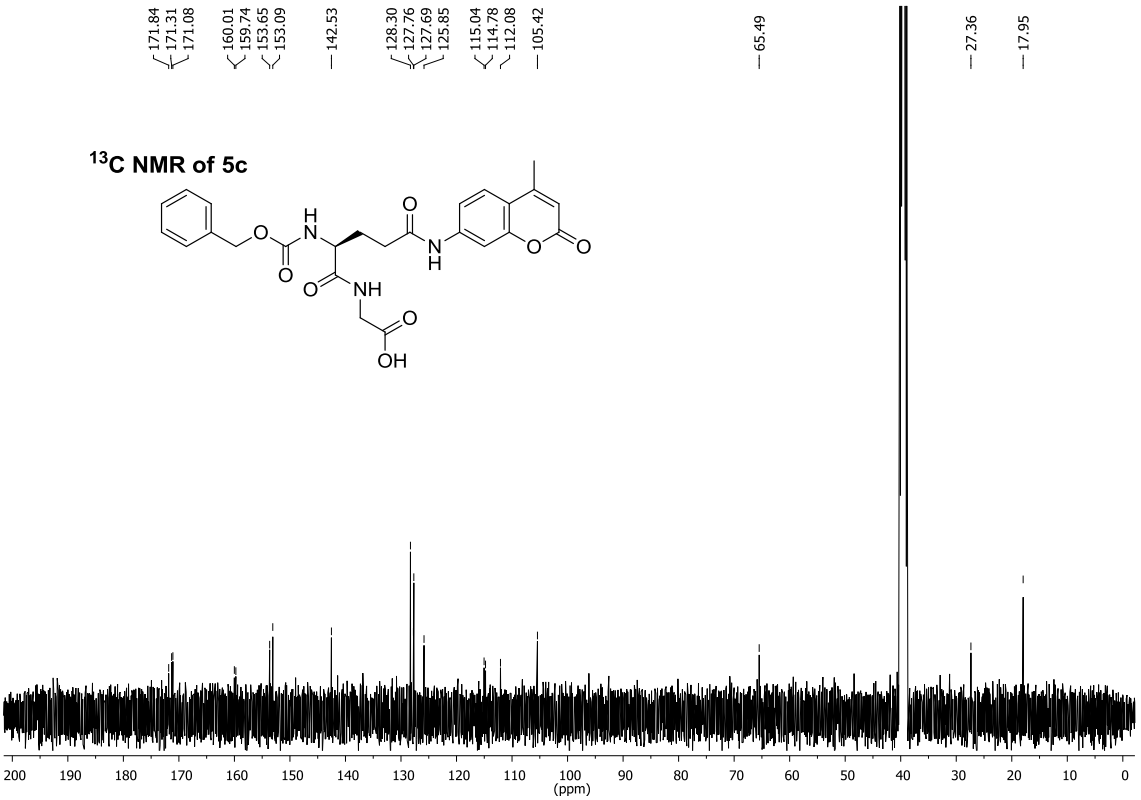
171.84
171.31
171.08
160.01
159.74
153.65
153.09
142.53
128.30
127.76
127.69
125.85
115.04
114.78
112.08
105.42
65.49
27.36
17.95
13C NMR of 5c
(ppm)

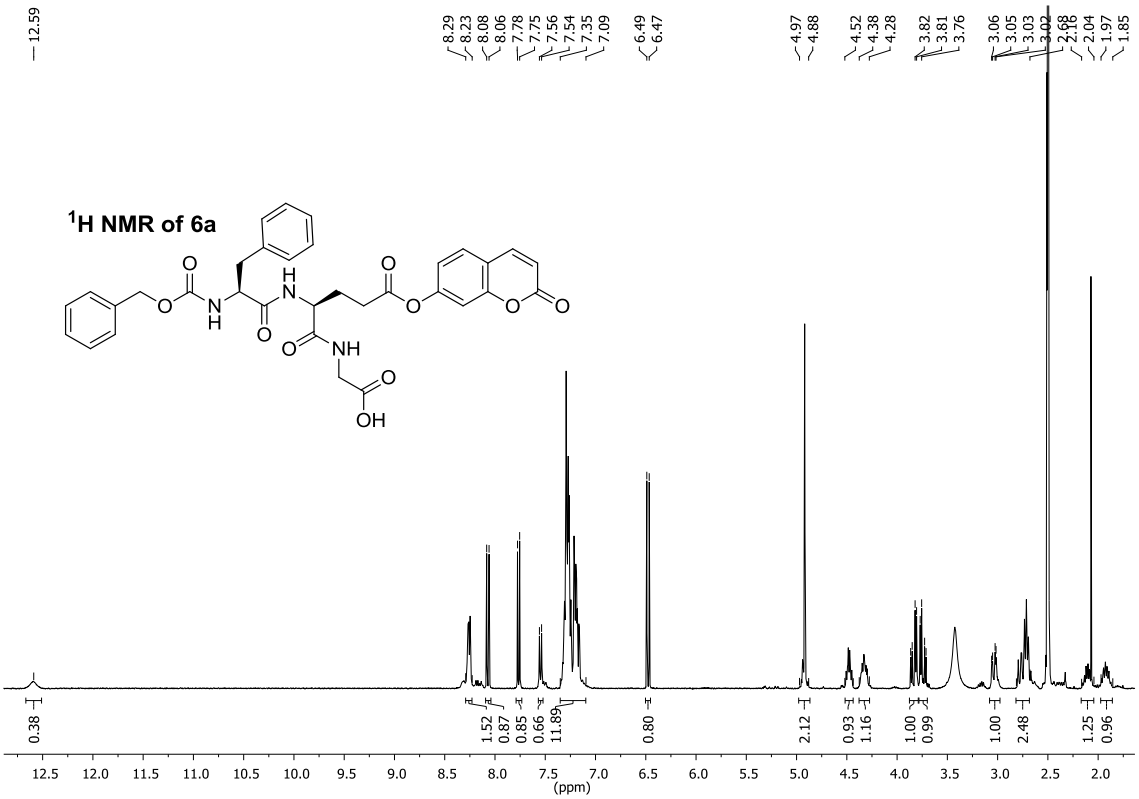

^{1}H NMR of 6a

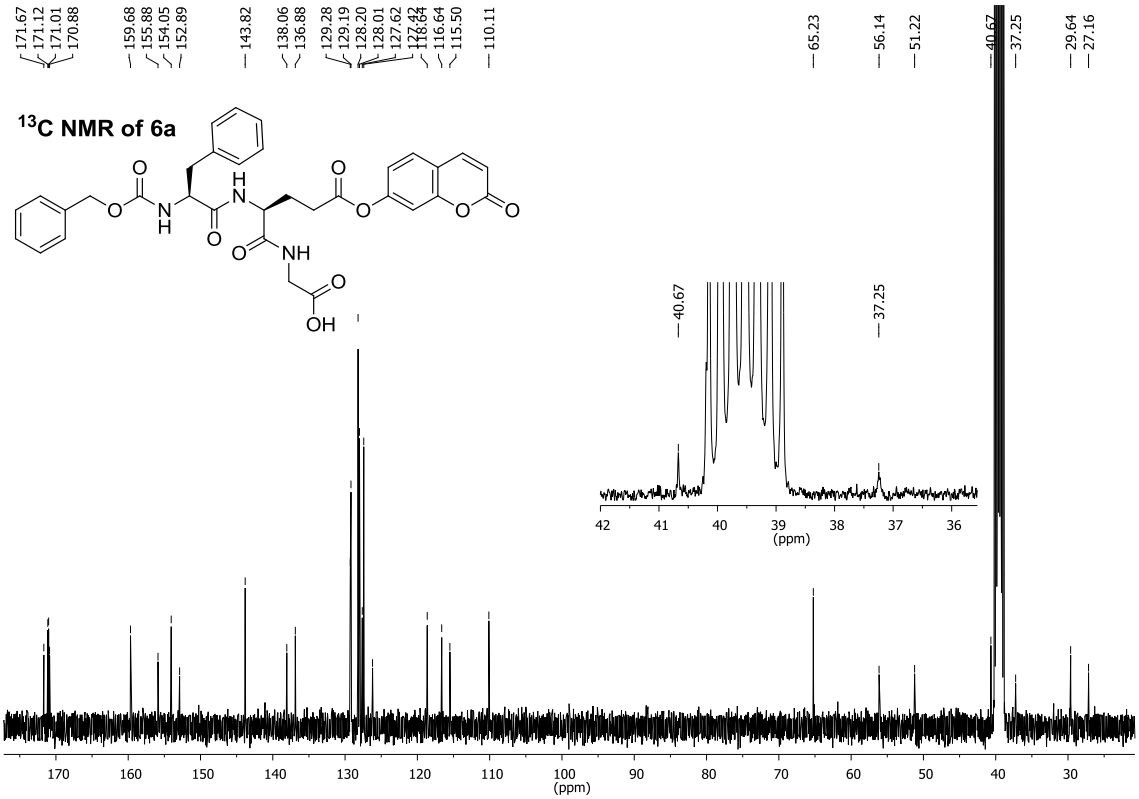

^{13}C NMR of 6a

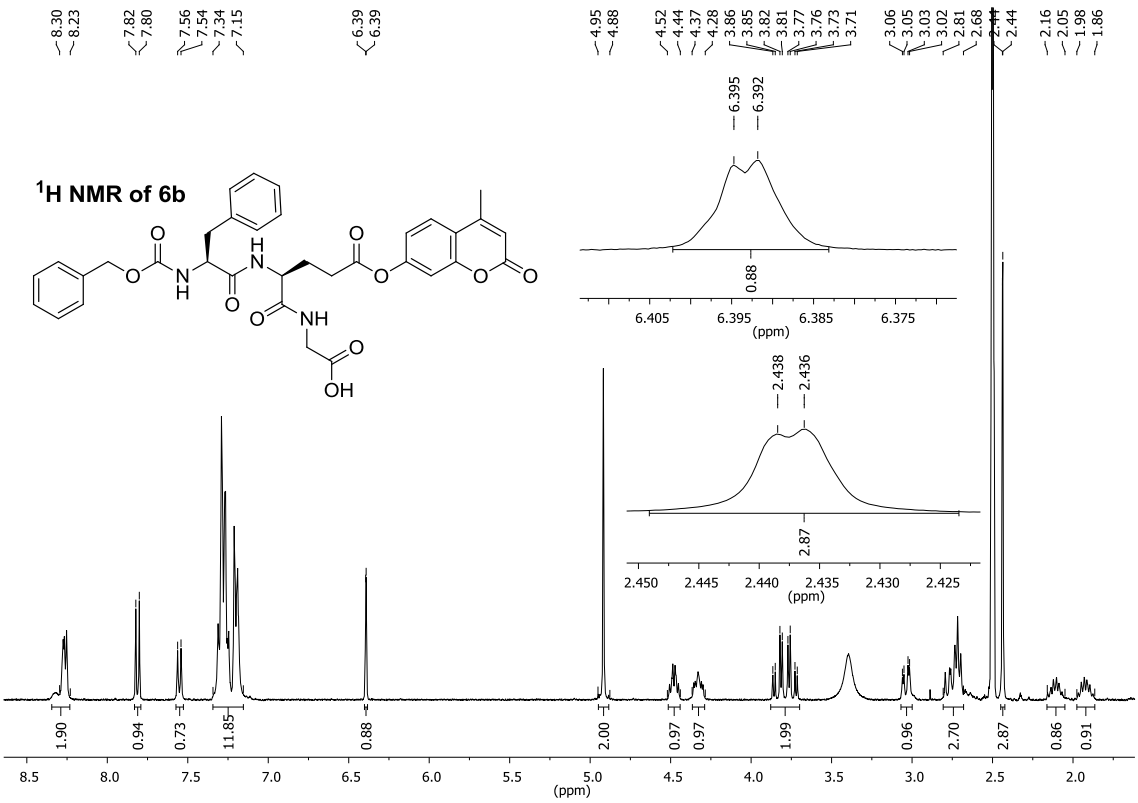
1H NMR of 6b
8.30
8.23
7.82
7.80
7.56
7.54
7.34
7.15
6.39
6.39
4.95
4.88
4.52
4.44
4.37
4.28
3.86
3.85
3.82
3.81
3.77
3.76
3.73
3.71
3.06
3.05
3.03
3.02
2.81
2.68
2.44
2.44
2.16
2.05
1.98
1.86
6.395
6.392
0.88
6.405
6.395
6.385
6.375
(ppm)
2.438
2.436
2.87
2.450
2.445
2.440
2.435
2.430
2.425
(ppm)
1.90
0.94
0.73
11.85
0.88
2.00
0.97
0.97
1.99
0.96
2.70
2.87
0.86
0.91
8.5
8.0
7.5
7.0
6.5
6.0
5.5
5.0
4.5
4.0
3.5
3.0
2.5
2.0
(ppm)

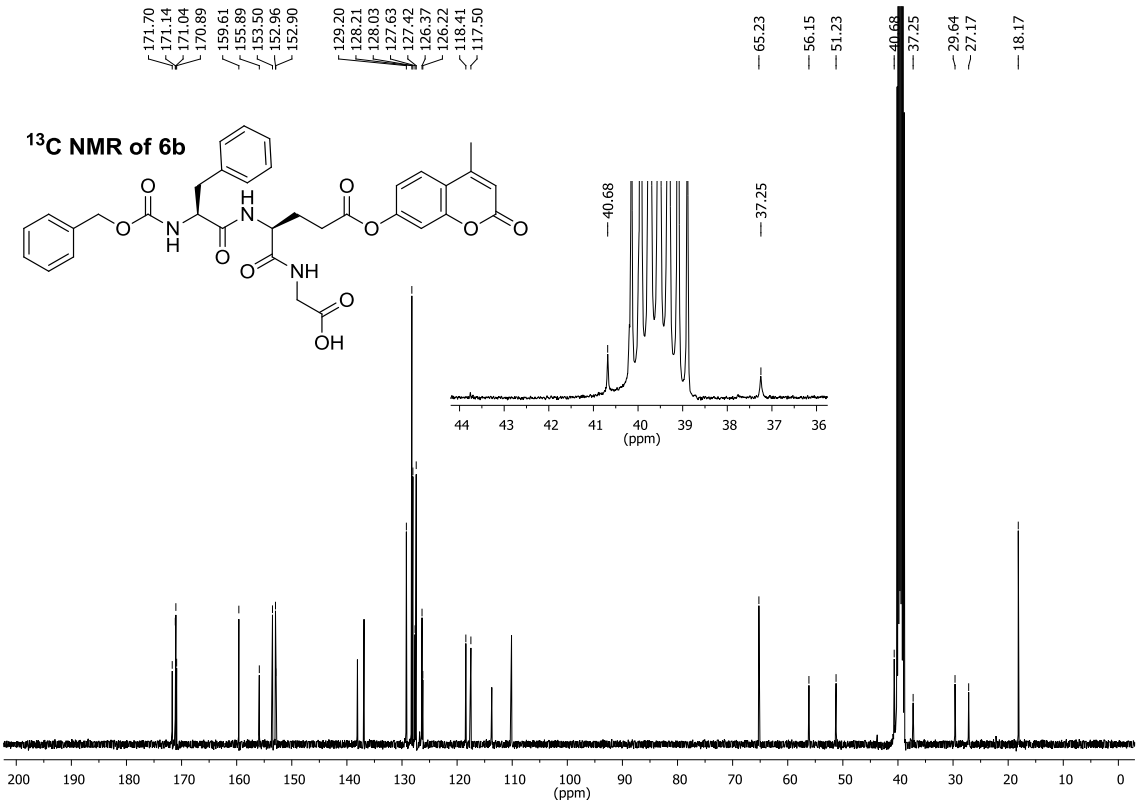
13C NMR of 6b
171.70
171.14
171.04
170.89
159.61
155.89
153.50
152.96
152.90
129.20
128.21
128.03
127.63
127.42
126.37
126.22
118.41
117.50
65.23
56.15
51.23
40.68
37.25
29.64
27.17
18.17
40.68
37.25
44
43
42
41
40
39
38
37
36
(ppm)
200
190
180
170
160
150
140
130
120
110
100
90
80
70
60
50
40
30
20
10
0
(ppm)

^{1}H NMR of 7

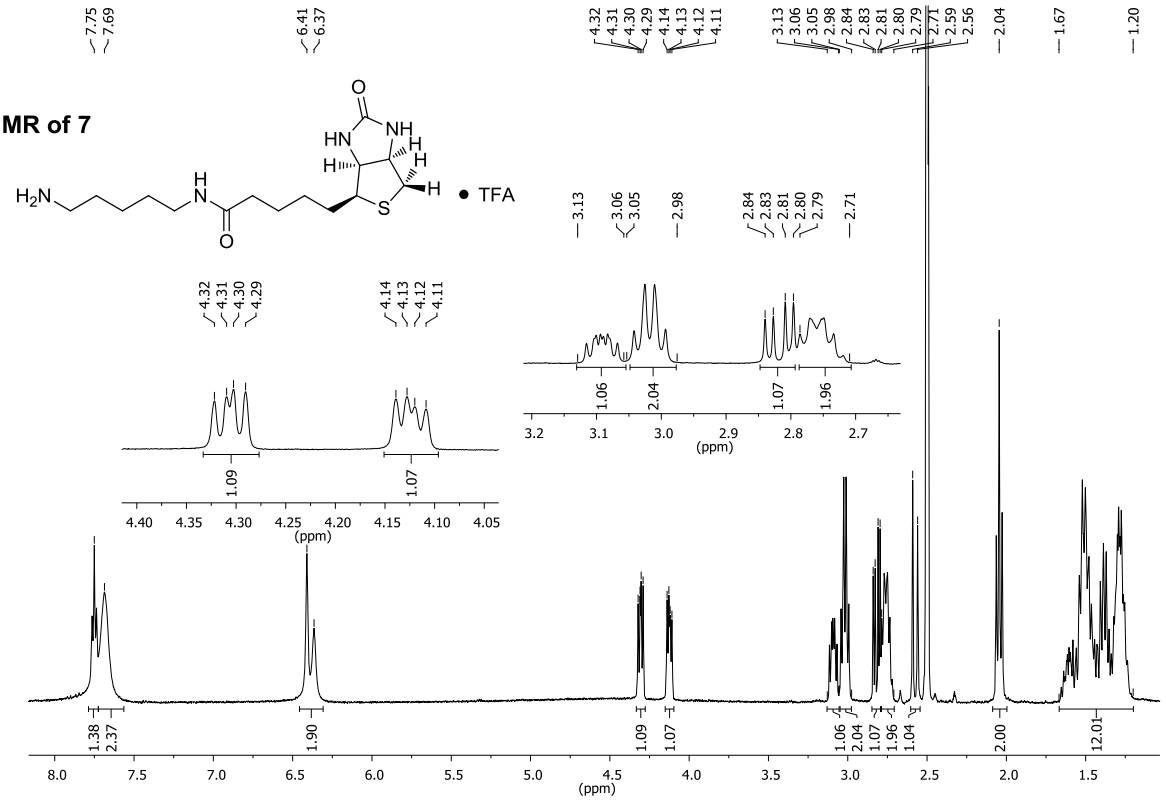

^{13}C NMR of 7

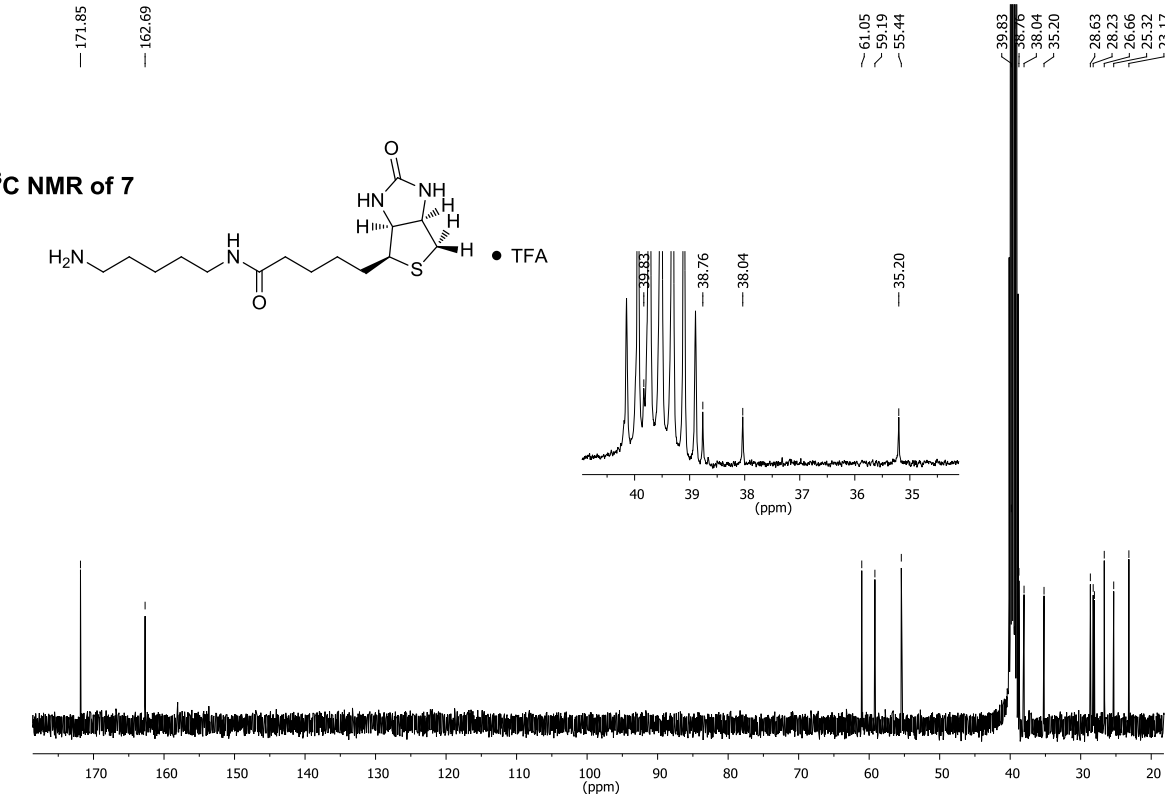

Literature for Supporting Information

[1] (a) P. Gagnon, X. Huang, E. Therrien, J. W. Keillor *Tetrahedron Lett.* **2002**, *43*, 7717-7719; (b) S. M. Gillet, J. N. Pelletier, J. W. Keillor *Anal. Biochem.* **2005**, *347*, 221-226.

[2] G. Schwarz, H. Alberts, H. R. Kricheldorf *Liebigs Ann. Chem.* **1981**, 1257-1270.

[3] J. Xu, Y. Fu, D. F. Luo, Y. Y. Jiang, B. Xiao, Z. J. Liu, T. J. Gong, L. Liu *J. Am. Chem. Soc.* **2011**, *133*, 15300-15303.

[4] I. Roy, O. Smith, C. M. Clouthier, J. W. Keillor *Protein Expr. Purif.* **2013**, *87*, 41-46.

[5] (a) I. Friligou, E. Papadimitriou, D. Gatos, J. Matsoukas, T. Tselios *Amino Acids* **2011**, *40*, 1431-1440; (b) S. L. Pedersen, A. P. Tofteng, L. Malik, K. J. Jensen *Chem. Soc. Rev.* **2012**, *41*, 1826-1844.

[6] J. D. K. Twibanire, T. B. Grindley *Org. Lett.* **2011**, *13*, 2988-2991.

[7] K. Barlos, O. Chatzi, D. Gatos, G. Stavropoulos *Int. J. Pept. Protein Res.* **1991**, *37*, 513-520.

[8] (a) M. Gude, J. Ryf, P. D. White *Lett. Peptide Sci.* **2002**, *9*, 203-206; (b) R. Wodtke, G. Ruiz-Gomez, M. Kuchar, M. T. Pisabarro, P. Novotna, M. Urbanova, J. Steinbach, J. Pietzsch, R. Löser *Org. Biomol. Chem.* **2015**, *13*, 1878-1896.

[9] M. E. Mahoney, A. Oliver, O. Einarsdottir, J. P. Konopelski *J. Org. Chem.* **2009**, *74*, 8212-8218.

[10] D. Seebach, E. Dubost, R. I. Mathad, B. Jaun, M. Limbach, M. Löweneck, O. Flögel, J. Gardiner, S. Capone, A. K. Beck, H. Widmer, D. Langenegger, D. Monna, D. Hoyer *Helv. Chim. Acta* **2008**, *91*, 1736-1786.

[11] R. Bollhagen, M. Schmiedberger, K. Barlos, E. Grell *J. Chem. Soc., Chem. Comm.* **1994**, 2559-2560.

[12] E. K. Woodman, J. G. K. Chaffey, P. A. Hopes, D. R. J. Hose, J. P. Gilday *Org. Process Res. Dev.* **2009**, *13*, 106-113.

[13] M. Vendrell, R. Ventura, A. Ewenson, M. Royo, F. Albericio *Tetrahedron Lett.* **2005**, *46*, 5383-5386.

[14] K. Hardes, M. Zouhir Hammamy, T. Steinmetzer *Anal. Biochem.* **2013**, *442*, 223-230.

[15] (a) B. Sjöberg *Z. Physik. Chem.* **1942**, *52B*, 209-221; (b) F. Lynen, S. Ochoa *Biochim. Biophys. Acta* **1953**, *12*, 299-314.

[16] Z. P. Gates, J. R. Stephan, D. J. Lee, S. B. H. Kent *Chem. Commun.* **2013**, *49*, 786-788.

[17] (a) J. C. Han, G. Y. Han *Anal. Biochem.* **1994**, *220*, 5-10; (b) E. B. Getz, M. Xiao, T. Chakrabarty, R. Cooke, P. R. Selvin *Anal. Biochem.* **1999**, *273*, 73-80.

[18] (a) J. Podlech, M. Gurrath, G. Müller In *Houben-Weyl Methods of Organic Chemistry, Vol. E22a "Synthesis of peptides and peptidomimetics",* (Eds.: Goodman, M.; Felix, A.; Moroder, L.; Toniolo, C.), G. Thieme, Stuttgart, **2003**, pp. 67; (b) M. Mergler, F. Dick *J. Pept. Sci.* **2004**, *10*, S2/145, http://www.bachem.com/fileadmin/user_upload/pdf/TechLib_Base-Induced_Glutarimide_Formation_During_Fmoc-Based_SPPS.pdf; (c) J. Zhu, R. E. Marchant *J. Pept. Sci.* **2008**, *14*, 690-696.

[19] S. Capasso, L. Mazzarella, F. Sica, A. Zagari *J. Chem. Soc., Chem. Commun.* **1991**, 1667-1668.

[20] A. Baici, *Kinetics of enzyme-modifier interactions*, Springer, Wien, **2015**, pp. 127-169.

[21] I. H. Segel, *Enzyme Kinetics - Behavior and analysis of rapid equilibrium and steady-state enzyme systems*, John Wiley & Sons, Hoboken, **1975**, pp. 170-176.

[22] I. B. Wilson, J. Alexander *J. Biol. Chem.* **1962**, *237*, 1323-1326.

[23] G. R. Hillmann, H. G. Mautner *Biochemistry* **1970**, *9*, 2633-2638.

[24] A. Case, R. L. Stein *Biochemistry* **2003**, *42*, 9466-9481.

[25] (a) J. E. Folk *J. Biol. Chem.* **1969**, *244*, 3707-3713; (b) J. W. Keillor, C. M. Clouthier, K. Y. Apperley, A. Akbar, A. Mulani *Bioorg. Chem.* **2014**, *57*, 186-197.

[26] (a) R. L. Stein, *Kinetics of enzyme action - essential principles for drug hunters*, John Wiley & Sons, Hoboken, **2011**, pp. 141-168; (b) A. Cornish-Bowden, *Fundamentals of enzyme kinetics*, Wiley-Blackwell, Weinheim, **2012**, pp. 204-210.

[27] A. Leblanc, C. Gravel, J. Labelle, J. W. Keillor *Biochemistry* **2001**, *40*, 8335-8342.

[28] I. H. Segel, *Enzyme Kinetics - Behavior and analysis of rapid equilibrium and steady-state enzyme systems*, John Wiley & Sons, Hoboken, **1975**, pp. 606-625.

[29] (a) K. Dalziel *Acta Chem. Scand.* **1957**, *10*, 1706-1723; (b) W. Schöpp, H. Sorger, H.-P. Kleber, H. Aurich *Eur. J. Biochem.* **1969**, *10*, 56-60.

[30] F. M. Dickinson In *Enzymology Labfax,* (Eds.: Engel, P. C.), BIOS Scientific Publishers Limited and Academic Press, Oxford and San Diego, **1996**, pp. 84-95.

[31] B. J. Egner, M. Cardno, M. Bradley *J. Chem. Soc., Chem. Commun.* **1995**, 2163-2164.

[32] A. Bernecker, R. Wieneke, R. Riedel, M. Seibt, A. Geyer, C. Steinem *J. Am. Chem. Soc.* **2010**, *132*, 1023-1031.

[33] (a) J. A. Glasel *Biochemistry* **1966**, *5*, 1851-1855; (b) J. H. Bradbury, R. N. Johnson *J. Magn. Reson.* **1979**, *35*, 217-222.